INSIGHTS INTO THE INTERCONNECTED BRAIN DURING (MULTI-)SENSORY PROCESSING

A CONCURRENT TMS-FMRI APPROACH

Dissertation

Zur Erlangung des Grades eines
Doktors der Naturwissenschaften

der Mathematisch-Naturwissenschaftlichen Fakultät
und
der Medizinischen Fakultät der Eberhard-Karls-Universität Tübingen

vorgelegt von:
Joana Leitão
aus Lissabon
Dezember, 2014

Tag der mündlichen Prüfung:	17. August 2015
Dekan der Fakultät für Biologie:	Prof. Dr. W. Rosenstiel
Dekan der Medizinischen Fakultät:	Prof. Dr. I. B. Autenrieth
1. Berichterstatter:	Prof. Dr. U. Noppeney
2. Berichterstatter:	Prof. Dr. C. Braun
3. Berichterstatter:	Prof. Dr. N. Weiskopf
Prüfungskommission:	Prof. Dr. U. Noppeney
	Prof. Dr. H. Preissl
	Prof. Dr. G. Lohmann
	Dr. A. Bartels

I hereby declare that I have produced the work entitled: *"Insights into the Interconnected Brain during (Multi-)sensory processing - A Concurrent TMS-fMRI Approach"*, submitted for the award of a doctorate, on my own (without external help), have used only the sources and aids indicated and have marked passages included from other works, whether verbatim or in content, as such. I swear upon oath that these statements are true and that I have not concealed anything. I am aware that making a false declaration under oath is punishable by a term of imprisonment of up to three years or by a fine.

Joana Leitão

Acknowledgments

I would like to start by thanking my thesis advisor, Uta Noppeney, for all the support and guidance she offered me throughout my studies. The scientific knowledge she has transmitted me is something I am very grateful for. I would also like to thank her for the opportunity of working in her new group in the University of Birmingham. This allowed me not only get to know another country and culture but also to become acquainted with a different work setting and different ways of doing things, which was certainly an enriching experience.

I would also like to thank Axel Thielscher for his collaboration in our projects throughout the entire period of my studies and for teaching me most of what I know about the method of transcranial magnetic stimulation and its combination with functional magnetic resonance imaging.

I am also grateful to my colleagues from the Cognitive Neuroimaging Group in Tübingen and the Computational Cognitive Neuroimaging Group in Birmingham for creating a great working atmosphere. To my colleagues in Tübingen a special thanks for all your assistance and availability during the time-consuming acquisition phase of my data. I would not have been able to do it without your help. Thank you especially to Ruthi, my mother chicken, who from the very beginning until the very end was always very supportive and helped me in so many ways. I would also like to thank Rémi, for making the journey between the two labs a much greater and funnier experience, and Tim, without whom the delivery process would have been a big ordeal.

Besides my direct colleagues I am also very grateful to Mario for his backstage tours into Psychtoolbox and computer graphics, after which everything made much more sense. His development of Psychtoolbox and his quick implementations of new features made my life so much easier during these last years. Thank you for all your support at work and beyond.

A very special thanks goes also to Natalie, who always unhesitatingly helped me at various levels during my studies. The conversations with her about research and beyond offered me new perspectives and transmitted me confidence about my work. Thank you also for teaching me Russian, хорошая девушка!

To all my friends that stayed throughout the years and the ones I gained along the way. Thank you for all the shared moments and for making my life more exciting. To the ones I met abroad, thank you for making me feel at home.

I am also extremely grateful to all the participants who were kind enough to lend their brains to my experiments. Without their motivation, cooperation and endurance in an always friendly and pleasant environment this work would not have been possible.

To my family, thank you very much. Mãe, Pai, Tia, ufa, já está! Thank you for all your support and encouragement and for being there for me during all the ups and downs. Ana e Maria, it is really good to have you as my sisters. I miss you very much. To the little ones, the stories I heard about you always made me smile! I wished I were there to be able to tell them myself.

And to José, who even from far away was always able to calm down the whirlpools in my head. It has been so good having you nearby now! Thank you for all your patience and for always making me laugh.

Abstract

The ability to appropriately respond to sensory information from our surroundings relies on the dynamic interplay between different and distributed brain regions, which is flexibly adapted according to current contexts and demands. By allowing direct monitoring of local and distal effects of transcranial magnetic stimulation (TMS), the concurrent application of TMS and functional magnetic resonance imaging (fMRI) provides a causal interventional approach to investigate this interconnected nature of the brain. In this dissertation, we used this methodology to investigate the neural mechanisms underlying (audio-)visual processing under different cognitive and experimental settings. In particular, given the functional heterogeneity of the intraparietal sulcus (IPS) in a number of different cognitive functions, a special focus was given to the functional role of this region during such processes. As a first step, we evaluated the causal involvement of the IPS during crossmodal deactivations by applying continuous repetitive TMS at different intensity levels to the right IPS and at the Vertex during three different sensory contexts (visual, auditory and fixation). Second, by engaging the attentional network in a demanding visual detection task we investigated how TMS at the right IPS influenced task-related activations, by applying bursts of TMS pulses over the right IPS and during a Sham condition. Moreover, given that additional sensory information might influence task performance in a beneficial or in a detrimental way, we further manipulated the bottom-up sensory context by introducing two different auditory contexts (present vs. absent). Third, to evaluate the differential effects of stimulating low-level sensory areas and higher-order association cortices, we compared the consequences of parietal and occipital stimulation on task-related activations during an identical experimental setting. Lastly, keeping the same visual detection task, we assessed the role of the IPS during perceptual decisions by categorizing participants' responses into hits, misses, false alarms and correct rejections and comparing conditions with matched visual input but different behavioural response categories and vice versa. Overall, our results provide causal evidence for the involvement of the right IPS in different stages of sensory processing. Moreover, they also reflect the ability of the concurrent TMS-fMRI approach to divide a global task-related network into those elements that are specifically associated to the targeted area.

Table of Contents

List of Abbreviations

A	Auditory Stimulation
AC	Anterior Cingulate
ANOVA	Analysis of Variance
AV	Audiovisual Stimulation
BA	Brodmann area
BOLD	Blood-Oxygenation-Level-Dependent
CR	Correct Rejections
dB	Decibel
EEG	Electroencephalography
EPI	Echo-Planar Imaging
FEF	Frontal Eye Fields
Fix	Fixation
FLASH	Fast Low-Angle Shot
fMRI	Functional Magnetic Resonance Imaging
FOV	Field-Of-View
FWE	Family-Wise Error
GABA	gamma-aminobutyric acid
GE	Gradient Echo
HRF	Hemodynamic Response Function
HRTF	Head-Related Transfer Function
Hz	Hertz
IPL	Inferior Parietal Lobe
IPS	Intraparietal Sulcus
LCD	Liquid Crystal Display
LGN	Lateral Geniculate Nucleus
LIP	Lateral Intraparietal Sulcus
MEP	Motor Evoked Potential
MFG	Middle Frontal Gyrus
mm	millimeter
MNI	Montreal Neurological Institute
mPFC	medial Prefrontal Gyrus
MRI	Magnetic Resonance Imaging
MR	Magnetic Resonance
ms	milliseconds
Occ	Occipital
PET	Positron Emission Tomography
PPC	Posterior Parietal Cortex
RF	Radiofrequency
RM-ANOVA	Repeated-measures Analysis of Variance
rMT	resting Motor Threshold
ROI	Region Of Interest
rTMS	repetitive Transcranial Magnetic Stimulation
s	seconds
SD	Standard Deviation
SDT	Signal Detection Theory
SFG	Superior Frontal Gyrus
SI	Primary Somatosensory Cortex
SMA	Supplementary Motor Area
SPM	Statistical Parametric Map
T	Tesla
TE	Time of Echo
TI	Time of Inversion
TMS	Transcranial Magnetic Stimulation
TPJ	Temporoparietal Junction
TR	Time of Repetition
V	Visual Stimulation
VLPFC	Ventral Lateral Prefrontal Cortex

List of Figures

List of Tables

1 Introduction

1.1 An ensemble of dynamic interconnected systems

Whether cortical functions are localized in defined regions of the cortex or are instead the result of interactions between different areas of the brain is a question that has had a central role throughout the history of neuroscience. Although the idea of cortical localization of function had been contemplated before, it was with Franz Joseph Gall that it started gaining significant attention (Finger, 1994a; Catani and Ffytche, 2005). Despite his flawed phrenology theories, Gall was crucial in establishing the notion that the cortex might contain various functionally specialized parts and his ideas influenced a number of prominent physicians at the time.

However, from its very beginnings phrenology was also the target of severe criticism. Marie-Jean-Pierre Flourens, who emphasized the importance of brain stimulation and ablation in animal studies as a scientific method, was one of its strongest opponents. His observations of recovery of function after ablation in birds led him to the contrasting idea of cortical equipotentiality, by which the cortex was thought to function as a whole (Finger, 1994a). Paradoxically, it was based on brain damage that cortical localization achieved serious acceptance when Paul Broca presented his case of motor aphasia after lesion in the frontal lobe in 1861 (Finger, 1994a). Further support for localization of function followed with other lesion-based evidence, like David Ferrier's ablation experiments of the motor cortex in monkeys and dogs, and the discovery of cytoarquitectonic maps by Korbinian Brodmann, amongst other things (Finger, 1994a).

By the end of the 19th century localization of function was a widespread belief, albeit not one without contestants. For instance, based on new findings about numerous connections between cells in the nervous system, Camillo Golgi argued that functionally localization was not supported by anatomical data and maintained a holistic approach towards brain function (Finger, 1994b). Others took a less drastic view and while they acknowledged localization for sensory or motor functions, they rejected the idea of specialized regions for complex cognitive processes. Essentially, for many researchers the fundamental problem with such lesion-based demonstrations rested on the fact that they equated the localization of symptoms with localization of function. In fact, as John Hughlings Jackson suggested, symptoms, while unquestionably recognized, could have arisen as secondary effects of brain damage on more distal structures (Finger, 1994b). Accordingly, it was proposed by Carl Wernicke and others that higher functions, such as speech, were the product of associative connections between areas storing sensory and motor images and that it was the disruption of these pathways that caused functional disorders, the so called disconnection syndromes (Catani and Ffytche, 2005).

While this theoretical framework was practically abandoned during the first half of the 20th century, it gained renewed interest in 1965 when it was reintroduced by Norman Geschwind. However, Geschwind's theory went one step beyond it by suggesting that the association cortex (in particular

the angular gyrus) acted as a relay station between different brain regions. Hence, even circumscribed lesions to the association cortex that did not cause damage to any of the connecting pathways would result in a disconnection syndrome (Catani and Ffytche, 2005). Geschwind's ideas influenced a number of modern neuroscientists and since then accumulating evidence for a distributed processing between functionally specialized and interconnected regions has been presented (e.g. Mesulam, 1990; Corbetta and Shulman, 2002; Bullmore and Sporns, 2009).

Interestingly, the emergence of new neuroimaging tools, in particular in the field of functional magnetic resonance imaging (fMRI), has recently sparked a renewed debate over the structure-function relationship of the brain. Following the traditional focus of fMRI research on localization, some researchers emphasize the role of cortical specialization with the ultimate goal of obtaining a "cognitively precise parts list" for the human brain (Kanwisher, 2010). Yet, with the development of new analytical methods, such as structural and functional connectivity measures, graph theoretical methods and machine learning approaches, the concept of the brain as a network has rapidly gained a large number of supporters (e.g. Bressler, 1995; McIntosh, 2000; Bressler and Tognoli, 2006; Rubinov and Sporns, 2010; Anderson et al., 2013), to the point that some even suggest that the notion of functional areas should be entirely renounced (Laurienti, 2014; Pessoa, 2014).

Notwithstanding the disagreement about the level of functional specificity of individual brain areas, current accounts still concur on the idea that complex cognitive brain functions must result from the collaborative interplay between distributed and interconnected brain regions (Friston and Price, 2011). Importantly, the observation that some regions can be associated with multiple functions indicates that this interplay is dynamic in nature, changing in a temporal and spatial scale according to current contexts and demands (Meehan and Bressler, 2012; Cole et al., 2013). One such region that has been implicated in several cognitive processes is the intraparietal sulcus, which will be the focus of the following section.

1.2 The Intraparietal Sulcus - A Hub in Control Mechanisms

The intraparietal sulcus (IPS) constitutes an important anatomical landmark in the brain. Located in the posterior parietal cortex, it extends posteriorly from the transverse occipital sulcus until more anteriorly to the post-central sulcus, thereby separating the parietal lobe in a superior and inferior part (Fig. 1.1). Possibly related to this strategic location in the brain and its ensuing connectivity pattern, the IPS has been shown to be functionally heterogeneous. In fact, both in humans and in nonhuman primates, IPS has been associated with numerous functions, such as spatial attention (Hopfinger et al., 2000; Corbetta and Shulman, 2002; Yantis et al., 2002; Silver et al., 2005), multisensory integration (Calvert et al., 2001; Sadaghiani et al., 2009; Beauchamp et al., 2010; Pasalar et al., 2010; Werner and Noppeney, 2010), coordination of visuomotor actions (Taubert et al., 2010; Reichenbach et al., 2011; Konen et al., 2013), numerical cognition (Dehaene et al., 2004; Ansari, 2007; Cohen Kadosh and Walsh, 2009; Jacob and Nieder, 2009) and perceptual decisions (Churchland et al., 2008; Tosoni et al., 2008; Freedman and Assad, 2011; Gould et al., 2012), suggesting that this region might act as convergence zone where multimodal inputs are integrated

according to current demands. The following sections review some of the existing evidence pertaining the involvement of this region in a selected set of different cognitive processes.

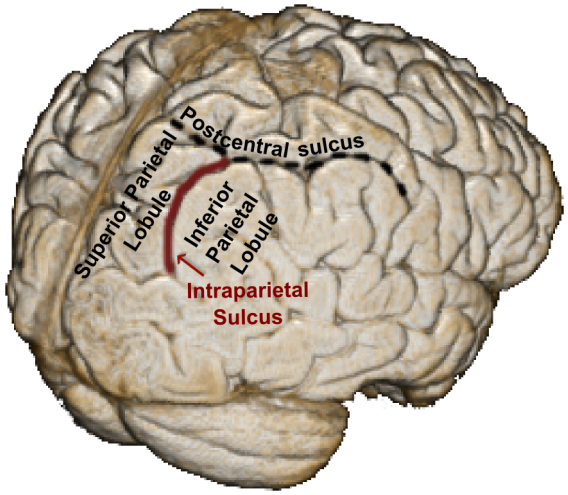

Figure 1.1. Anatomy of the (right) parietal lobe. The intraparietal sulcus (in red) extends from the transverse occipital sulcus until the postcentral sulcus and separates the parietal lobe in the superior and inferior parietal lobules.

1.2.1 Top-down and Bottom-up Mechanisms in Attentional Selection Processes

Selective attention entails the ability to dynamically focus on objects or events that are currently relevant for behaviour. This selection depends on both bottom-up, stimulus-driven factors that reflect physical properties of the sensory events and top-down factors reflecting our current goals and intentions. Correspondingly, at the neural level, steering attention to behaviourally relevant events involves the dynamic interaction between sensory brain areas and attentional control systems. In fact, accumulating evidence has demonstrated that attentional top-down signals can modulate activity in sensory cortical areas. These top-down biases are thought to facilitate processing of objects from the attended stimulus feature, which can occur through several different mechanisms.

For instance, top-down signals can modulate stimulus-evoked responses by enhancing neural responses by a multiplicative gain factor for attended relative to unattended stimulus attributes. Most of the evidence comes from investigations in the visual domain, where neurophysiological studies in non-human primates have demonstrated that these gain control mechanisms can occur in both primary and extrastriate visual areas (Motter, 1993; Luck et al., 1997; McAdams and Maunsell, 1999; Treue and Martínez Trujillo, 1999). Further evidence comes from functional imaging and magneto- and electroencephalography studies in humans that respectively reported increases in Blood-oxygen-level dependent (BOLD) signal and changes in oscillatory and event-related activity that are assumed to enhance neural processing for the attended stimulus feature (Heinze et al., 1994; Mangun et al., 1998; Tootell et al., 1998; Friston and Büchel, 2000). In particular, studies that investigated attentional top-down influences as a function of the attended stimulus attribute have demonstrated that selective attention modulates activations in extrastriate areas that are specialized in processing the selected attribute (Corbetta et al., 1990; Clark et al., 1997; O'Craven et al., 1997).

Outside the visual domain, attention-induced stimulus-evoked response increases have likewise been reported in the auditory (Hubel et al., 1959; Hillyard et al., 1973; Alho et al., 1994) and somatosensory sensory systems (Hsiao et al., 1993; Burton et al., 1999; Johansen-Berg et al., 2000).

In addition to modulate stimulus-evoked responses, attentional top-down biases can also occur in the absence of sensory stimulation. These top-down modulations are characterised by an increase in baseline activity that occurs when observers are directing attention to the relevant stimulus feature in expectation of incoming of sensory information. For instance, when attention is directed to a certain position in space, enhanced baseline activation and oscillatory activity modulations can be observed in retinotopic visual areas (Kastner et al., 1999; Hopfinger et al., 2000; Worden et al., 2000; Thut et al., 2006) and somatotopic somatosensory cortices (Macaluso et al., 2003) that represent the attended spatial location. Likewise, increases in preparatory activity have also been shown in auditory cortices (for a review see Fritz et al., 2007) and for non-spatial stimulus attributes in corresponding feature selective areas (Chawla et al., 1999; McMains et al., 2007).

Functionally, baseline shifts and stimulus-evoked modulations are thought to bias neural processing in favour of the attended stimulus feature. This sacrifices in-depth processing of other coinciding stimuli, which correspondingly results in an improved behavioural performance (Serences and Kastner, 2014). Accordingly, another mechanism by which attention can modulate processing in sensory cortices is through suppressive effects for distracting or unattended stimuli properties (Moran and Desimone, 1985; Pinsk et al., 2004; Hopf et al., 2005; Seidl et al., 2012). Along similar lines, preparatory activity has also shown to be modulated by the knowledge about distractor presence, suggesting that preparatory activity might be involved in the suppression of task-irrelevant information (Serences et al., 2004; Munneke et al., 2011).

Numerous functional imaging studies have identified a distributed frontoparietal network, comprising the IPS and the frontal eye fields, as the source for these top-down attentional modulations. The IPS, in particular, has shown increased baseline activations during expectation of visual stimuli (Kastner et al., 1999; Serences et al., 2004). In fact, using variations of Posner's endogenous spatial cueing paradigm (Posner, 1980) that separates cue-induced preparatory attentional signals from signals related to the detection of visual targets, neuroimaging studies have demonstrated that the IPS exhibits sustained increased activations in response to attention-directing cues, which is interpreted as representing a critical role of this region during voluntary attentional control (Corbetta et al., 2000; Hopfinger et al., 2000; Kincade et al., 2005). This cue-driven activity is not exclusive to spatial properties of the stimuli but can equally be observed when attention is directed to other non-spatial stimuli features within and across sensory modalities (Egner et al., 2008; Smith et al., 2010).

Additionally, spatial attentional modulations in this region have shown to be topographically organized in accordance to the spatial position that is covertly attended (Silver et al., 2005; Saygin and Sereno, 2008). Moreover, spatially selective attention modulations can also occur in a stimulus-driven fashion. For instance, Serences and Yantis (2007) showed activation increases in the IPS for target-coloured distractors presented contralaterally to the voluntarily attended side relative to distractors that did not share any features with the target stimulus. These results suggest that target-coloured distractors are endowed with higher attentional priority in this region because they share a

feature with the behavioural relevant stimulus. In the same vein, using a sustained spatial attention task that manipulated the location of attention and the location of the perceptually salient stimuli, Geng and Mangun (2009) showed that IPS activations were strongly modulated by perceptually salient stimuli that were presented outside the attended location.

Collectively, these findings indicate that the IPS is not exclusively involved in voluntary attentional control but is likewise sensitive to sensory-driven properties of the attended stimulus. Due to these functional characteristics it has been suggested that the IPS encodes an attentional priority map of the environment that is characterized by the integration of sensory-driven and top-down signals according to current perceptual or behavioural salience (Gottlieb, 2007; Ptak, 2012).

1.2.2 Perceptual decision-making

An appropriate interaction with the world relies on our ability to select a specific action based on sensory evidence arising from a frequently noisy environment. More often than not, this involves making a categorical choice between two possible alternatives.

The connection between noisy sensory evidence and response choice has been formalised in an influential model of decision-making. In the framework of signal detection theory (SDT) (Green and Swets, 1966), it is assumed that choices are determined based on a deterministic decision rule, in which noisy sensory evidence is compared to a certain criterion value that establishes a boundary between the two response options along an internal response axis. Importantly, this criterion value reflects response strategies undertaken by the observer and is completely independent of the detectability of the sensory event. Hence, this model successfully accounts for the observation that different task instructions can result in distinct behavioural outcomes despite identical sensory stimulation. However, it overlooks an important component of decision-making, namely the time needed to complete a decision.

Indeed, the crucial effect of time during a decision process is readily observable in the speed-accuracy trade-off phenomenon, whereby instructions to respond rapidly result in less accurate responses, whereas the converse occurs when accuracy is emphasised (Bogacz et al., 2010). Sequential sampling models provide an extension to SDT by incorporating time in the decision process (Ratcliff and Smith, 2004). In fact, whereas different types of sequential models (e.g. drift diffusion, random walk models, etc.) differ in the way they model evidence acquisition or define the stopping criterion, they all concur in the assumption that perceptual decisions are formed by the temporal accumulation of noisy sensory evidence until a decision threshold indicating one or the other response alternatives is reached. Therefore, accumulator models have the advantage of providing precise predictions about the relationship between response times and accuracy.

Additionally, entailed in a decision process are subjective evaluations about the decision itself that reflect among other things the level of confidence about the selected option or the awareness of an incorrect choice. These metacognitive abilities constitute a crucial aspect in decision-making, as they can determine the outcome of subsequent decisions. While largely overlooked in early models of decision-making, these components have been increasingly acknowledged in recent expansions of

the above-mentioned models (Maniscalco and Lau, 2012; Yeung and Summerfield, 2012; Fleming and Lau, 2014).

Consistent with the multiplicity of processes associated with decision-making, accumulating studies have shown that the neural underpinnings of perceptual decisions encompass a widespread network of areas that include sensory, frontal and parietal cortices, as well motor and premotor regions (Kim and Shadlen, 1999; Heekeren et al., 2004, 2006; de Lafuente and Romo, 2006; Pleger et al., 2006; Thielscher and Pessoa, 2007; Noppeney et al., 2010). Embedded in this network, the IPS has been consistently implicated in various aspects of decision-making (Hanks et al., 2006; Churchland et al., 2008; Tosoni et al., 2008; Rorie et al., 2010; Freedman and Assad, 2011; Ploran et al., 2011; Gould et al., 2012; Filimon et al., 2013).

For instance, using a discrimination task, in which monkeys had to indicate the direction of motion via saccadic eye movements to one of two visual targets, Shadlen and Newsome (2001) showed that the activity of single neurons in the lateral intraparietal sulcus (LIP) was predictive of the behavioural outcome at the end of the trial in a way that did not depend on the accuracy of the response. Specifically, by placing one choice-target inside the neurons' receptive field and the other at a distant location, they showed that neural activity gradually increased when the response choice at the end of the trial corresponded to the target inside the neuron's receptive field, while the opposite pattern was observed for the alternative response option. This predictive activity emerged early in the trial and was gradually more reliable over time. Moreover, its timing and magnitude was modulated by the strength of motion signal contained in the stimulus. Collectively, these results suggest that LIP neurons integrate sensory evidence that is relevant for the selection of a response. Hence, much like behavioural data, physiological responses in this region are also successfully predicted by the evidence accumulator model, a finding that has since been replicated (Roitman and Shadlen, 2002; Churchland et al., 2008). Similar conclusions were adduced in a recent fMRI study that employed an equivalent motion discrimination task while parametrically manipulating the level of motion coherence (Kayser et al., 2010). Specifically, Kayser and colleagues were able to confirm their prediction that if the IPS functions as an accumulator in humans, BOLD activations in this region, which they assumed are correlated with integrated neural activity, should vary inversely with increasing motion coherence.

Moreover, it has also been proposed that the IPS encodes choice confidence in non-human primates (Kiani and Shadlen, 2009). In a similar experimental procedure as the one presented above, monkeys executed saccadic eye movements to indicate their response in a motion discrimination task, in which task difficulty was now manipulated by varying motion coherence and stimulus duration. However, in half of the trials monkeys were additionally given the option to renounce to committing to a choice by making saccadic eye movements to a third target that was associated with a certain but smaller reward. Behaviourally, their results show that monkeys used this option more often when sensory evidence was weak (i.e. for low motion coherence and short stimulus durations). Moreover, for almost all levels of task difficulty, response accuracy was improved in trials where monkeys waived this option relative to trials in which they were not given this possibility at all, thus suggesting that the "opting out" choice was based on evaluations about the level of confidence on each trial. Interestingly, extracellular recordings from LIP neurons showed that firing rates during

"opt-out" trials reached only an intermediate level of activity that was reduced in comparison to trials in which the response option corresponded to targets in the receptive field of the recorded neuron, but increased relative to trials that represented opposite response option. Hence, the authors concluded that LIP neurons not only reflect the formation of a decision, but also encode the subjective confidence associated with a choice.

1.2.3 Control in a Multisensory Environment

Our experience of the world relies upon information received through multiple sensory channels, each providing us with distinctive impressions of the surroundings. Extraordinarily, instead of considering each piece of information in isolation, the brain tries to combine all sensory signals into a unified and coherent percept in order to achieve an enhanced understanding of the environment.

Behaviourally, the ability to integrate information from different sensory modalities presents several advantages. For instance, the detection, discrimination and categorization of external stimuli can be dramatically enhanced when multiple sensory sources are available, in particular in a situation in which individual signals happen to be degraded or unreliable (e.g. Shams and Kim, 2010; Werner and Noppeney, 2010; Chen et al., 2011; Fiebelkorn et al., 2011). Similarly, combined sensory information can also result in speeded responses relative to their corresponding unisensory presentation (Hershenson, 1962; Forster et al., 2002; Diederich and Colonius, 2004; Senkowski et al., 2006; Hecht et al., 2008). Crucially, whether or not different sensory signals are integrated strongly depends on their temporal and spatial relation. Indeed, only stimuli that are in close temporal and spatial proximity are inferred to have originated from a common source and will consequently be integrated (Calvert et al., 2004; Macaluso and Driver, 2005). Interestingly, these spatial and temporal constraints can sometimes alter the quality of the sensory percept, as reflected by illusions like the ventriloquist effect (Thurlow and Jack, 1973) or the double flash illusion (Shams et al., 2002). These illusions suggest that information from a multisensory event is not blindly combined, but instead processed by weighting the contribution of each modality by its reliability for the relevant property (i.e. space in the ventriloquist effect and time in the double flash illusion) (e.g. Alais and Burr, 2004; Ernst and Bülthoff, 2004; Helbig and Ernst, 2007).

On account of this multitude of behavioural consequences, a great deal of research in both human and non-human primates has been dedicated to the identification of the neural correlates of multisensory integration. At the cortical level, multisensory integration was traditionally assumed to follow a hierarchical processing path, characterized by extensive analyses of each individual modality in its respective unisensory cortex before information from all different sensory inputs was relayed to higher-order association areas in order to be combined there. This assumption was supported by early anatomical, electrophysiological and hemodynamic studies that identified multisensory convergence zones based on their connectivity patterns with multiple sensory-specific cortices and their ability to respond to information from multiple sensory modalities (for reviews see Macaluso and Driver, 2005; Cappe et al., 2009).

However, the prevailing notion that multisensory integration is deferred until later processing stages has recently been challenged by evidence showing that primary sensory cortices do not exclusively

process information from their respective sensory modality (Macaluso and Driver, 2005; Schroeder and Foxe, 2005; Ghazanfar and Schroeder, 2006; Kayser and Logothetis, 2007; Driver and Noesselt, 2008). In fact, modulatory effects in sensory-specific cortices due to multisensory stimulation have been extensively demonstrated in both humans (Büchel et al., 1998; Amedi et al., 2002; Miller and D'Esposito, 2005; Werner and Noppeney, 2010, 2011) and non-human primates (e.g. Kayser et al., 2005, 2007). In particular, a recent fMRI study showed that the nature of these modulations strongly depends on the current sensory context (Werner and Noppeney, 2011). Indeed, their results show that whereas inputs from the non-preferred sensory modality amplified responses to concurrently presented inputs from the preferred sensory modality, they induced deactivations when presented alone (see also Haxby et al., 1994; Kawashima et al., 1995; Laurienti et al., 2002).

The neural mechanisms that support these multisensory effects in primary sensory areas are currently not fully understood. Based on electrophysiological evidence showing multisensory integration at very short latencies (Giard and Peronnet, 1999; Foxe et al., 2000; Molholm et al., 2002; Murray et al., 2005), it has been proposed that low-level multisensory interactions are mediated via feedforward thalamocortical (Cappe et al., 2009; Tyll et al., 2011) and direct connectivity between sensory areas (Falchier et al., 2002; Rockland and Ojima, 2003). Yet, a contrasting, whilst not incompatible, interpretation suggests that these modulations are mediated via top-down influences from higher-order association cortices, thereby reflecting the implementation of attentional control in a multisensory environment (for reviews see Macaluso and Driver, 2005; Driver and Noesselt, 2008; Talsma et al., 2010).

The IPS is among the higher-order association areas displaying the criteria characteristic to a multisensory convergence zone. For instance, using moving visual, auditory and tactile stimuli, Bremmer et al. (2001) showed increased activations in bilateral human intraparietal sulci in response to all three sensory types. These findings converge with single-cell recordings in non-human primates showing that neurons of the ventral and lateral intraparietal areas respond to stimuli arising from different sensory inputs (Colby et al., 1993; Cohen et al., 2005; Schlack et al., 2005; Russ et al., 2006; Avillac et al., 2007). Further evidence comes from studies that found anatomical connectivity pathways between these regions and cortical areas associated with different sensory modalities (Hyvärinen, 1982; Maunsell and van Essen, 1983; Boussaoud et al., 1990; Lewis and Van Essen, 2000).

Moreover, consistent with its involvement in attentional control in a unisensory (visual) context (see section 1.2.1), numerous studies have demonstrated that the parietal cortex also plays a critical role in multisensory attentional control (Macaluso, 2000; Macaluso et al., 2003; McDonald et al., 2003; Santangelo et al., 2009; Smith et al., 2010). In particular, Macaluso et al. (2003) used a discrimination task that manipulated the direction of attention (left vs. right), the presence of bilateral visuo-tactile stimulation (presence vs. absent) and the task-relevant modality (vision vs. touch) in order to investigate crossmodal relationships in spatial selective attention. As expected, they found that attending to unimodal visual and tactile stimuli increased preparatory activations contralaterally to the attended side in the respective sensory cortices. Moreover, equivalent multimodal spatial effects (i.e. effects of comparing attend to left vs. attend to right pooled over both tactile and visual task-relevant modalities) were found in the intraparietal sulci and the lateral

occipital gyri, thus suggesting that the former might be involved in controlling the direction of attention across different sensory modalities.
In conclusion, multisensory interactions have been demonstrated in a distributed neural network encompassing, subcortical, primary sensory and higher-order association areas. Included in the latter, the IPS has been shown to be involved in multisensory processing during various contextual settings.

1.2.4 Summary

The evidence depicted above demonstrates some of functions encompassed by the IPS from the point of view of three distinct experimental frameworks. Moreover, it implicitly illustrates that the aspects addressed in these sections are tightly interwoven. For instance, attending to a stimulus location can increase behavioural performance (i.e. perceptual decisions were influenced), which can further be modulated by the presence of sensory inputs from different modalities. Thus, the IPS, with its heterogeneous functions and distributed connectivity pattern, effectively reflects the interconnected nature of the brain.

1.3 Concurrent TMS-fMRI

In the past years, fMRI has provided invaluable evidence concerning the mechanisms underlying complex brain functions. On the one hand, many fMRI studies took advantage of its high spatial resolution to identify functionally specialized brain areas (Kanwisher et al., 1997; Epstein and Kanwisher, 1998). On the other hand, the possibility of simultaneously visualizing activity changes across the entire brain revealed that any given cognitive process results in distributed patterns of activation (e.g. Gitelman et al., 1999; Corbetta and Shulman, 2002; Gazzaley et al., 2004; Fairhall and Ishai, 2007; Price, 2010). This observation lead to two fundamental questions: (i) are all the regions actually necessary for the task at hand and (ii) are they (and if yes, how) all interconnected. Unfortunately, the correlational nature of standard fMRI methods precludes inferences in this regard. In contrast, by reversibly perturbing ongoing neural processing, Transcranial Magnetic Stimulation (TMS) can causally implicate the stimulated region. Moreover, TMS effects are not necessarily circumscribed to the stimulated site but can propagate to remote areas of the brain, which renders TMS as a promising tool for studying brain connectivity. Indeed, remote effects of TMS can readily be observed in its most common demonstration, whereby a single TMS pulse over the primary motor cortex produces a contralateral muscular contraction in the hand. However, when applied outside the motor cortex, TMS studies often have to rely on behavioural measures to characterize TMS-induced effects and inferences have to be restricted to the stimulated region. Hence, much like in lesion studies, when TMS is used in isolation there is a risk of overlooking distal consequences of TMS and confounding them with effects originating in the stimulated site. Consequently, in order to understand how neural processing is modulated from a network perspective, TMS-induced changes in neural activity need to be monitored directly by combining this methodology with other neuroimaging techniques.

Almost two decades ago, the concurrent combination of fMRI and TMS was considered as being impossible. However, in their seminal studies Bohning and colleagues (1997, 1998) successfully demonstrated the technical feasibility of this combination, and since then concurrent TMS-fMRI has proven useful in the investigation of the interconnected nature of the brain, as will be shown below. This section provides a brief overview of the main technical and practical issues arising from the combination of both techniques and reviews some of the most prominent studies that applied this methodology to investigate sensory and cognitive brain networks.

1.3.1 Methodological considerations

Concurrent TMS-fMRI is a technically challenging methodology that needs to overcome problems arising from the interference between the magnetic fields inherent to each individual technique. Given that the work developed in this dissertation made use of an already established TMS-fMRI set-up (Moisa et al., 2009) without making any explicit contributions to its development, a comprehensive account of the technical difficulties in combining both techniques is outside the scope of this dissertation. Yet, a description of the main technical complications is still warranted. This section will summarize some of the most prominent technical and practical problems arising from combining the two techniques.

Technical aspects

One apparent complication arising from the combination of the two methods is that the mere presence of the TMS coil inside the scanner bore generates inhomogeneities in the static magnetic field of the scanner, which can lead to local (i.e. up to 2 cm underneath the coil) geometric distortions and signal drop-outs in the echo-planar images (EPI) (Baudewig et al., 2000; Bestmann et al., 2003a). Generally, since the distance between the cortical surface and the skull typically exceeds 2 cm, these artefacts do not cause very severe problems in human studies (Baudewig et al., 2000; Bestmann et al., 2003a). Furthermore, in a recent study, Bungert et al. (2012) reported a way to further reduce this type of artefacts by 75-85% through the use of passive shimming. Shimming strategies are generally applied to eliminate inhomogeneities inside the magnetic field of the scanner. While active shimming is achieved by adjustable currents flowing through specialized coils that generate a corrective magnetic field, passive shimming typically makes use of small metal sheets that are placed inside the scanner bore in order to counteract magnetic field distortions. By appropriately placing such metal sheets on the TMS coil, the authors were able to significantly reduce inhomogeneities in the magnetic field caused by the presence of the TMS coil. As this shimming strategy can be easily incorporated in the TMS coil, it should be beneficial in future concurrent TMS-fMRI studies.

Local field inhomogeneities can also arise through small leakage currents from the TMS coil (Weiskopf et al., 2009). Importantly, owing to the coil's finite resistance, these leakage currents that arise from the high-voltage capacitors used in the stimulator circuitry can emerge even when no pulses are being applied. Since leakage currents are dependent on the stimulator output intensity, this type of artefacts is particularly problematic in parametric TMS designs (i.e. studies that

parametrically manipulate TMS intensities). Yet, this problem can be circumvented by introducing an additional switch in the stimulator circuitry that bypasses the TMS coil when no pulses are being discharged (Weiskopf et al., 2009).

Another general problem is the propagation of radiofrequency (RF) noise into the scanner, which can significantly decrease the signal-to-noise of the data. Indeed, even when the TMS stimulator is placed outside the scanner room, the cable connecting the stimulator to the TMS coil can function as an antenna that transmits RF noise inside the originally shielded scanner environment. These external RF signals can be detected by the magnetic resonance (MR) receiver coils, resulting in image artefacts and consequently in a reduction of the signal-to-noise ratio of the MR data. One solution is to use a high-current filter to eliminate the RF noise caused by the stimulator (Moisa et al., 2009). However, it should be noted for practical purposes that the introduction of these filters attenuates the TMS output intensity by 6-8%.

Finally, dynamic artefacts are related to the application of a TMS pulse and are particularly problematic as they correlate with the TMS paradigm. Different effects can occur depending on the timing of the pulse relative to image acquisition. Typically, an EPI sequence comprises three main steps that are repeated for each slice in each acquired volume: a slice-selective RF excitation step, a phase encoding step and a frequency encoding step, also termed readout, that occurs during data acquisition. Applying a TMS pulse during RF excitation can destroy the specificity of the RF pulse. Consequently, not only can subsequent images of the perturbed slice be affected, but nearby slices might show strong signal fluctuations as well. These fluctuations can be in the order of the physiological BOLD changes and can thus result in false-positive activations (Bestmann et al., 2003a). On the other hand, applying the TMS pulse during the readout phase does not produce these carry-over effects. However, depending on the time point at which the pulse is applied during readout, severe signal dropouts or high-frequency image distortions can occur (Bestmann et al., 2003a). One possibility to approach these artefacts is to apply TMS during readout and substitute the affected images by interpolation between their temporal neighbors. Alternatively, TMS can be applied in temporal gaps between slice or volume acquisitions, which was the strategy adopted in the work presented in this dissertation. Indeed, it has been shown that if the time between the application of a TMS pulse and the subsequent EPI section is long enough (typically ≥ 100ms) only negligible effects in image quality can be observed (Bestmann et al., 2003a). While this strategy avoids interpolation errors and allows the application of pulse trains of any given length, it has the disadvantage of reducing the temporal resolution of the functional data and precluding jittering of the TMS application relative to the MR acquisition.

So far, focus was given to how TMS influences the magnetic field of the scanner and how this affects image quality. However, the interaction between the magnetic fields of both techniques is of course bidirectional. Indeed, one of the first considerations in early combinations of TMS and fMRI was related to the integrity of the TMS coil. TMS coils used inside the scanner need to be free of any ferromagnetic materials and have to be reinforced to withstand the strong forces and high currents that the coil is subjected to. In this respect, figure of eight coils, in which the torques in the two coil loops go in opposite directions, are in principle more beneficial (Bohning et al., 2003b).

Furthermore, a recent study went beyond the physical impact on the TMS coil and investigated how the induced TMS magnetic field was affected by the static magnetic field from the scanner (Yau et al., 2014). By measuring TMS induced voltage changes in a search coil and positioning the TMS coil at different orientations and locations (inside the bore vs. fringe field of the scanner), they showed that TMS fields measured in the fringe field were sensitive to coil manipulation, whereas TMS fields inside the scanner remained relatively constant, thereby providing further validation for concurrent TMS-fMRI studies.

To summarize, the combination of TMS and fMRI is now feasible provided certain technical problems are accounted for. However, these also implicate some constraints in the set of parameters that can be used for each individual technique.

Practical aspects

There are also some practical considerations that need to be addressed when applying this methodology. One practical aspect pertains the considerable space constraints for TMS coil positioning inside the scanner, which limits the choices for possible target stimulation locations. In addition, accurate positioning of the TMS coil over the targeted area is further complicated by the impossibility to rely on neuronavigation systems that achieve high spatial accuracy for coil positioning outside the scanner (Ettinger et al., 1998; Schönfeldt-Lecuona et al., 2005). Methods for coil positioning inside the scanner have been developed that allow for an accurate placement in concurrent TMS-fMRI studies, as validated by stimulation over the motor system (Bohning et al., 2003a; Denslow et al., 2005a; Moisa et al., 2009; Yau et al., 2013). In other studies vitamin capsules and water tubes have been attached to the TMS coil, rendering it visible in fast anatomical images that can be acquired between runs (Bohning et al., 2000, 2003c; Nahas et al., 2001; Sack et al., 2007). However, this method only allows for *a posteriori* reconstruction of the coil position, thus precluding online optimization of coil placement. Despite this disadvantage, this was also the strategy adopted in the studies comprising this dissertation.

Moreover, the application of a TMS pulse is generally accompanied by auditory and somatosensory sensations and potentially elicits startle effects. These non-specific TMS side effects need to be carefully controlled for, as it might otherwise be difficult to disentangle them from true TMS effects. A standard procedure relies on the introduction of a control position that is thought to be unrelated to the cognitive processes under investigation. Commonly the vertex, which is determined individually as the highest point of the skull located medially between both hemispheres, is used for these purposes (e.g. Ruff et al., 2006), although other regions have been used as well (e.g. Sack et al., 2007). Alternatively, TMS studies outside the scanner often rely on a sham control condition that typically involves tilting the TMS coil by 90° thereby eliciting the same auditory co-activations without effectively stimulating the brain. Hitherto, these Sham control conditions, aside from precluding TMS-induced somatosensory sensations, were not suitable for TMS inside the scanner due to space restrictions. Yet, a control sham condition that takes advantage of the quadratic decay of the TMS-induced magnetic field with increasing distance from the coil has proven successful in

eliciting equivalent auditory and somatosensory TMS side effects without effective brain stimulation throughout a series of studies presented in this dissertation (chapters 3 to 5).

Additionally, concurrent TMS-fMRI studies often adopt a parametric approach, in which different TMS intensities are used based on the fact that low TMS intensities are not as effective in inducing neural effects whilst creating comparable TMS side effects (e.g. Ruff et al., 2006, 2008; Blankenburg et al., 2010). In principle, this approach has the advantage of rendering each stimulation location as its own control condition, thereby creating more comparable settings between experimental and control conditions, as these could be acquired in the same experimental session. Yet, whereas side effects elicited by different TMS intensities might be qualitatively similar it does not immediately follow that they are quantitatively comparable as well. This can have important implications when investigating sensory systems, an issue that will be addressed in Chapter 2.

In fact, the preceding point alerts to the problem of choosing an appropriate TMS intensity. Commonly, TMS intensities are chosen individually in relation to the resting motor threshold (rMT), which is defined as the minimum intensity necessary to elicit muscle twitches (typically 5 out of 10) in a relaxed finger when the TMS coil is placed over the corresponding motor cortical representation. With the exception of studies stimulating the visual cortex, where intensities are frequently set relative to the phosphene threshold (e.g. Silvanto et al., 2005; Romei et al., 2007; De Graaf et al., 2012), this approach of determining TMS intensities is employed even for studies outside the motor system (e.g. Chambers et al., 2004; Oliver et al., 2009; Feredoes et al., 2011; Bien et al., 2012; Heinen et al., 2013). This procedure is based on the fact that the motor cortex is the only region over which TMS can elicit overt effects that can be measured in an objective fashion (phosphene threshold relies on participants subjective report). However, there is controversial evidence about whether an intensity that is suitable for one area automatically transfers to other regions (Stewart et al., 2001; Boroojerdi et al., 2002; Antal et al., 2004; but see Deblieck et al., 2008; Oliver et al., 2009). Additionally, individual resting motor thresholds are typically very variable, depending on factors such as posture (Ackermann et al., 1991), mental activity (Izumi et al., 1995; Abbruzzese et al., 1996), or variations in sensory input (Leon-Sarmiento et al., 2005). For these reasons, in studies investigating processes outside the motor system, fixed intensities across participants are often preferred, in order to minimize this type of variability (Sack et al., 2007; Ruff et al., 2008; Blankenburg et al., 2010). Accordingly, in the studies presented in this dissertation we also opted to employ fixed TMS intensities across participants.

However, it should be reinforced that even with a constant TMS intensity different effects might be elicited depending on the current state of the network. Indeed, the same intensity that is thought to be ineffective in one situation might prove to have an effect in a different setting (e.g. resting vs. active motor threshold). In terms of hemodynamic response, different effects can also be observed in remote brain areas and in the stimulated region in response to the same TMS intensity. Specifically, it has been shown that TMS over the motor cortex at intensities below the rMT can result in activations in remote functionally connected areas of the brain, without eliciting an increase in activations under the stimulated area (Bestmann et al., 2003b, 2004; Hanakawa et al., 2009). On the other hand, TMS above rMT induced activation increases in both stimulated and distant interconnected brain areas (Bestmann et al., 2003b, 2004; Hanakawa et al., 2009). This can be

further complicated by interactions between different parameters that can be manipulated in a TMS protocol (e.g. frequency, intensity, train length). Consequently, in order to allow for more informed interpretations in concurrent TMS-fMRI studies more research on the relationship between different combinations of TMS parameters and their ensuing hemodynamic response is necessary. Moreover, a better understanding of the underlying neural mechanisms of TMS is likewise required. In the following section some of the current knowledge about these topics will be presented.

1.3.2 What are we actually measuring?

TMS is based on the principles of electromagnetic induction. By applying a brief pulse of current through a stimulation coil held on the subject's scalp, a time-varying magnetic field perpendicular to the current is produced. In turn, this magnetic field induces an electrical current in the brain. If the right stimulation parameters are used, the induced current will depolarize cortical neurons and generate action potentials (Cowey, 2005).

Despite its extensive application in neuroscience, the exact mechanisms under which TMS exerts its effects on cortical circuits remain, however, largely unknown. In humans, most of the knowledge comes from research on the motor system, partially because TMS effects on the motor cortex can be directly measured as motor evoked potentials (MEPs) in the targeted muscle. As an example, in a series of studies based on recordings from epidural electrodes implanted in the spinal tract, Di Lazarro and colleagues (for a review see Di Lazzaro et al., 2012) showed that the effects of TMS on the descending volleys depend on the intensity used for stimulation. Indeed, at low intensities and with the appropriate coil orientation TMS evoked a single wave, termed I-wave (I = indirect), which is thought to originate from the activation of monosynaptic cortico-cortical connections projecting onto corticospinal neurons. With increasing intensity the descending volleys became more and more complex, showing multiple subsequent volleys (late I-waves). Yet, when a certain intensity level was reached an early volley was observed prior to the first I-wave. This volley, termed D-wave, is believed to reflect the direct excitation of axons from pyramidal tract neurons and, under appropriate conditions, can be apparent even at MEP threshold intensity.

Pharmacological experiments have provided additional characterization of the physiology of motor measures elicited by TMS (for a review see Ziemann, 2004). For instance, it has been shown that late I-waves, as opposed to the first I-wave, are sensitive to several pharmacological manipulations. These changes in MEPs are likely to reflect synaptic excitability and can occur even without alterations in the motor threshold, indicating that these two measures are related to different physiological processes. Indeed, the use of drugs that block voltage-gated sodium channels, which are essential in the regulation of axon excitability, resulted in increased motor thresholds, thereby suggesting that this measure actually reflects axon excitability.

Outside the motor system, animal studies have provided significant contributions to the understanding of how TMS affects neurophysiological mechanisms in the stimulated area and how local effects are propagated to remote areas of the brain (Moliadze et al., 2003, 2005; Aydin-Abidin et al., 2006; Allen et al., 2007; de Labra et al., 2007). For instance, using extracellular single-units recordings in the primary visual cortex of anaesthetised cats, Moliadze et al. (2003) showed that

single TMS pulses over the occipital cortex elicited excitatory activity that was followed by inhibitory neuronal processes lasting up to a few seconds. Furthermore, higher TMS intensities additionally elicited an early suppression of activity that preceded this initial facilitation, which the authors interpreted as being the result of activating local inhibitory circuits. In another study using the same animal model, de Labra et al. (2007) investigated the cortical influences on thalamic responses by applying TMS at two different frequencies over the visual cortex. They showed that independently of TMS frequency parameters, TMS to visual cortex inhibited cells of the dorsal lateral geniculate nucleus (LGN) by specifically decreasing the sustained component of the response. Still, in the concurrent combination with fMRI this matter is further complicated by the difficulty of translating these neural effects into hemodynamic signals (Ekstrom, 2010). For example, depending on which area of the brain is considered, BOLD decreases have been associated with both decreases and increases in neural activity (Shmuel et al., 2006; Schridde et al., 2008). In a recent study, Allen et al. (2007) provided an integrated view on the effects of TMS by combining electrophysiological and hemodynamic recordings during the application of short bursts of TMS over the visual cortex of anaesthetized cats. Their results showed long lasting neural and hemodynamic TMS effects that depended on the current state of the stimulated region and covaried with the duration and frequency parameters of TMS stimulation. Critically, TMS-induced neural effects were tightly coupled with corresponding hemodynamic changes, which is of particular relevance for understanding TMS effects in concurrent TMS-fMRI studies.

Further evidence comes from animal studies that applied microstimulation during fMRI and showed that the BOLD effects of microstimulation can spread beyond the stimulated area (Tolias et al., 2005; Sultan et al., 2007; Ekstrom et al., 2008). In particular, Logothetis et al. (2010) combined microstimulation, neurophysiology, microinjection and fMRI to investigate the effects of electric stimulation on cortical signal propagation. Electric stimulation of the LGN in monkeys reduced BOLD responses in its projection regions in the visual cortex. These effects were strongly contingent on the employed stimulation frequency. In fact, high frequencies elicited positive responses in areas connected monosynaptically to the LGN (i.e. primary visual cortex), whereas extrastriate visual areas continued to show negative responses. Intracortical recordings in V1 revealed that these effects at the BOLD level were paralleled by a short excitatory response that was followed by a pronounced and long-lasting inhibition. Thus, the authors proposed that the deactivation of extrastriate cortex might result from synaptic inhibition of V1 projection neurons. To further test this hypothesis they injected GABA antagonists in V1, which resulted in a reversal of the activation pattern in extrastriate visual cortex, thereby providing additional evidence for their premise. Altogether, their results are important as they emphasize how local neural circuitry can have an impact on the propagation of externally induced stimulation.

In conclusion, these studies have provided invaluable evidence about the underlying neural mechanisms of externally induced stimulation and their relation with hemodynamic signals. Nonetheless, they also demonstrate that interpretations about TMS-evoked effects as measured with fMRI are not straightforward and should be made with some caution.

1.3.3 Previous studies using concurrent TMS-fMRI

Early investigations with concurrent TMS-fMRI applied TMS over the primary motor cortex to examine how TMS affected neural activity at the BOLD level (Bohning et al., 2000, 2003c; Bestmann et al., 2003b, 2005; Denslow et al., 2005b). Importantly, this early studies focused on the effects of different TMS protocols on hemodynamic responses and revealed that TMS can have a distributed impact on BOLD activations that depends on the state of the network. Since then, the field has moved beyond the motor system and applied this methodology to causally map sensory and cognitive brain networks, which will be the main focus of this section.

Most of the studies applying concurrent TMS-fMRI outside the motor cortex focused on the visual system and in particular on how TMS can influence top-down modulations in visual cortices. In fact, in a series of studies, Ruff and colleagues set out to test whether TMS effects differ across distinct regions of the dorsal attentional network (Ruff et al., 2006, 2008, 2009). Specifically, the authors examined how applying bursts of 5 pulses of TMS (9 Hz) at either the left of right frontal eye fields (FEF) or intraparietal sulci (IPS) influenced processing in retinotopic visual areas in dependence of the current visual input. Participants were instructed to passively fixate the centre of the screen while TMS was applied during rest or during the presentation of moving and flickering visual stimuli. Regardless of the presence or absence of visual input, TMS at the right FEF induced an increase in activations in regions of early visual cortex (V1 to V4) representing the peripheral visual field, while decreasing BOLD signal for representations of the central visual field. Moreover, these effects at the neural level were accompanied by a selective improvement of the perceived contrast for peripheral visual stimuli, as revealed by an additional psychophysical experiment. On the other hand, left FEF-TMS effects were restricted to representations of the central visual field, for which similar activation decreases were observed. Interestingly, and contrasting results from the stimulation of frontal areas, right IPS-TMS effects depended strongly on bottom-up visual stimulation. In fact, high vs. low right IPS-TMS positively affected early visual areas only in the absence of visual stimulation, while it decreased activation in V5/MT+ exclusively during the presentation of moving visual stimuli. Conversely, TMS over the left IPS did not produce any observable effects. Overall, these findings underline how frontal and parietal regions can modulate activation in visual cortices in qualitatively distinct ways. Moreover, they also provide evidence for a right-lateralized dominance of frontoparietal influences upon visual areas.

Going one step further, Blankenburg et al. (2010) used concurrent TMS-fMRI to investigate how top-down modulations of the right posterior parietal cortex (PPC) on visual areas depended on the current attentional state. Participants were presented with a bilateral visual display and performed a spatial attention task involving sustained covert attention to either the left or right visual hemifield. As expected, attending to the left vs. the right resulted in activations in the right visual cortex and vice-versa for the opposite comparison. Interestingly, however, applying high vs. low intensity TMS to the PPC simultaneously with the visual display increased this differential effect in the fusiform gyrus. Critically, the bottom-up visual input and response requirements were kept constant across conditions, implying that these attentional-state-dependent TMS effects on visual areas were modulated in a purely top-down manner. Hence, these results reveal that parietal TMS effects on

visual areas depend not only on the level of bottom-up visual input but also on the cognitive state of the stimulated area.

The previous studies used concurrent TMS-fMRI to investigate remote physiological influences that were independent of any behavioural consequences of TMS. Conversely, Sack et al. (2007) were the first who explicitly evaluated whether TMS-induced impairments on a visuospatial task were explained solely by local brain activity changes underneath the stimulated area or were rather paralleled by a more widespread perturbation of task-related activity. Participants were presented with identical images of an analogue clock and performed an angle or a control colour discrimination task while TMS was applied over the left or the right IPS. Behavioural impairments were specific to the visuospatial task during right IPS-TMS and correlated with a decrease in activation in a right lateralized network of frontoparietal areas. Hence, these findings suggest that the ensuing neural effects actually contributed to the observed behavioural impairments. However, as the authors point out themselves, these interpretations should be taken with care as these remote neural effects might have alternatively resulted from the perturbed behaviour instead of being its cause.

Contrasting the considerable amount of studies stimulating over the parietal cortex in the investigation of visuospatial processing, the number of concurrent TMS-fMRI studies targeting the occipital cortex directly is very scarce. To the best of our knowledge, Caparelli et al. (2010) were the only applying occipital TMS inside the scanner. This study applied this methodology to investigate mechanisms of phosphene perception. However, the relevance of this study is mitigated by several methodological limitations and will hence not be considered further.

Outside the visual domain, the number of studies is also quite limited. In one example, Blankenburg et al. (2008) used concurrent TMS-fMRI to examine interhemispheric effects of parietal TMS on somatosensory responses. By manipulating the presence of right-wrist median nerve stimulation, which provides input to the left primary somatosensory cortex (SI), the authors showed that high vs. low TMS to the right parietal cortex increased BOLD activity in the left SI during right-wrist stimulation, whereas decreases were induced in the same area in the absence of somatosensory input. In a follow-up TMS experiment outside the scanner these results were paralleled by an enhancement of somatosensory detection on the ipsi-lateral right hand. As speculated by a previous offline TMS study showing identical behavioural results (Seyal et al., 1995), these effects might reflect interhemispheric corticothalamic interactions. Indeed, the bilateral thalami exhibited a similar activation pattern as the left SI, suggesting that these facilitatory effects during the presence of somatosensory input may involve thalamic circuitry.

Taken together, the studies reviewed here show that TMS can have effects in remote interconnected areas of the brain and that these remote influences might be related to TMS-induced changes in behaviour. On the other hand, these findings also demonstrate that TMS effects in remote areas are state-dependent in the sense that they may differ according to current sensory and cognitive contexts. In conclusion, concurrent TMS-fMRI has proven to be a useful tool in the understanding of the dynamic interconnected brain.

1.4 Organization of the current work

In order to appropriately interact with the environment the brain needs to flexibly adapt to constantly changing circumstances. Accumulating evidence suggests that this flexibility arises from the collaborative interplay between distributed and interconnected brain regions that dynamically change their functional connectivity patterns in order to accommodate a wide diversity of different task demands (Meehan and Bressler, 2012; Cole et al., 2013). The dynamic nature of these interactions is noticeably apparent in the intraparietal sulcus (IPS), a region that has been associated with a number of different cognitive functions such as top-down attentional control, multisensory integration, perceptual decisions, coordination of visuomotor actions and numerical cognition, to name a few. By allowing the monitoring of causal interactions between different brain regions, concurrent TMS-fMRI constitutes a promising tool for studying this interconnected nature of the brain. The present work used this methodology to investigate the underlying neural mechanisms of (audio-) visual processing during different experimental contexts, with a special focus on the causal functional role of the IPS during theses processes.

Specifically, in **Chapter 2** we evaluated the involvement of the IPS in the generation of crossmodal deactivations. Alongside feedforward thalamocortical and direct connectivity between sensory areas, it has been proposed that crossmodal effects on sensory-specific cortices might be mediated by feedback signals from higher order association areas such as the IPS. We explicitly tested this hypothesis by applying repetitive TMS (1.9Hz) at no, low, and high intensity over the right intraparietal sulcus (IPS) and the vertex and by evaluating the ensuing effects on visual and auditory cortices during three different sensory contexts: visual, auditory, and no stimulation.

In **Chapter 3** we investigated how disturbances to IPS activity affected ongoing task-related activations during a demanding visual detection task that involved covert attention to the left visual field. In fact, whether we are able to detect a particular event in our surroundings depends on the interaction between bottom-up sensory information and top-down mechanisms that are driven by our current goals and intentions. In this context, the parietal cortex has been proposed as a source of top-down attentional control in visual areas that not only mediates goal-directed behaviour, but also integrates stimulus-driven information. Moreover, since the detection of sensory stimuli can be additionally influenced by co-occurring task-irrelevant sensory events, we further investigated the effects of different sensory contexts by introducing auditory stimuli as an additional contextual factor across runs. In contrast to the study presented in Chapter 2, in this chapter we adopted a stimulus-locked TMS protocol that consisted of short bursts of four TMS pulses (10 Hz) applied at 100 ms after stimulus onset. This change of protocol was associated with the task and visual stimulation used in the Chapter 3 and is in accordance with TMS protocols that are used in visual detection paradigms (e.g. Chambers et al., 2004; Oliver et al., 2009; Heinen et al., 2011). In fact, instead of a continuous sensory stimulation for a period of 20 seconds as in the study presented in Chapter 2, the task in the Chapter 3 involved the detection of briefly presented visual stimuli. In addition, in recognition of experiences gained from Chapter 2, we abandoned the parametric TMS approach and introduced a new Sham control condition that took advantage of the quadratic decay of the TMS-induced magnetic field.

In the first two chapters we perturbed IPS activity to investigate how this influenced task-related activations and specifically how it modulated top-down activations in low-level sensory areas, in particular in the visual cortex. However, given the recurrent interchange of feedback and feedforward information between these brain structures during perceptual processes (Mumford, 1992; Lamme and Roelfsema, 2000; Rauss and Pourtois, 2013), it is important to evaluate the effects of stimulating low-level sensory areas and to examine in which way these differ from those provoked by stimulation of higher-order association cortices under equivalent circumstances. In order to do so, in **Chapter 4** we extended our experimental design from Chapter 3 by including an additional experimental TMS site over the right occipital cortex. The use of the same experimental design and participants allowed us to assess putative differential effects of each experimental TMS site by independently comparing them with the Sham condition.

Finally, in **Chapter 5** we assessed the causal role of the right IPS during perceptual processes from the perspective of perceptual decision-making. Indeed, the experimental study of visual perception relies on participants' subjective reports, which result from a decision process that selects between possible response options. Numerous neurophysiological and neuroimaging studies have shown that the IPS is consistently recruited during perceptual decisions (Hanks et al., 2006; Churchland et al., 2008; Tosoni et al., 2008; Rorie et al., 2010; Freedman and Assad, 2011; Ploran et al., 2011; Gould et al., 2012; Filimon et al., 2013). By categorizing participants' responses into hits, misses, false alarms and correct rejections, we adapted the experimental design used in Chapter 3 to investigate how disturbances to IPS activity influence the neural systems underlying perceptual decisions.

Chapter 2

Effects of parietal TMS on visual and auditory processing at the primary cortical level – A concurrent TMS-fMRI Study

Joana Leitão[1,3], **Axel Thielscher**[1,2], Sebastian Werner[1], Rolf Pohmann[1,2] and Uta Noppeney[1,2,3]

[1]Cognitive Neuroimaging Group, Max Planck Institute for Biological Cybernetics, Tübingen, Germany

[2]High-field Magnetic Resonance Centre, Max Planck Institute for Biological Cybernetics, Tübingen, Germany

[3]Computational Neuroscience and Cognitive Robotics Centre, University of Birmingham, Birmingham, UK

Published in Cerebral Cortex April 2013;23:873±884; doi:10.1093/cercor/bhs078

This chapter contains the full transcription of the above-mentioned paper, with the exception that table and figure numbering have been changed to adhere with the overall numbering of the dissertation.

Author contributions

Leitão, Thielscher and Noppeney designed the experiment. Stimuli were programmed and designed by Leitão with the support of Werner. Thielscher contributed with TMS expertise. Pohmann programmed the MRI sequence. Data was collected by Leitão. Leitão analysed the data with help of Thielscher and Noppeney. Leitão, Thielscher and Noppeney wrote the manuscript.

Acknowledgments

This work was supported by the Max Planck Society. We thank Mario Kleiner for assistance with Psychtoolbox programming, Mario Moisa for helping with the TMS-fMRI setup, Natalia Zaretskaya for helping with the eye tracker setup, and all members of the Cognitive Neuroimaging Group.

Abstract

Accumulating evidence suggests that multisensory interactions emerge already at the primary cortical level. Specifically, auditory inputs were shown to suppress activations in visual cortices when presented alone but amplify the blood oxygen level-dependent (BOLD) responses to concurrent visual inputs (and vice versa). This concurrent transcranial magnetic stimulation-functional magnetic resonance imaging (TMS-fMRI) study applied repetitive TMS trains at no, low, and high intensity over right intraparietal sulcus (IPS) and vertex to investigate top-down influences on visual and auditory cortices under 3 sensory contexts: visual, auditory, and no stimulation. IPS-TMS increased activations in auditory cortices irrespective of sensory context as a result of direct and nonspecific auditory TMS side effects. In contrast, IPS-TMS modulated activations in the visual cortex in a state-dependent fashion: it deactivated the visual cortex under no and auditory stimulation but amplified the BOLD response to visual stimulation. However, only the response amplification to visual stimulation was selective for IPS-TMS, while the deactivations observed for IPS- and Vertex-TMS resulted from crossmodal deactivations induced by auditory activity to TMS sounds. TMS to IPS may increase the responses in visual (or auditory) cortices to visual (or auditory) stimulation via a gain control mechanism or crossmodal interactions. Collectively, our results demonstrate that understanding TMS effects on (uni)sensory processing requires a multisensory perspective.

Keywords: crossmodal deactivations, interleaved/concurrent TMS-fMRI, multisensory integration, multisensory interactions, right intraparietal sulcus

Introduction

Multisensory integration was traditionally thought to be deferred until later processing stages in higher order association cortices. Recent evidence from neuroanatomy, electrophysiology and functional imaging in humans, nonhuman primates, and other species suggests that sensory inputs interact already at the primary, putatively unisensory, cortical level (Macaluso and Driver 2005; Schroeder and Foxe 2005; Ghazanfar and Schroeder 2006). Specifically, in human functional imaging studies, the effect of inputs from the nonpreferred sensory modality on activations in primary sensory cortices depends on the presence or absence of concurrent sensory inputs from the preferred modality (Laurienti et al. 2002; Johnson and Zatorre 2005). For instance, auditory inputs suppressed activations in visual cortices when presented alone but amplified the blood oxygen level-dependent (BOLD) response to concurrent visual inputs (and vice versa). In other words, competitive interactions (= crossmodal deactivations) between sensory cortices for unisensory stimulation mutated into cooperative interactions (= superadditive response enhancement) for multisensory stimulation (Werner and Noppeney 2010a, 2011).

The neural mechanisms that mediate these ‘‘inhibitory’’ and ‘‘excitatory’’ audiovisual interactions at the primary cortical level are currently unclear. Several functional architectures have been proposed such as feedforward thalamocortical, direct connectivity between sensory areas, and feedback from higher order association areas such as the intraparietal sulcus (IPS) or the superior temporal sulcus (Calvert 2001; Schroeder et al. 2003; Beauchamp et al. 2004; Hackett et al. 2007; Driver and Noesselt 2008; Sadaghiani et al. 2009). Recent electroencephalography and transcranial magnetic stimulation (TMS) studies have supported thalamocortical and direct mechanisms by demonstrating multisensory interactions at less than 100 ms poststimulus (Foxe et al. 2000; Molholm et al. 2002; Murray et al. 2005; Romei et al. 2007; Cappe et al. 2010; Raij et al. 2010). Yet, given the sluggishness of the BOLD response, functional magnetic resonance imaging (fMRI) activations in primary sensory cortices may reflect a compound of early and late interactions. Indeed, a recent study combining fMRI and effective connectivity analyses (i.e., dynamic causal modeling) suggested that low-level audiovisual interactions may be mediated by both direct/thalamocortical influences and top-down effects from higher order association areas (Werner and Noppeney 2010a). From a cognitive perspective, these top-down effects may also reflect crossmodal modulation of attentional resources (Shomstein and Yantis 2004; Johnson and Zatorre 2005, 2006; Werner and Noppeney 2011). Thus, the IPS with its connectivity to visual or auditory cortices (Hyvarinen 1982; Maunsell and van Essen 1983; Boussaoud et al. 1990; Lewis and Van Essen 2000a) has been implicated in crossmodal attentional selection and switching (Macaluso et al. 2000; Rushworth et al. 2001; Yantis et al. 2002; Macaluso, Eimer, et al. 2003; Pessoa et al. 2009; Santangelo et al. 2009).

Concurrent (or interleaved) TMS-fMRI provides an alternative, technically challenging, causal interventional approach to study the effect that one region exerts over another brain area. Focusing on motor, sensory, and higher order cognitive processing, a number of recent studies have

demonstrated an effect of TMS not only on the directly stimulated brain area but also on remote interconnected regions (Baudewig et al. 2001; Sack et al. 2007; Bestmann et al. 2008; Blankenburg et al. 2008; Ruff et al. 2008; 2009; Blankenburg et al. 2010). For instance, application of TMS to right but not left IPS induced functional changes in a widespread right hemispheric frontoparietal system and concurrent impairments of visuospatial processing (Sack et al. 2007). More relevant for the aim of the current study, IPS-TMS has also been shown to influence activations in visual and somatosensory cortices in a state-dependent fashion. Even though IPS-TMS increased activation in both visual and somatosensory cortices, this response amplification was observed in different contexts. In the primary visual cortices, IPS-TMS increased activations only in the absence of visual stimulation; it did not influence responses to visual stimulation (Ruff et al. 2008). In contrast, in the somatosensory cortices, IPS-TMS suppressed activations in the absence of somatosensory stimulation yet amplified the response to somatosensory stimuli (Blankenburg et al. 2008). These are surprising and puzzling results. They raise the question whether IPS may influence sensory processing from different modalities in fundamentally different ways.

This study pursued several aims: First, we investigated the influence of IPS-TMS on visual and auditory processing in the same experimental setting and subjects using a random effects approach. This is essential because studies have previously often included only very few subjects, so that differences between somatosensory and visual studies may not necessarily reflect differences between sensory systems but simply result from intersubject variability. Second, we investigated and interpreted the TMS effects not only from the classical unisensory perspective but also within a multisensory framework. Given previous research, we hypothesized that in particular deactivations in sensory cortices may be mediated via crossmodal mechanisms. To address these questions, we investigated the role of top-down influences from the right IPS on the activation profile in the visual and auditory cortices under 3 sensory contexts: visual, auditory, and no stimulation. To control for nonspecific TMS effects, we applied trains of repetitive TMS (rTMS; 1.9 Hz for 20 s) at no, low, and high intensity over right IPS and vertex. We hypothesized that high (vs. low and no) TMS to right IPS would alter the BOLD responses to sensory signals and the activation level in the absence of stimulation in both visual and auditory cortices as our a priori regions of interest.

Materials and Methods

Participants

Twenty participants (7 males; mean age: 25.2 years; standard deviation [SD]: 2.5; 2 left handed) with no history of neurological or psychiatric illness took part in this concurrent TMS-fMRI experiment. Participants had normal or corrected-to-normal vision and reported normal hearing. All participants gave informed consent prior to participation, and the study was approved by the Human Research Ethics Committee of the Medical Faculty at the University of Tübingen.

Experimental Design

The 3 x 3 x 2 factorial design manipulated: 1) sensory context (visual [V], auditory [A], and fixation [Fix]), 2) TMS stimulation intensity (no TMS, low TMS, and high TMS), and 3) TMS location (right IPS and vertex). TMS was applied at no, low, or high intensity either to right IPS or to vertex as a control site. Hence, as shown in Figure 2.1, the experimental design included 9 conditions for each TMS site amounting to 18 conditions in total.

This design enabled us to investigate the effect of IPS-TMS on auditory (or visual)-evoked activations in auditory (or visual) cortices. Moreover, from the multisensory perspective, we were able to investigate how IPS-TMS affects crossmodal deactivations such as auditory (or visual)-evoked deactivations in visual (or auditory) cortices.

Participants were presented with blocks of fixation, auditory, and visual stimulation (block duration: 20 s; Fig. 2.1). They fixated a white fixation cross presented throughout the entire run in the center of the screen. To maintain participants' attention, they responded to rare auditory (a brief beep, frequency: 700 Hz, duration: 300 ms) and visual (a red fixation cross, duration: 300 ms) targets, which were presented in auditory and visual blocks, respectively.

Because of the static magnetic field of the MR scanner, the amplitude of the TMS clicks was amplified to 87.1 dB (low TMS intensity) and 97.3 dB (high TMS intensity). To attenuate these differences in auditory stimulation for low and high TMS intensity, we used dampening headphones and created pseudo-TMS clicks by recording the auditory click produced by a TMS pulse. Pseudo-TMS clicks were presented at 1.9 Hz (= frequency of rTMS stimulation) throughout the entire experiment, that is, in auditory, visual, fixation, and baseline blocks. In the TMS blocks, pseudo-clicks and TMS pulses were synchronized. Simultaneous recording of pseudo-clicks and real TMS pulses confirmed the perfect synchronization of the pseudo-TMS clicks and TMS pulses. Despite all these efforts, the auditory side effects were not completely equated for high and low TMS conditions most likely also because of additional bone conduction.

The activation blocks of 20 s alternated with 20 s baseline periods (Fig. 2.1B). We manipulated TMS intensity and the sensory stimulation context over blocks and the TMS location across sessions. The sequence of conditions was pseudo-randomized and counterbalanced within and across participants.

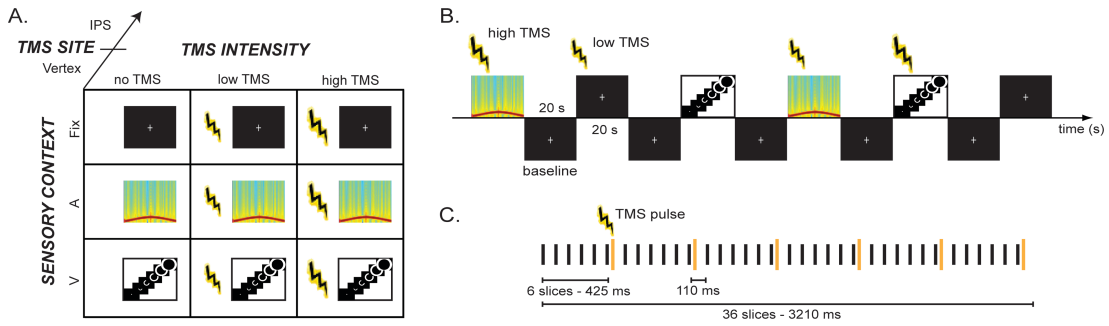

Figure 2.1. Experimental procedure. **(A)** 3 x 3 x 2 factorial design manipulating: 1) sensory context (visual [V, expanding-contracting ring], auditory [A, frequency modulated pure tone as illustrated by time-frequency spectrogram], and fixation [Fix]), 2) TMS stimulation intensity (no TMS, low TMS, and high TMS), and 3) TMS location (right IPS and vertex). **(B)** Example and timing of 20 s activation blocks that were interleaved with 20 s baseline periods (stimuli for illustrational purposes only). **(C)** Illustration of the concurrent TMS-fMRI protocol for one scan. 1.9 Hz rTMS was applied by delivering a TMS pulse 10 ms after every sixth slice followed by a gap of 100 ms.

There were 5 runs per TMS stimulation location, each run included 2 blocks of each condition amounting to a total of 10 blocks per condition. In each run, 6 of the 24 condition blocks contained targets, amounting to a total of 3 visual and 3 auditory targets per run.

Stimuli and Stimuli Presentation

The visual stimulus consisted of a periodically expanding and contracting white ring (diameter minimum: 1.7°, maximum: 17.5° visual angle; width minimum: 0°, maximum: 2.95° visual angle; length of temporal period: 600 ms) presented on a black background with a white fixation cross in the center of the ring. The visual stimulus was presented continuously in blocks of 20 s.

The auditory stimulus was created with Adobe Audition 2.0 by modulating a sinusoidal tone using the pitch bender function. This created an auditory stimulus that was basically equivalent to a sinusoidally frequency modulated pure tone with a carrier frequency (fc) of 375 Hz and a modulation frequency ($f_{auditory}$) of 2.35 Hz. The maximum frequency deviation, Df, equaled 225 Hz. The duration of each brief auditory stimulus was 425 ms. Thirty-six auditory stimuli were sequentially presented with an interstimulus interval of 110 ms in blocks of 20 s.

Visual and auditory stimuli were presented separately using Psychophysics Toolbox version 3 (Brainard 1997; Kleiner et al. 2007) running on MATLAB 7.5 (MathWorks Inc., MA, USA) and a Macintosh laptop running OS-X 10.5.6 (Apple Inc., CA, USA). The visual stimulus was back projected onto a frosted Plexiglas screen using a LCD projector (JVC Ltd., Yokohama, Japan) visible to the participant through a mirror mounted on the MR head coil. Auditory stimuli were presented via the Siemens pneumatic system, where the standard pneumatic headphones were replaced by E-A-RLINK 3A 420-2005 insert earphones (EST! Medizintechnik AG, Reutlingen, Germany) and dampening headphones (3M Occupational Health & Environmental Safety, MN, USA) used to reduce the clicking sound produced by the TMS pulses. Note that both the insert earphones and the dampening headphones are made out of plastic and hence cannot have interfered with the fMRI signal. In addition to this passive dampening strategy, the effects of the auditory TMS

clicks were reduced by camouflaging them with the pseudoclicks. Subjects indicated their responses (i.e., target detection task) using a MR-compatible custom-built button device connected to the stimulus computer.

TMS Stimulation Sites

TMS was applied over right IPS as experimental and vertex as a control site. For IPS-TMS, we adopted the Talairach coordinates (x = 38, y = –44, z = 46) as a published activation peak for multisensory motion (Bremmer et al. 2001). Bremmer et al. (2001) identified this region as being commonly activated by visual, auditory, and tactile motion. Since our stimuli also elicited the impression of looming versus receding motion, this multisensory motion area seemed ideal for the purposes of this study. However, please note that these coordinates are close to those reported in numerous studies investigating audiovisual integration (Bushara et al. 1999; Corbetta et al. 2000; Lewis et al. 2000; Calvert 2001; Werner and Noppeney 2011). Furthermore, since these coordinates were also very close to the IPS-TMS location in Ruff et al. (2008), they also enabled a comparison across the 2 studies.

The structural scans of each individual were normalized into Montreal Neurological Institute (MNI) space using unified segmentation. After transforming the Talairach coordinates from Bremmer et al. (2001) into MNI space, individual IPS scalp locations were determined by inverse transforming the new MNI coordinates into native space using the parameters obtained from spatial normalization and computing the intersection between the skull and a perpendicular vector through those coordinates. A posteriori reconstruction of the coil position (for methodological details, see Data Acquisition and TMS Procedures) enabled the calculation of the mean coordinates for TMS stimulation. This showed that, across participants, the target IPS coordinates were obtained with a mean deviance of 5.25 mm ± 3.88 (mean, SD), which is considered to be an acceptable value, in comparison to the spatial accuracy obtained when positioning TMS outside the scanner (Schonfeldt-Lecuona et al. 2005).

For Vertex-TMS, the MNI coordinates were determined individually as the highest point of the skull located medially between both hemispheres using a Neuronavigation System (BrainView, Frauenhofer IPA, Stuttgart, Germany). A posteriori reconstruction of the coil position (for methodological details, see Data Acquisition and TMS Procedures) enabled the calculation of the mean coordinates for vertex stimulation across subjects (x = 2 mm ± 3.56 [mean, SD], y = –32.5 mm ± 7 [mean, SD], z = 85 mm ± 4.4 [mean, SD]). Note that both y- and z-coordinates will depend on individual skull geometries. A posteriori reconstruction of the coil position also allowed us to verify that the individual vertex locations were always anterior to or at (in 4 subjects) the intersection of the postcentral gyri from both hemispheres. Thus, our vertex stimulation site is a well-suited control condition, since it is expected to induce comparable somatosensory and auditory side effects without influencing visual or auditory processing directly (Ruff et al. 2006: Supplementary Material).

Data Acquisition and TMS Procedures

A 3-T TIM Trio System (Siemens, Erlangen, Germany) was used to acquire both high-resolution structural images (176 sagittal slices, time repetition [TR] = 2300 ms, time echo [TE] = 2.98 ms,

time to inversion [TI] = 1100 ms, flip angle = 9°, field of view [FOV] = 240 mm x 256 mm, image matrix = 240x256, voxel size = 1 mm x 1 mm x 1 mm) and T2*- weighted axial echoplanar images (EPIs) with BOLD contrast (gradient echo [GE]-EPI, Cartesian k-space sampling, TR = 3210 ms, TE = 40 ms, flip angle = 90°, FOV = 192 mm x 192 mm, image matrix 64x64, 36 slices acquired sequentially in ascending direction, 3 mm x 3 mm x 3 mm voxels, slice thickness 2.6 mm, interslice gap 0.4 mm). A total of 298 volume images were acquired for each run.

After each EPI run, a fast structural image (fast low-angle shot [FLASH], 100 slices, 128x128 matrix, voxel size = 2x2x3 mm, TR = 452 ms, TE = 2.46 ms) was acquired to enable a posteriori reconstruction of the TMS coil position inside the scanner. The TMS coil was marked with water tubes to enable the automatic coregistration of the coil representation in the FLASH images with a pre-acquired reference image of the coil. In addition, the subject's head in the FLASH images was coregistered to the high-resolution structural scan. Thereby, we were able to determine the coil position inside the scanner with respect to an individual's structural MRI that was also used for neuronavigation.

The EPI sequence was adapted for concurrent TMS-fMRI experiments by introducing gaps of 110 ms after every 425 ms in the GE-EPI sequence. Each gap was introduced to allow the delivery of one TMS pulse 10 ms after each sixth slice acquisition without interference with image quality (Bestmann et al. 2003). Hence, rTMS was applied at 1.9 Hz, that is, every 535 ms (Fig. 2.1C), using the same coil-holding device as in Moisa et al. (2009). This TMS protocol was employed for 3 reasons. First, a repetition rate of about 2Hz has previously been shown to induce reliable excitation but only moderate after effects, rendering them ideal for online studies (Arai et al. 2005). Second, the continuous rhythmic TMS pattern lend itself to masking procedures with pseudo-TMS clicks and constant auditory input throughout the entire block. Third, blocks of 2 Hz stimulation have previously been shown to induce significant and constant brain activation throughout the entire duration of the block in a previous concurrent TMS-fMRI experiment (Moisa et al. 2010).

Biphasic stimuli were delivered using a MagPro X100 stimulator (MagVenture, Denmark) and a MR-compatible figure of eight TMS coil (MRi-B88). Unlike TMS over motor and visual cortices, it is not possible to perform a direct measurement (like motor-evoked potentials or phosphenes) of the TMS effects during IPS stimulation. Therefore, one standard approach is to calibrate the intensity of IPS-TMS based on an individual's resting motor threshold. Yet, the existence of a correlation between TMS thresholds for different cortical structures is controversially discussed (Stewart et al. 2001; Boroojerdi et al. 2002; Antal et al. 2004; but see Deblieck et al. 2008; Oliver et al. 2009). Furthermore, individual resting motor thresholds are typically very variable, depending on factors such as posture (Ackermann et al. 1991), mental activity (Izumi et al. 1995; Abbruzzese et al. 1996), or variations in sensory input (Leon-Sarmiento et al. 2005). To minimize the variance of the IPS-TMS effects, we applied TMS at 3 intensities consistently across all subjects. Based on a previous study performed with this coil in this lab, the mean resting motor threshold for this coil was estimated as 55% of the total stimulator output (M Moisa, personal communication). Hence, low and high TMS intensities were set consistently for all participants to 60% and 120% of the mean resting motor threshold for the used coil. This corresponded to 33% (low TMS) and 66% (high TMS) of the total stimulator output. For the no TMS condition, the stimulator output was set to 0%.

Motivated by the experimental choices made in previous studies, low intensity TMS blocks were introduced as an additional control condition that is thought to induce similar side effects as high intensity TMS in the absence of specific TMS effects (Ruff et al. 2006; Blankenburg et al. 2010). However, our study clearly demonstrates that high TMS induces significantly stronger auditory activations as nonspecific TMS side effects than low TMS. This was the case despite additional masking procedures that were not even employed in previous studies. These findings suggest that low TMS cannot adequately control for nonspecific TMS side effects. Importantly, because of the brain's multisensory organization, the nonspecific TMS-induced auditory activations can have an effect in both auditory and other sensory cortices, thereby rendering the interpretation of TMS effects difficult not only in auditory but in all sensory systems.

Conversely, it is difficult to prove that low TMS to IPS does not induce any direct IPS stimulation. In support of subthreshold noneffective IPS stimulation, we observed no significant state-dependent effects for low TMS in our region of interest, when using the statistical thresholds generally applied in this study. In other words, at this threshold of significance, no interactions were revealed between low > no TMS intensity and visual > auditory stimulation ($[V > A]_{\text{low IPS-TMS}} > [V > A]_{\text{no IPS-TMS}}$) when imposing the additional constraint of ($[V > A]_{\text{low IPS-TMS}} > [V > A]_{\text{low Vertex-TMS}}$). Likewise, the interactions between low > no TMS intensity with 1) visual > fixation or 2) fixation > auditory stimulation were not significant. Nevertheless, classical statistics is in principle not able to prove the absence of an effect. Indeed, at a low uncorrected level of significance ($p < 0.05$, $z = 2.3$), we observed an effect in the calcarine sulcus for ($[V > A]_{\text{low IPS-TMS}} > [V > A]_{\text{no IPS-TMS}}$). It is therefore conceivable that low intensity TMS may induce very small and unreliable (i.e., variable) suprathreshold effects in IPS depending on the prior activity level of IPS. For instance, subthreshold TMS stimulation of IPS may turn into suprathreshold TMS under auditory or visual stimulation. While our data provide no strong evidence for this mechanism, it is premature to completely ignore these effects.

Given these critical considerations about the putative direct and indirect effects of low intensity TMS, we will identify main- and state-dependent TMS effects using high TMS > no TMS as our main contrast and high TMS > low TMS as an additional statistical constraint at a lower threshold of significance using the inclusive masking option.

Extensive image quality tests of our setup (see previous reports: Moisa et al. 2009; Moisa et al. 2010: Supplementary Material) revealed only negligible TMS artifacts on the EPI images. Specifically, these tests scanned for radiofrequency noise induced by the TMS setup, compared the signal-to-fluctuation-noise ratios with and without TMS, quantified the amount of signal dropout and distortions in the EPI images, and validated the effectiveness of the methods to suppress TMS-induced leakage currents. Furthermore, in the current study, we acquired EPI data with a phantom under different sensory stimulation conditions and TMS stimulation intensities. Comparing each ''activation condition'' against baseline (height threshold: $p < 0.001$ uncorrected) yielded only nonsignificant and randomly distributed activation patterns.

fMRI Data Analysis: Preprocessing

The fMRI data were analyzed using SPM8 (Wellcome Department of Imaging Neuroscience, London; www.fil.ion.ucl.ac.uk/spm) (Friston et al. 1995). Scans from each subject were realigned using the first as a reference, unwarped, spatially normalized into MNI space, resampled to a spatial resolution of 2x2x2 mm^3, and spatially smoothed with a Gaussian kernel of 8 mm full-width at half-maximum. The time series of all voxels were high-pass filtered to 1/128 Hz. The first 3 volumes were discarded to allow for T1-equilibration effects.

fMRI Data Analysis: Modeling and Statistics

The fMRI experiment was modeled using regressors obtained by convolving each activation block with a canonical hemodynamic response function (HRF; n.b., an additional analysis including the canonical HRF and the temporal derivative as 2 basis functions yielded basically equivalent results). In addition to modeling the 9 conditions in our 3x3x3 factorial design separately for each IPS-TMS and Vertex-TMS session, the statistical model included the 6 visual and auditory target blocks and their respective target onsets (after convolving each event-related unit impulse with the HRF) to account for potential attentional differences between blocks with and without targets. The reported statistical comparisons were limited to blocks without targets. Nuisance covariates included the realignment parameters to account for residual motion artifacts.

To allow for a random effects analysis and inferences at the population level, the contrast images (each condition > baseline) were entered in a second level ANOVA (Friston et al. 1999). At the second level, we evaluated the following statistical comparisons.

Effect of Sensory Context

Sensory-evoked activations were identified by comparing V (resp. A) > baseline (only no TMS conditions pooled over IPS and vertex). With respect to the deactivations, we were interested only in crossmodal deactivations. In other words, our aim was to identify 1) deactivations induced by auditory stimulation selectively in visual processing areas, that is, areas that are activated by visual stimulation and 2) deactivations induced by visual stimulation selectively in auditory processing areas, that is, areas that are activated by auditory stimulation. Operationally, we hence identified auditory-induced deactivations within the visual activation system by inclusively masking the auditory-induced deactivations (A < baseline) with the visual-induced activations (V > baseline). Conversely, we identified visual-induced deactivations within the auditory activation system by inclusively masking the visual-induced deactivations (V < baseline) with the auditory-induced activations (A > baseline).

Effect of TMS Intensity

The effect of TMS intensity was selectively tested for by comparing high IPS-TMS > no IPS-TMS (pooled across conditions). The effect of TMS intensity can be caused either as a confounding nonspecific side effect of the auditory TMS clicks or via direct ‘‘true’’ TMS effects. To dissociate

the activations mediated by the 2 mechanisms, we have employed the following analysis strategy: first, since nonspecific TMS effects should be common to IPS and vertex stimulation, they were identified by inclusively masking the effect of TMS intensity for IPS-TMS (i.e., high IPS-TMS > no IPS-TMS) with 1) high Vertex-TMS > no Vertex-TMS. Furthermore, since high intensity TMS was also shown to induce more auditory activations than low intensity TMS, we additionally inclusively masked with 2) high Vertex-TMS > low Vertex-TMS intensity.
Second, specific effects of IPS-TMS should, in contrast, be selective for high intensity TMS and the IPS stimulation site. Hence, specific TMS effects were identified by inclusively masking the main effect of IPSTMS with 1) high IPS-TMS > low IPS-TMS and 2) high IPS-TMS > high Vertex-TMS. The application of 2 constraints increases the specificity of our statistical comparison.

Interaction between TMS Effects and Sensory Context: State-Dependent TMS Effect

Primarily, we were interested in state-dependent TMS effects, that is, TMS effects that depend on the sensory stimulation context. Since crossmodal deactivations were identified reliably only for auditory stimulation, we selectively investigated whether the TMS effect on the BOLD signal in visual cortices depended on sensory context. Specifically, we investigated whether TMS to IPS modulates visual induced activations and auditory-induced deactivations in the visual cortex in a different manner.
Given the role of IPS in attentional selection, we hypothesized that IPS-TMS would induce a more effective assignment of attentional resources to the stimulated sensory system and conversely withdraw attentional resources from the nonstimulated sensory system. At the neural level, we therefore expected IPS-TMS to jointly amplify 1) activation decreases in visual cortex during auditory stimulation and 2) activation increases during visual stimulation. Hence, we tested for the interaction between visual versus auditory stimulation and high versus no IPS-TMS intensity ($[V > A]_{\text{high IPS-TMS}} > [V > A]_{\text{no IPS-TMS}}$). To control for nonspecific TMS effects, we imposed 2 additional constraints using inclusive masking with the following contrasts: 1) the interaction between visual versus auditory stimulation and high versus low IPS-TMS intensity ($[V > A]_{\text{high IPS-TMS}} > [V > A]_{\text{low IPS-TMS}}$) and 2) the interaction between visual versus auditory stimulation and high IPS-TMS versus high Vertex-TMS ($[V > A]_{\text{high IPS-TMS}} > [V > A]_{\text{high Vertex-TMS}}$).
To dissociate whether these state-dependent TMS effects reflect TMS effects on visually induced activations or auditory-induced deactivations, we tested separately for interactions between TMS intensity and 1) visual > fixation ($[V > Fix]_{\text{high IPS-TMS}} > [V > Fix]_{\text{no IPS-TMS}}$) or 2) fixation > auditory ($[Fix > A]_{\text{high IPS-TMS}} > [Fix > A]_{\text{no IPS-TMS}}$). For each interaction contrast, we imposed additional constraints (e.g., interaction between V > Fix with 1) high > low TMS and 2) high IPS-TMS > high Vertex-TMS) following the same rationale as described above using inclusive masking.

Search Volume Constraints

The effects were tested for 1) within the entire brain and, based on our a priori hypothesis, 2) in the visual and auditory cortices, and 3) motion area hMT+/V5+ as our regions of interest. All regions of interest were defined using the SPM Anatomy Toolbox (Eickhoff et al. 2005). The anatomical mask

for the entire visual cortex included 6402 voxels within the bilateral cytoarchitectonic maps BA17, BA18, and hOC5; the anatomical mask for the visual motion area hMT+/V5+ included 163 voxels in the bilateral cytoarchitectonic maps hOC5; the anatomical mask for the auditory cortex encompassed 973 voxels in the bilateral cytoarchitectonic maps TE 1.0, TE 1.1, and TE 1.2.

Unless stated otherwise, we report activation at $p < 0.05$ corrected at the voxel level for multiple comparisons (family-wise error rate) based on Gaussian Random Field theory within the entire brain and in our regions of interest. Additional constraints on statistical effects were imposed using inclusive masks thresholded consistently at 0.01 uncorrected.

Results

The data were analyzed in 3 steps. First, we identified stimulus-evoked activations and deactivations in the primary visual and auditory cortices under conditions of no TMS. Second, we tested for the main effect of TMS by directly comparing high and no TMS intensities. Third, we characterized state-dependent effects of TMS in visual cortex by testing for the interaction between sensory context and TMS intensity. The effects were tested for within the entire brain and the visual and auditory cortices as our primary regions of interest.

Effects of Sensory Context

Stimulus-Evoked Activations

To identify stimulus-evoked activations, we compared sensory stimulation relative to baseline in the absence of TMS stimulation. As expected, visual stimulation induced activations in calcarine sulci and bilateral V5/MT+ and auditory stimulation in bilateral superior temporal gyri (Fig. 2.2 and Table 2.1). Visual stimulation also induced significant activations in the right middle frontal gyrus and in the right superior parietal lobule (Table 2.1).

Stimulus-Evoked Deactivations

Deactivations induced by auditory stimulation were identified within the visual activation system by comparing A < baseline masked with V > baseline. As expected, this comparison showed deactivations within the cuneus, specifically the calcarine sulci extending into the lingual gyri (Fig. 2.2B(i) and Table 2.1).

Likewise, deactivations induced by visual stimulation were identified within the auditory activation system by comparing V < baseline masked with A > baseline. At an uncorrected level of significance, this comparison revealed deactivations in Heschls' gyri bilaterally (Fig. 2.2B(ii) and Table 2.1). The deactivations within the auditory system were less pronounced than in the visual system, most likely because the auditory system was continuously driven by pseudo- and true TMS auditory clicks.

Effect of IPS-TMS:
High > No TMS—Specific Direct and Nonspecific Indirect TMS Effects

As expected, high versus no IPS-TMS revealed significant activations in the auditory cortices. This main effect of TMS could reflect either auditory stimulation by the TMS clicks as confounds (=nonspecific indirect TMS effect) or true top-down modulatory effects from TMS-IPS stimulation (=specific direct TMS effects). To dissociate the contributions of these 2 mechanisms to the auditory activations, we imposed additional constraints using the inclusive masking option (see Materials and Methods).

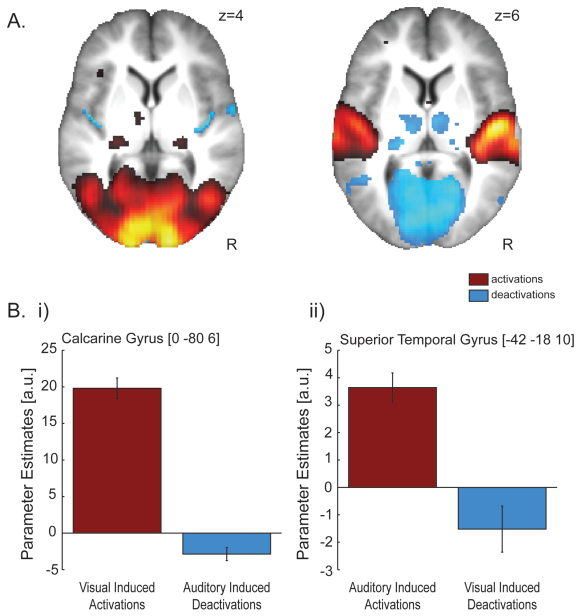

Figure 2.2. Visual- and auditory-induced activations and deactivations during no TMS blocks. **(A)** Visual- (left) and auditory (right)-induced activations (red) and deactivations (blue) are displayed on axial slices of a mean image created by averaging the subjects' normalized structural images. For illustrational purposes only, the effects are displayed at a height threshold of $p < 0.01$ uncorrected. Extent threshold > 0 voxels. Visual (resp. auditory)-induced deactivations are inclusively masked additionally with A>baseline (resp. V>baseline) at $p < 0.01$ uncorrected. **(B)** Parameter estimates (mean ± standard error of the mean, RFX model) for visual and auditory stimulation pooled (i.e., summed) across TMS stimulation locations (IPS and vertex) are displayed for the given coordinates (5activation peak) within the (i) calcarine gyrus and (ii) the superior temporal gyrus. The bar graphs represent the size of the effect in nondimensional units (corresponding to % whole-brain mean).

Specific Direct TMS Effects

True IPS-TMS effects should be selective and enhanced for 1) high > low IPS-TMS and 2) high IPS > high Vertex-TMS. Imposing these 2 additional constraints revealed activations in the left superior temporal gyrus extending into the left rolandic operculum (Fig. 2.3A and Table 2.2). Even though the activations were left lateralized, at a lower threshold of significance ($p < 0.05$ uncorrected), they were also observed in the right hemisphere (Fig. 2.3A). Imposing simultaneously 2 statistical constraints using the inclusive masking option renders our statistical results more specific.

The presence of high IPS-TMS > high Vertex-TMS effects in the auditory cortices of both hemispheres (in the absence of any significant effects for high Vertex-TMS > high IPS-TMS) suggests that they are mediated via top-down effects induced by IPS-TMS rather than being a result of unbalanced auditory TMS inputs to the 2 ears.

Nonspecific Indirect TMS Effects

Nonspecific TMS effects due to auditory confounds should be present for both IPS and vertex stimulation. Hence, they should be revealed when masking the main effect of TMS (i.e., high vs. no IPS-TMS) with 1) high > no Vertex-TMS and 2) high > low Vertex-TMS. Indeed, imposing these additional constraints revealed again significant activations in the left Heschl's gyrus and in the

bilateral superior temporal gyri extending to the rolandic operculi that were partially overlapping with the activations attributed to true TMS effects (Fig. 2.3A and Table 2.2).

Similar activations in auditory cortices were also obtained when masking high IPS-TMS > low IPS-TMS with 1) high > no Vertex-TMS and 2) high > low Vertex-TMS indicating that low TMS does not control for auditory and somatosensory side effects. Hence, from a unisensory perspective, low TMS cannot be considered a good control condition (as previously suggested) to evaluate remote TMS effects on auditory processing or activations within the auditory cortex, even when extensive measures are applied to control for the auditory TMS side effects as in the current study. More importantly, from a multisensory perspective, it does not form a valid control condition for any type of uni- or multisensory experiment, since activations in auditory cortex can have pronounced nonlinear influences on processing in other sensory systems (see Discussion).

Interactions between TMS Intensity and Sensory Context: State-Dependent TMS Effects

To investigate whether IPS-TMS jointly amplified visual-induced activations and auditory-induced deactivations within the occipital cortex, we tested for the interaction between V > A and TMS intensity (high > no TMS). To control for TMS side effects, we imposed 2 additional constraints: a significant interaction 1) between V > A and high > low TMS and 2) between V > A and high IPS >

Table 2.1 Effects of stimulus evoked (de-)activations (pooled over all no TMS conditions)

Brain Regions	*MNI Coordinates (mm)*			*Z Score*	p_{FWE}*-value*
	x	y	z		
Stimulus Evoked Activations					
A > baseline					
Left Superior Temporal Gyrus	-54	-14	2	> 6	< 0.001#
Right Superior Temporal Gyrus	56	-10	0	> 6	< 0.001#
V > baseline					
Left Calcarine Gyrus	-4	-92	-6	> 8	< 0.001*
Left V5+/MT+	-44	-70	2	> 8	< 0.001**
Right V5+/MT+	46	-70	0	> 8	< 0.001**
Right Middle Occipital Gyrus	38	-92	0	> 8	< 0.001*
Right Middle Frontal Gyrus	50	0	54	5.83	< 0.001
Right Superior Parietal Lobule	28	-50	48	5.71	< 0.001
Stimulus Evoked Deactivations					
A < baseline (inclusively masked with V > baseline)					
Calcarine Gyrus	0	-80	6	5.58	< 0.001*
Left Lingual Gyrus	-20	-62	2	5.46	< 0.001*
Left Cuneus	-2	-98	22	4.77	0.002*
V < baseline (inclusively masked with A > baseline)					
Left Insula Lobe	-40	-14	8	4.90	0.016
Left Heschl's Gyrus	-42	-18	10	3.13	0.001 (uncorr)
Right Heschl's Gyrus	48	-10	6	2.71	0.003 (uncorr)

p-values are corrected for multiple comparisons within the entire brain, the visual cortex *, the MT/V5+ **, or the auditory cortex #, see Materials&Methods

high Vertex-TMS (for further details, see Materials and Methods). These interaction contrasts jointly revealed effects in the cuneus that were located in Brodmann area 18 based on cytoarchitectonic probability maps (Fig. 2.3B and Table 2.2). As shown in the parameter estimate plots, IPS-TMS amplifies the activations to visual stimuli and the deactivations to auditory stimuli (Fig. 2.3B). However, the response suppression in the visual cortex during TMS stimulation was comparable for 1) auditory and fixation conditions and 2) IPS- and Vertex-TMS stimulation sites. Indeed, the interactions between A < Fix and 1) TMS intensity or 2) TMS site were not significant.

In contrast, while Vertex-TMS also suppressed activation during visual stimulation, IPS-TMS increased the visual-induced activations relative to fixation as confirmed statistically in a significant interaction between V > Fix and TMS intensity (as well as TMS site) (Table 2.2). Collectively, these results suggest that IPS-TMS selectively enhances the response to visual stimuli in the visual cortex.

Table 2.2. TMS-induced effects

Brain Regions	*MNI Coordinates (mm)*			*Z Score*	*Z Score masking 1)*	*Z Score masking 2)*	p_{FWE}-*value*
	x	y	z				
Effect of TMS intensity							
Non-specific TMS effects on auditory cortex							
High IPS-TMS > no IPS-TMS (inclusively masked with (i) High Vertex-TMS > no Vertex-TMS and (ii) High Vertex-TMS > low Vertex-TMS)							
Left Superior Temporal	-54	-32	20	> 8	7.41	5.10	< 0.001
	-54	-28	10	5.95	3.79	2.51	< 0.001#
Right Superior Temporal	40	-32	14	4.72	2.89	2.41	< 0.001#
	40	-22	2	4.18	2.37	2.92	0.003#
Right Rolandic Operculum	46	-32	20	7.52	6.23	5.83	< 0.001
Left Rolandic Operculum	-36	-32	18	6.22	3.61	2.82	< 0.001#
Left Heschl's Gyrus	-36	-24	6	5.95	4.26	2.73	< 0.001#
Specific TMS effects on auditory cortex							
High IPS-TMS > no IPS-TMS (inclusively masked with (i) High IPS-TMS > low IPS-TMS and (ii) High IPS-TMS > high Vertex-TMS)							
Left Superior Temporal	-54	-32	20	> 7	7.10	3.96	< 0.001
	-54	-4	4	5.12	5.33	2.36	< 0.001#
Left Rolandic Operculum	-58	0	4	6.97	6.70	3.69	< 0.001
	-36	-32	18	6.22	3.52	3.42	< 0.001#
Right Superior Temporal	60	-28	18	6.57	5.48	2.43	< 0.001
Interaction between TMS Effects and Sensory Context							
TMS induced enhancement of activation differences between visual and auditory processing							
[V > A] high IPS-TMS > [V > A] no IPS-TMS (inclusively masked with (i) [V > A] high IPS-TMS > [V > A] low IPS-TMS and (ii) [V > A] high IPS-TMS > [V > A] high Vertex-TMS)							
Right Cuneus	2	-88	26	4.31	2.91	2.49	0.012*
	6	-90	24	4.04	2.34	2.34	0.038*
TMS induced enhancement of visual activations							
[V > Fix] high IPS-TMS > [V > Fix] no IPS-TMS (inclusively masked with (i) [V > Fix] high IPS-TMS > [V > Fix] low IPS-TMS and (ii) [V > Fix] high IPS-TMS > [V > Fix] high Vertex-TMS)							
Right Cuneus	0	-92	24	4.36	4.36	2.42	0.01*
	8	-84	18	4.04	4.05	2.76	0.032*

p-values are corrected for multiple comparisons within the entire brain, the visual cortex *, or the auditory cortex #, see Materials&Methods

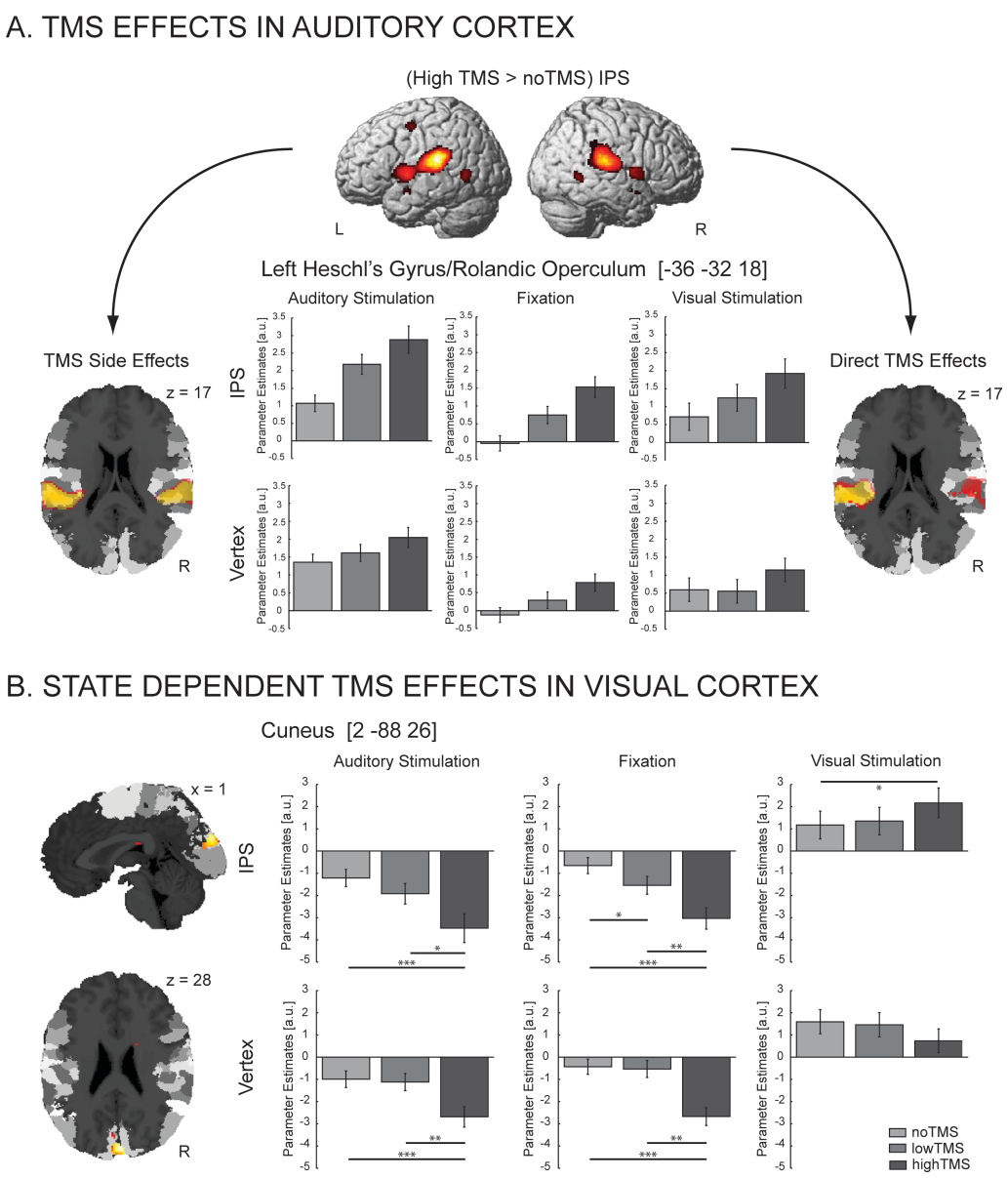

Figure 2.3. (A) (*center top*) Increased activations for high relative to no intensity IPS-TMS pooled (i.e., summed) across sensory stimulation contexts are rendered on a template of the whole brain. Height threshold of $p<0.01$ uncorrected, no extent threshold, for illustrational purposes only. (*center bottom*) Parameter estimates (mean±standard error of the mean, RFX model) for no TMS (light gray), low intensity TMS (medium gray), and high intensity TMS (dark gray) in the cuneus at the given coordinates (i.e., activation peaks) are shown separately for auditory (left), fixation (middle), and visual (right) contexts. The bar graphs represent the size of the effect in nondimensional units (corresponding to % whole-brain mean). (*left bottom*) Nonspecific TMS effects were identified by inclusively masking the effects of high>no IPS-TMS with 1) high>no Vertex-TMS intensity and 2) high>low Vertex-TMS intensity at $p < 0.01$ (yellow) and $p < 0.05$ (red) uncorrected. (*right bottom*) Specific ''true'' TMS effects were identified by inclusively masking the effects of high>no IPS-TMS with 1) high>low IPS-TMS intensity and 2) high IPS-TMS>high Vertex-TMS intensity at $p<0.01$ (yellow) and $p<0.05$ (red) uncorrected. Effects are displayed on axial slices of cytoarchitectonic maps (Eickhoff et al. 2005). **(B)** TMS effects that depend on sensory stimulation context. (*left*) Interactions between TMS intensity and sensory stimulation ($[V>A]_{\text{high IPS-TMS}} > [V>A]_{\text{no IPS-TMS}}$) are displayed on sagittal and axial slices of cytoarchitectonic maps (Eickhoff et al. 2005). Height threshold: $p<0.01$, uncorrected (for illustrational purposes only). Extent threshold > 0 voxels. The effects are inclusively masked

By contrast, the suppressive TMS effects during auditory stimulation and fixation are more likely to be caused by the TMS clicks as side effects that are common to vertex and IPS-TMS sites rather than true neural TMS effects.

Eye Monitoring (Outside the Scanner)

To ensure that the observed activation pattern did not result from eye movements, twitches, and startle effects, a subset of 6 subjects participated in an additional TMS experiment that was performed outside the scanner with identical paradigm and parameters. The TMS stimulation protocol was also identical, except for the TMS intensities that were newly defined as 30% (low TMS) and 60% (high TMS) of total output to account for the absence of the high-current filter that was used in the fMRI experiment to prevent MR images from being affected by RF noise (Moisa et al. 2009). For each subject, data in 2 runs were acquired for each TMS location.

Horizontal and vertical eye movements were recorded using a ViewPoint Eyetracker system (Arrington Research Inc., Scottsdale, AZ, USA) (220 Hz sampling rate). Eye position data were automatically corrected for blinks. For each subject, the mean distance (degrees) from the fixation cross, the number of saccades (defined by eye velocity threshold > 30°/s), and the number of blinks were quantified.

The 3 indices were independently entered into a 3-way repeated measures analysis of variance (RM-ANOVA) with the factors TMS stimulation location (right IPS and vertex), TMS intensity (no TMS, low TMS, and high TMS), and sensory modality (A, V, and Fix). None of the 3 RM-ANOVAs revealed any significant main effects or interactions demonstrating that differences in eye movements are unlikely to account for the observed activation profile in our fMRI data.

---

with 1) the interaction between visual versus auditory stimulation and high versus low IPS-TMS intensity ($[V>A]_{high\ IPS\text{-}TMS} > [V>A]_{low\ IPS\text{-}TMS}$) and 2) the interaction between visual versus auditory stimulation and high IPS-TMS versus high Vertex-TMS ($[V>A]_{high\ IPS\text{-}TMS} > [V>A]_{high\ Vertex\text{-}TMS}$) at $p<0.01$ uncorrected. (*right*) Parameter estimates (mean±standard error of the mean, RFX model) for no TMS (light gray), low intensity TMS (medium gray), and high intensity TMS (dark gray) in the cuneus at the given coordinates (i.e., activation peaks) are shown separately for auditory (left), fixation (middle), and visual (right) contexts. The bar graphs represent the size of the effect in nondimensional units (corresponding to % whole-brain mean). For illustrational purposes, the stars indicate the significance of the tests comparing individual conditions at the activation peak (uncorrected; ***significant at $p<0.001$, **significant at $p<0.01$, *significant at $p<0.05$).

Discussion

This concurrent TMS-fMRI study investigated the effect of IPSTMS on the (de)activations in the visual and auditory cortices under 3 sensory contexts: auditory, no, and visual stimulation. Our results demonstrate that IPS-TMS generally increased activations in the auditory cortex irrespective of the sensory stimulation context. Comparing IPS-TMS and Vertex-TMS suggests that this increase in activation level in the auditory cortices results from both co-activations induced by TMS clicks and top-down effects from IPS. In contrast, IPS-TMS influenced activations in the visual cortex in a state-dependent fashion: IPS-TMS suppressed activation in the cuneus under auditory and no stimulation but amplified the response to visual stimulation. Since TMS to the vertex as a control site exerted a comparable suppression in the visual cortex under auditory and no stimulation, the suppressive effects may be mediated via crossmodal inhibitory mechanisms as a consequence of the activations in auditory cortices due to the TMS clicks. Nevertheless, the amplification of visual-induced responses in the cuneus was selectively observed for IPS-TMS. The visual-evoked activations may be enhanced by IPS-TMS directly via mechanisms of gain control or indirectly by modulating the interactions with the auditory cortex.

Previous functional imaging studies have demonstrated that the BOLD responses in sensory cortices are increased for signals of the preferred sensory modality but suppressed for signals from the nonpreferred sensory modality (Haxby et al. 1994; Kawashima et al. 1995; Laurienti et al. 2002). Indeed, our study replicates these findings: auditory stimulation induced activations in auditory cortices but deactivations in visual cortices. Conversely, visual stimulation induced activations in visual cortices but deactivations in auditory cortices (though at a lower threshold of significance). These crossmodal deactivations may be mediated via thalamic mechanisms, sparse direct connectivity between sensory areas or top-down modulation from higher order association areas such as IPS (Lewis and Van Essen 2000b; Falchier et al. 2002; Macaluso, Driver, et al. 2003; Rockland and Ojima 2003; Musacchia and Schroeder 2009; Werner and Noppeney 2010b; Beer et al. 2011). From a cognitive perspective, the seesaw relationship between visual and auditory cortices under unisensory stimulation may reflect competition of sensory signals from multiple modalities for common attentional resources. For instance, an auditory signal may withdraw attentional resources from visual processing leading to deactivations in the visual cortex and vice versa (Shomstein and Yantis 2004; Johnson and Zatorre 2005, 2006; Werner and Noppeney 2011).

Given the prominent role of IPS in crossmodal attention and attentional switching (Macaluso et al. 2000; Rushworth et al. 2001; Yantis et al. 2002; Macaluso, Eimer, et al. 2003; Pessoa et al. 2009), we therefore hypothesized that TMS to the IPS may alter and potentially enhance this seesaw relationship. Specifically, within the visual cortex, it should amplify visual-induced activations and auditory-induced deactivations. Since the auditory cortex was perturbed by the auditory TMS pseudo-clicks, we expected state-dependent effects primarily in visual cortices and TMS main effects in auditory cortices.

Indeed, TMS increased activations in the auditory cortices irrespective of sensory stimulation context. Importantly, a more fine-grained analysis approach suggested that this activation increase might be mediated via 2 distinct mechanisms (Fig. 2.4A). First and not surprisingly, the TMS clicks induced auditory activations as a nonspecific side effect irrespective of whether TMS was applied to IPS or vertex (Blankenburg et al. 2008; Hanakawa et al. 2009). Second and more importantly, IPS-TMS increased activations in auditory cortices bilaterally even relative to Vertex-TMS with no auditory activations being observed for the opposite comparison (i.e., high Vertex-TMS > high IPS-TMS). These results suggest that IPS-TMS may not only increase activations in the auditory cortex via nonspecific auditory confounds but possibly also via top-down effects from IPS. Since the real and pseudo-TMS clicks strongly perturbed the auditory cortex even in the fixation or visual stimulation conditions, it is not surprising that the auditory deactivations were attenuated, and the TMS effects were not state dependent.

In contrast, in the visual cortex IPS-TMS increased the auditory-induced deactivations as well as the visual-induced activations. IPS-TMS similarly induced deactivations in the visual cortex in the absence of any stimulation. At first sight, these state-dependent TMS effects seem to be in accordance with our hypothesis. Yet, the response profile we observed in the visual cortex may not necessarily reflect true state-dependent IPS-TMS effects, but as we will argue below be generated by a mixture of true and nonspecific TMS side effects similarly to the TMS effects in the auditory cortices. Taking the multisensory nature of the neocortex serious (Ghazanfar and Schroeder 2006), activations and deactivations in the visual cortices can in principle be mediated via audiovisual interactions as a consequence of the TMS side effects on activations in the auditory cortex. In line with this conjecture, a recent study (Werner and Noppeney 2011) demonstrated that auditory input suppressed activations in the visual cortex but amplified the BOLD response to concurrent visual inputs. Since high relative to low intensity clicks increased activations in the auditory cortex, it is conceivable that the auditory cortex in turn induces deactivations in the visual cortex in the absence of visual stimulation but amplifies the response to concurrent visual stimulation. In other words, the auditory TMS clicks themselves can induce BOLD effects in the auditory cortex that exert different influence on the visual cortex depending on the sensory stimulation context. This multisensory perspective is important because it highlights that BOLD effects due to TMS side effects in the auditory cortex emerge 1) not only in the auditory cortex and 2) in a nonlinear fashion (i.e., they interact with the sensory stimulation context). Therefore, they can impede not only the interpretation of the main effect of TMS intensity but also interactions between TMS intensity and sensory stimulation context. In short, they cannot simply be eliminated or ignored when considering state-dependent TMS effects in unisensory processing (as has been argued in previous studies). Instead, even state-dependent TMS effects need to be carefully considered in the context of stimulation conditions to other control sites (e.g., vertex).

Indeed, TMS to the vertex as a control site induced a comparable deactivation in visual cortices under auditory and no stimulation suggesting that our IPS-TMS stimulation was not effective in modulating crossmodal deactivations. While an absence of an effect needs to be interpreted with caution, it may point to a role of recently advocated thalamic mechanisms in mediating crossmodal deactivations (Hackett et al. 1998; Schroeder et al. 2003; de la Mothe et al. 2006; Cappe et al. 2009).

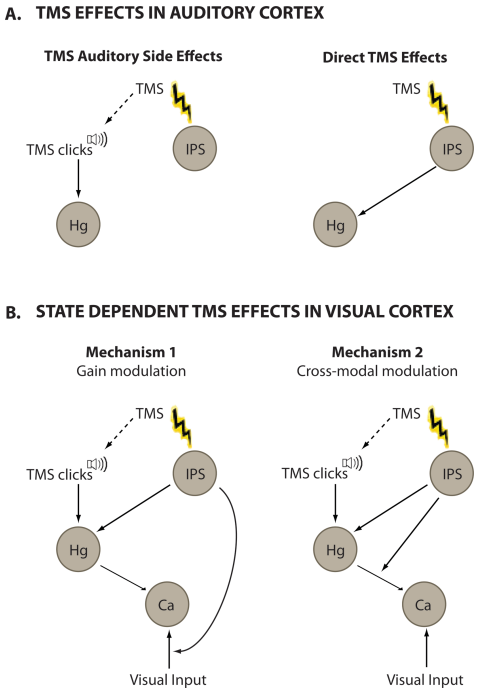

Figure 2.4. Mechanisms of TMS effects in auditory and visual cortices. **(A)** TMS effects in auditory cortex. (*left*) Auditory clicks produced by TMS pulses induce auditory coactivations in auditory cortices (nonspecific mechanism). (*right*) IPSTMS exerts top-down effects on the neural activity in auditory cortices (specific mechanism). **(B)** State-dependent TMS effects in visual cortex. (*left*) IPS-TMS increases visual activations directly via multiplicative gain control. (*right*) IPS-TMS modulates the effect of neural activity in auditory cortices (induced by TMS clicks) on activations in the visual cortex via crossmodal interactions.

So possibly, competition between sensory signals in multiple modalities may already be arbitrated via gating mechanisms at the thalamic level. Obviously, this suggestion remains speculative and needs to be substantiated in future studies demonstrating for instance a positive effect of thalamic lesions or perturbations on crossmodal deactivations.

While the effect of IPS- and Vertex-TMS was comparable for the deactivations, it differed for the visual-induced activations. Here, IPS-TMS amplified the response to the visual stimulus, while Vertex-TMS reduced the visual response. Importantly, this pattern of results contrasts with a recent study reporting an activation increase in the visual cortex for IPS-TMS only during fixation but not during visual stimulation (Ruff et al. 2008). The discrepancies between the 2 studies may be the result of differences in the protocols of TMS stimulation. While Ruff et al. (2008) applied short high-frequency TMS bursts (i.e., 3 bursts of 5 TMS pulses at 9 Hz), we applied 20 s of continuous rTMS at 1.9 Hz throughout the entire stimulation block. Indeed, previous studies have demonstrated that differences in stimulation frequencies and length of TMS stimulation may induce distinct and even opposite TMS effects (Paus et al. 1998; Speer et al. 2003; Moisa et al. 2010). Alternatively, discrepancies may result from different visual stimuli. While we used expanding and contracting visual stimuli, Ruff et al. (2008) presented random whole pattern movement that changed its color or shape every 500 ms. Finally, TMS effects may vary considerably across subjects. Since Ruff et al. (2008) was one of the first pioneering studies using concurrent TMS-fMRI to investigate the role of IPS on visual processing, the study was based on a small number of subjects that did not enable a random effects analysis for inferences across the entire population.

By contrast, our results do converge with the recent findings reported for the somatosensory cortex, where again IPS-TMS induced a deactivation in the somatosensory cortex under no wrist stimulation but amplified the BOLD response to wrist stimulation (Blankenburg et al. 2008). These convergent findings may suggest that the activation profile may generalize across primary sensory cortices. Yet, since Blankenburg et al. (2008) did not include a stimulation control site, it still remains to be investigated whether the deactivations reflect true TMS effects or may also be mediated via crossmodal interactions that depend on TMS auditory side effects.

Nevertheless, Blankenburg et al. (2008) and the current study consistently demonstrate that IPS-TMS amplifies the response to inputs from the preferred modality in primary sensory cortices (i.e., response to visual/auditory/somatosensory stimuli in primary visual/auditory/somatosensory cortex). We argue that TMS-IPS can modulate stimulus-evoked activations via at least 2 complementary mechanisms (Fig. 2.4B). First, from a unisensory perspective, IPS may increase visual activations via multiplicative gain control. Here, IPS may determine the gain of stimulus-evoked responses in visual cortices as in mechanisms of attentional top-down modulation within the visual system (McAdams and Maunsell 1999; Friston and Buchel 2000; Salinas and Sejnowski 2001; Martinez-Trujillo and Treue 2004; Womelsdorf et al. 2008). For instance, O'Craven et al. (1997) showed that attending to moving compared with stationary dots significantly increased activation in the visual motion area. Alternatively, from a multisensory perspective, IPS-TMS (but not Vertex-TMS) may modulate the effect of concurrent auditory TMS clicks on the BOLD response in the visual cortex via crossmodal mechanisms. Here, IPS-TMS modulates the effect of neural activity in the auditory cortex (induced by the TMS clicks) on activations in the visual cortex. This second multisensory mechanism may seem contrived when thinking in traditional unisensory terms. However, it emerges as a potential complementary mechanism when considering the pervasiveness of multisensory interactions within neocortex as shown in recent neuroimaging and neurophysiological research (Ghazanfar and Schroeder 2006; Kayser and Logothetis 2007). It alerts us to interpretational ambiguities and limitations of current TMS stimulation techniques that elicit nonspecific auditory and somatosensory side effects thus automatically turning unisensory into multisensory TMS stimulation experiments.

References

Abbruzzese G, Trompetto C, Schieppati M. 1996. The excitability of the human motor cortex increases during execution and mental imagination of sequential but not repetitive finger movements. Exp Brain Res. 111:465--472.

Ackermann H, Scholz E, Koehler W, Dichgans J. 1991. Influence of posture and voluntary background contraction upon compound muscle action potentials from anterior tibial and soleus muscle following transcranial magnetic stimulation. Electroencephalogr Clin Neurophysiol. 81:71--80.

Antal A, Nitsche MA, Kincses TZ, Lampe C, Paulus W. 2004. No correlation between moving phosphene and motor thresholds: a transcranial magnetic stimulation study. Neuroreport. 15:297--302.

Arai N, Okabe S, Furubayashi T, Terao Y, Yuasa K, Ugawa Y. 2005. Comparison between short train, monophasic and biphasic repetitive transcranial magnetic stimulation (rTMS) of the human motor cortex. Clin Neurophysiol. 116:605--613.

Baudewig J, Siebner HR, Bestmann S, Tergau F, Tings T, PaulusW, Frahm J. 2001. Functional MRI of cortical activations induced by transcranial magnetic stimulation (TMS). Neuroreport. 12:3543--3548.

Beauchamp MS, Argall BD, Bodurka J, Duyn JH, Martin A. 2004. Unraveling multisensory integration: patchy organization within human STS multisensory cortex. Nat Neurosci. 7:1190--1192.

Beer AL, Plank T, Greenlee MW. 2011. Diffusion tensor imaging shows white matter tracts between human auditory and visual cortex. Exp Brain Res. 213:299--308.

Bestmann S, Baudewig J, Frahm J. 2003. On the synchronization of transcranial magnetic stimulation and functional echo-planar imaging. J Magn Reson Imaging. 17:309--316.

Bestmann S, Swayne O, Blankenburg F, Ruff CC, Haggard P, Weiskopf N, Josephs O, Driver J, Rothwell JC, Ward NS. 2008. Dorsal premotor cortex exerts state-dependent causal influences on activity in contralateral primary motor and dorsal premotor cortex. Cereb Cortex. 18:1281--1291.

Blankenburg F, Ruff CC, Bestmann S, Bjoertomt O, Eshel N, Josephs O, Weiskopf N, Driver J. 2008. Interhemispheric effect of parietal TMS on somatosensory response confirmed directly with concurrent TMS-fMRI. J Neurosci. 28:13202--13208.

Blankenburg F, Ruff CC, Bestmann S, Bjoertomt O, Josephs O, Deichmann R, Driver J. 2010. Studying the role of human parietal cortex in visuospatial attention with concurrent TMS-fMRI. Cereb Cortex. 20:2702--2711.

Boroojerdi B, Meister IG, Foltys H, Sparing R, Cohen LG, Topper R. 2002. Visual and motor cortex excitability: a transcranial magnetic stimulation study. Clin Neurophysiol. 113:1501--1504.

Boussaoud D, Ungerleider LG, Desimone R. 1990. Pathways for motion analysis: cortical connections of the medial superior temporal and fundus of the superior temporal visual areas in the macaque. J Comp Neurol. 296:462--495.

Brainard DH. 1997. The Psychophysics Toolbox. Spat Vis. 10:433--436.

Bremmer F, Schlack A, Shah NJ, Zafiris O, Kubischik M, Hoffmann K, Zilles K, Fink GR. 2001. Polymodal motion processing in posterior parietal and premotor cortex: a human fMRI study strongly implies equivalencies between humans and monkeys. Neuron. 29:287--296.

Bushara KO, Weeks RA, Ishii K, Catalan MJ, Tian B, Rauschecker JP, Hallett M. 1999. Modality-specific frontal and parietal areas for auditory and visual spatial localization in humans. Nat Neurosci. 2:759--766.

Calvert GA. 2001. Crossmodal processing in the human brain: insights from functional neuroimaging studies. Cereb Cortex. 11:1110--1123.

Cappe C, Morel A, Barone P, Rouiller EM. 2009. The thalamocortical projection systems in primate: an anatomical support for multisensory and sensorimotor interplay. Cereb Cortex. 19:2025--2037.

Cappe C, Thut G, Romei V, Murray MM. 2010. Auditory-visual multisensory interactions in humans: timing, topography, directionality, and sources. J Neurosci. 30:12572--12580.

Corbetta M, Kincade JM, Ollinger JM, McAvoy MP, Shulman GL. 2000. Voluntary orienting is dissociated from target detection in human posterior parietal cortex. Nat Neurosci. 3:292--297.

de la Mothe LA, Blumell S, Kajikawa Y, Hackett TA. 2006. Thalamic connections of the auditory cortex in marmoset monkeys: core and medial belt regions. J Comp Neurol. 496:72--96.

Deblieck C, Thompson B, Iacoboni M, Wu AD. 2008. Correlation between motor and phosphene thresholds: a transcranial magnetic stimulation study. Hum Brain Mapp. 29:662--670.

Driver J, Noesselt T. 2008. Multisensory interplay reveals crossmodal influences on 'sensory-specific' brain regions, neural responses, and judgments. Neuron. 57:11--23.

Eickhoff SB, Stephan KE, Mohlberg H, Grefkes C, Fink GR, Amunts K, Zilles K. 2005. A new SPM toolbox for combining probabilistic cytoarchitectonic maps and functional imaging data. Neuroimage. 25:1325--1335.

Falchier A, Clavagnier S, Barone P, Kennedy H. 2002. Anatomical evidence of multimodal integration in primate striate cortex. J Neurosci. 22:5749--5759.

Foxe JJ, Morocz IA, Murray MM, Higgins BA, Javitt DC, Schroeder CE. 2000. Multisensory auditory-somatosensory interactions in early cortical processing revealed by high-density electrical mapping. Brain Res Cogn Brain Res. 10:77--83.

Friston K, Holmes A, Worsley KJ, Poline JB, Frith C, Frackowiak R. 1995. Statistical parametric mapping: a general linear approach. Hum Brain Mapp. 2:22.

Friston KJ, Buchel C. 2000. Attentional modulation of effective connectivity from V2 to V5/MT in humans. Proc Natl Acad Sci U S A. 97:7591--7596.

Friston KJ, Holmes AP, Price CJ, Buchel C, Worsley KJ. 1999. Multisubject fMRI studies and conjunction analyses. Neuroimage. 10:385--396.

Ghazanfar AA, Schroeder CE. 2006. Is neocortex essentially multisensory? Trends Cogn Sci. 10:278--285.

Hackett TA, De La Mothe LA, Ulbert I, Karmos G, Smiley J, Schroeder CE. 2007. Multisensory convergence in auditory cortex, II. Thalamocortical connections of the caudal superior temporal plane. J Comp Neurol. 502:924--952.

Hackett TA, Stepniewska I, Kaas JH. 1998. Thalamocortical connections of the parabelt auditory cortex in macaque monkeys. J Comp Neurol. 400:271--286.

Hanakawa T, Mima T, Matsumoto R, Abe M, Inouchi M, Urayama S, Anami K, Honda M, Fukuyama H. 2009. Stimulus-response profile during single-pulse transcranial magnetic stimulation to the primary motor cortex. Cereb Cortex. 19:2605--2615.

Haxby JV, Horwitz B, Ungerleider LG, Maisog JM, Pietrini P, Grady CL. 1994. The functional organization of human extrastriate cortex: a PET-rCBF study of selective attention to faces and locations. J Neurosci. 14:6336--6353.

Hyvarinen J. 1982. Posterior parietal lobe of the primate brain. Physiol Rev. 62:1060--1129.

Izumi S, Findley TW, Ikai T, Andrews J, Daum M, Chino N. 1995. Facilitatory effect of thinking about movement on motor-evoked potentials to transcranial magnetic stimulation of the brain. Am J Phys Med Rehabil. 74:207--213.

Johnson JA, Zatorre RJ. 2005. Attention to simultaneous unrelated auditory and visual events: behavioral and neural correlates. Cereb Cortex. 15:1609--1620.

Johnson JA, Zatorre RJ. 2006. Neural substrates for dividing and focusing attention between simultaneous auditory and visual events. Neuroimage. 31:1673--1681.

Kawashima R, O'Sullivan BT, Roland PE. 1995. Positron-emission tomography studies of cross-modality inhibition in selective attentional tasks: closing the ''mind's eye''. Proc Natl Acad Sci U S A. 92:5969--5972.

Kayser C, Logothetis NK. 2007. Do early sensory cortices integrate cross-modal information? Brain Struct Funct. 212:121--132.

Kleiner M, Baarmand MM, Pelli D. 2007. What's new in Psychtoolbox-3? Perception. 36(ECVP Abstract Supplement):14.

Laurienti PJ, Burdette JH, Wallace MT, Yen YF, Field AS, Stein BE. 2002. Deactivation of sensory-specific cortex by cross-modal stimuli. J Cogn Neurosci. 14:420--429.

Leon-Sarmiento FE, Bara-Jimenez W, Wassermann EM. 2005. Visual deprivation effects on human motor cortex excitability. Neurosci Lett. 389:17--20.

Lewis JW, Beauchamp MS, DeYoe EA. 2000. A comparison of visual and auditory motion processing in human cerebral cortex. Cereb Cortex. 10:873--888.

Lewis JW, Van Essen DC. 2000a. Corticocortical connections of visual, sensorimotor, and multimodal processing areas in the parietal lobe of the macaque monkey. J Comp Neurol. 428:112--137.

Lewis JW, Van Essen DC. 2000b. Mapping of architectonic subdivisions in the macaque monkey, with emphasis on parieto-occipital cortex. J Comp Neurol. 428:79--111.

Macaluso E, Driver J. 2005. Multisensory spatial interactions: a window onto functional integration in the human brain. Trends Neurosci. 28:264--271.

Macaluso E, Driver J, Frith CD. 2003. Multimodal spatial representations engaged in human parietal cortex during both saccadic and manual spatial orienting. Curr Biol. 13:990--999.

Macaluso E, Eimer M, Frith CD, Driver J. 2003. Preparatory states in crossmodal spatial attention: spatial specificity and possible control mechanisms. Exp Brain Res. 149:62--74.

Macaluso E, Frith CD, Driver J. 2000. Modulation of human visual cortex by crossmodal spatial attention. Science. 289:1206--1208.

Martinez-Trujillo JC, Treue S. 2004. Feature-based attention increases the selectivity of population responses in primate visual cortex. Curr Biol. 14:744--751.

Maunsell JH, van Essen DC. 1983. The connections of the middle temporal visual area (MT) and their relationship to a cortical hierarchy in the macaque monkey. J Neurosci. 3:2563--2586.

McAdams CJ, Maunsell JH. 1999. Effects of attention on the reliability of individual neurons in monkey visual cortex. Neuron. 23:765--773.

Moisa M, Pohmann R, Ewald L, Thielscher A. 2009. New coil positioning method for interleaved transcranial magnetic stimulation (TMS)/functional MRI (fMRI) and its validation in a motor cortex study. J Magn Reson Imaging. 29:189--197.

Moisa M, Pohmann R, Uludag K, Thielscher A. 2010. Interleaved TMS/CASL: comparison of different rTMS protocols. Neuroimage. 49:612--620.

Molholm S, Ritter W, Murray MM, Javitt DC, Schroeder CE, Foxe JJ. 2002. Multisensory auditory-visual interactions during early sensory processing in humans: a high-density electrical mapping study. Brain Res Cogn Brain Res. 14:115--128.

Murray MM, Molholm S, Michel CM, Heslenfeld DJ, Ritter W, Javitt DC, Schroeder CE, Foxe JJ. 2005. Grabbing your ear: rapid auditory-somatosensory multisensory interactions in low-level sensory cortices are not constrained by stimulus alignment. Cereb Cortex. 15:963--974.

Musacchia G, Schroeder CE. 2009. Neuronal mechanisms, response dynamics and perceptual functions of multisensory interactions in auditory cortex. Hear Res. 258:72--79.

O'Craven KM, Rosen BR, Kwong KK, Treisman A, Savoy RL. 1997. Voluntary attention modulates fMRI activity in human MT-MST. Neuron. 18:591--598.

Oliver R, Bjoertomt O, Driver J, Greenwood R, Rothwell J. 2009. Novel 'hunting' method using transcranial magnetic stimulation over parietal cortex disrupts visuospatial sensitivity in relation to motor thresholds. Neuropsychologia. 47:3152--3161.

Paus T, Jech R, Thompson CJ, Comeau R, Peters T, Evans AC. 1998. Dose-dependent reduction of cerebral blood flow during rapid-rate transcranial magnetic stimulation of the human sensorimotor cortex. J Neurophysiol. 79:1102--1107.

Pessoa L, Rossi A, Japee S, Desimone R, Ungerleider LG. 2009. Attentional control during the transient updating of cue information. Brain Res. 1247:149--158.

Raij T, Ahveninen J, Lin FH, Witzel T, Jaaskelainen IP, Letham B, Israeli E, Sahyoun C, Vasios C, Stufflebeam S, et al. 2010. Onset timing of cross-sensory activations and multisensory interactions in auditory and visual sensory cortices. Eur J Neurosci. 31:1772--1782.

Rockland KS, Ojima H. 2003. Multisensory convergence in calcarine visual areas in macaque monkey. Int J Psychophysiol. 50:19--26.

Romei V, Murray MM, Merabet LB, Thut G. 2007. Occipital transcranial magnetic stimulation has opposing effects on visual and auditory stimulus detection: implications for multisensory interactions. J Neurosci. 27:11465--11472.

Ruff CC, Bestmann S, Blankenburg F, Bjoertomt O, Josephs O, Weiskopf N, Deichmann R, Driver J. 2008. Distinct causal influences of parietal versus frontal areas on human visual cortex: evidence from concurrent TMS-fMRI. Cereb Cortex. 18:817--827.

Ruff CC, Blankenburg F, Bjoertomt O, Bestmann S, Freeman E, Haynes JD, Rees G, Josephs O, Deichmann R, Driver J. 2006. Concurrent TMS-fMRI and psychophysics reveal frontal influences on human retinotopic visual cortex. Curr Biol. 16:1479--1488.

Ruff CC, Blankenburg F, Bjoertomt O, Bestmann S, Weiskopf N, Driver J. 2009. Hemispheric differences in frontal and parietal influences on human occipital cortex: direct confirmation with concurrent TMSfMRI. J Cogn Neurosci. 21:1146--1161.

Rushworth MF, Paus T, Sipila PK. 2001. Attention systems and the organization of the human parietal cortex. J Neurosci. 21:5262--5271.

Sack AT, Kohler A, Bestmann S, Linden DE, Dechent P, Goebel R, Baudewig J. 2007. Imaging the brain activity changes underlying impaired visuospatial judgments: simultaneous FMRI, TMS, and behavioral studies. Cereb Cortex. 17:2841--2852.

Sadaghiani S, Maier JX, Noppeney U. 2009. Natural, metaphoric, and linguistic auditory direction signals have distinct influences on visual motion processing. J Neurosci. 29:6490--6499.

Salinas E, Sejnowski TJ. 2001. Gain modulation in the central nervous system: where behavior, neurophysiology, and computation meet. Neuroscientist. 7:430--440.

Santangelo V, Olivetti Belardinelli M, Spence C, Macaluso E. 2009. Interactions between voluntary and stimulus-driven spatial attention mechanisms across sensory modalities. J Cogn Neurosci. 21:2384--2397.

Schonfeldt-Lecuona C, Thielscher A, Freudenmann RW, Kron M, Spitzer M, Herwig U. 2005. Accuracy of stereotaxic positioning of transcranial magnetic stimulation. Brain Topogr. 17:253--259.

Schroeder CE, Foxe J. 2005. Multisensory contributions to low-level, 'unisensory' processing. Curr Opin Neurobiol. 15:454--458.

Schroeder CE, Smiley J, Fu KG, McGinnis T, O'Connell MN, Hackett TA. 2003. Anatomical mechanisms and functional implications of multisensory convergence in early cortical processing. Int J Psychophysiol. 50:5--17.

Shomstein S, Yantis S. 2004. Control of attention shifts between vision and audition in human cortex. J Neurosci. 24:10702--10706.

Speer AM, Willis MW, Herscovitch P, Daube-Witherspoon M, Shelton JR, Benson BE, Post RM, Wassermann EM. 2003. Intensity-dependent regional cerebral blood flow during 1-Hz repetitive transcranial magnetic stimulation (rTMS) in healthy volunteers studied with H215O positron emission tomography: II. Effects of prefrontal cortex rTMS. Biol Psychiatry. 54:826--832.

Stewart LM, Walsh V, Rothwell JC. 2001. Motor and phosphine thresholds: a transcranial magnetic stimulation correlation study. Neuropsychologia. 39:415--419.

Werner S, Noppeney U. 2010a. Distinct functional contributions of primary sensory and association areas to audiovisual integration in object categorization. J Neurosci. 30:2662--2675.

Werner S, Noppeney U. 2010b. Superadditive responses in superior temporal sulcus predict audiovisual benefits in object categorization. Cereb Cortex. 20:1829--1842.

Werner S, Noppeney U. 2011. The contributions of transient and sustained response codes to audiovisual integration. Cereb Cortex. 21:920--931.

Womelsdorf T, Anton-Erxleben K, Treue S. 2008. Receptive field shift and shrinkage in macaque middle temporal area through attentional gain modulation. J Neurosci. 28:8934--8944.

Yantis S, Schwarzbach J, Serences JT, Carlson RL, Steinmetz MA, Pekar JJ, Courtney SM. 2002. Transient neural activity in human parietal cortex during spatial attention shifts. Nat Neurosci. 5:995--1002.

Chapter 3

Bottom-up and Top-down Interactions revealed by concurrent TMS-fMRI under different sensory contexts

Joana Leitão[1,2], Axel Thielscher[1,3,4], Johannes Tuennerhoff[1], Uta Noppeney[1,2]

[1]Max Planck Institute for biological Cybernetics, 72076 Tübingen, Germany

[2]Computational Neuroscience and Cognitive Robotics Centre, University of Birmingham, B15 2TT Birmingham, UK

[3]Department of Electrical Engineering, Technical University of Denmark, 2800 Lyngby, Denmark

[4]DRCMR, Copenhagen University Hospital Hvidovre, 2650 Hvidovre, Denmark

An updated version of this chapter has been published since the submission of the thesis in:
J. of Neuroscience, August 2015; 35(32):11445–11457; doi: 10.1523/JNEUROSCI.0939-15.2015

Author contributions

Leitão and Noppeney designed the experiment. Stimuli were programmed and designed by Leitão. Thielscher contributed with TMS expertise. Leitão collected the data with the support of Tuennerhoff. Leitão analysed the data with the help of Noppeney. Leitão wrote the manuscript with the help of Thielscher and Noppeney.

Acknowledgments

This work was supported by the European Research Council and the Max Planck Society. The authors would like to thank Julian Hofmeister and Simone Götze for helping with data acquisition, Mario Kleiner for technical assistance and the medical doctors Daniel Zaldivar, Johannes Schultz and Matthias Munk for their availability during data acquisition and participants' screening. The authors declare no competing financial interests.

Abstract

Behaviour emerges from the interaction between neural processes representing stimulus-driven and goal-directed factors. The intraparietal sulcus (IPS) has been repeatedly identified as a source of top-down attentional control in visual areas that not only mediates goal-directed behaviour, but also integrates stimulus-driven information. The present study used concurrent TMS-fMRI to investigate the causal role of the right anterior IPS during a demanding visual detection task that manipulated the bottom-up visual input. We applied 4 pulses of TMS (10Hz) over the right IPS and during a Sham condition, while participants detected the presence/absence of a task-relevant visual input presented at their left lower visual field. Given that in natural conditions task-relevant sensory information rarely appears in isolation but is instead inserted in a stream of task-irrelevant multisensory signals, we further manipulated the bottom-up sensory context by introducing auditory stimuli across runs presented at target onset. Behaviourally, auditory stimuli resulted in accelerated responses. Conversely, TMS did not influence task performance, thereby ensuring unconfounded fMRI data. Our results show that IPS-TMS eliminated target-evoked activation increases in the right inferior parietal lobe, whilst having opposite effects in right occipito-temporal visual areas. This pattern reflects a complex interplay between these regions in the processing of task-relevant information during high attentional demands. Moreover, in the right posterior/middle insula and areas of the ventral lateral prefrontal cortex interactions between task-relevant bottom-up and top-down signals were diminished in the auditory context, suggesting that the extra auditory input attenuated the need for top-down influences in these regions.

Keywords: interleaved/concurrent TMS-fMRI, right anterior parietal cortex, top-down goal-directed behaviour vs. bottom-up stimulus-driven information, task-relevant processing, multisensory context

Introduction

An adequate interaction with the environment entails the ability to detect relevant sensory events embedded in a continuous stream of multisensory signals. In addition to bottom-up sensory information, it is now well established that detection of sensory events equally depends on top-down modulatory signals that can influence perceptual representations according to current behavioural relevance. For instance, top-down attention-related signals can increase activations in extrastriate areas merely by anticipation of behaviourally relevant visual stimuli (Kastner et al., 1999).

At the neural level, steering attention to relevant sensory events is associated with a distributed network of frontoparietal regions (e.g. Kastner and Pinsk, 2004; Serences and Yantis, 2006). Traditional research on attentional control emphasize a division between a dorsal part, involved in endogenous voluntary control that responds to current task requirements, and a ventral part associated with bottom-up attention driven by behaviourally relevant events in the environment (Corbetta and Shulman, 2002). However, this dichotomy is challenged by evidence showing stimulus-driven and expectancy effects in the dorsal and ventral networks, respectively (for review, see Macaluso and Doricchi, 2013). In particular, as a core node of the dorsal attentional network, the intraparietal sulcus (IPS) also displays response patterns consistent with a "salience map" that provides topographical representations of the visual field in accordance to the perceptual or behavioural salience of objects in the environment (e.g. Gottlieb, 2007; Swisher et al., 2007). Directing attention to behavioural relevant events is thus a multifaceted process that requires a dynamic interplay between attentional control systems and sensory brain regions.

Concurrent (or interleaved) TMS-fMRI provides a causal interventional approach to investigate online influences from the stimulated region on interconnected brain areas. Recently, several TMS-fMRI studies have established that TMS is able to modulate activity in remote areas of the brain and that these modulations critically depend on the current state of these areas (Sack et al., 2007; Ruff et al., 2008; Blankenburg et al., 2010; Moisa et al., 2012; Leitão et al., 2013).

The present study employed this methodology to evaluate the role of IPS in attentional control. Specifically, we investigated how TMS-induced disturbances to the right IPS influence task-contingent activations in other pertinent brain areas under different sensory contexts. To engage the attentional network participants performed a demanding visual detection task that manipulated the bottom-up visual input in a peripheral visual location. Participants maintained covert attention to the left lower visual field and indicated their percept of a small visual stimulus presented there on 50% of the trials. Simultaneously, bursts of 4 TMS pulses (10 Hz) were applied to the right anterior IPS, while Sham-TMS was used as a control condition. Moreover, we further manipulated the bottom-up sensory context across runs by introducing two different auditory contexts (present vs. absent). This experimental design allowed us to (i) examine how perturbation of IPS activity during an attentionally demanding visual detection task modulated task-related activations in other nodes of the attentional network and visual areas and (ii) to investigate how task processing might be influenced by the current bottom-up sensory context.

Material & Methods

Participants

Ten right-handed participants (4 male; mean age: 31.5 years; standard deviation: 8.1; Edinburgh Handedness inventory score (mean ± SD) of 78±16.8) participated in the experiment. Participants had no history of neurological illness, had normal or corrected-to-normal vision and reported normal hearing. All participants gave informed consent prior to participation and the study was approved by the Human Research Ethics Committee of the Medical Faculty at the University of Tübingen.

Experimental Design & Task

The 2x2x2 factorial design manipulated: (i) task-relevant visual input (V present, V absent), (ii) TMS condition (right anterior IPS, Sham) and (iii) auditory context (A present, A absent) (Fig. 3.1A).

In a visual detection paradigm, participants reported their percept (seen/unseen) of a visual stimulus presented in their left lower visual field, while at the same time fixating on a cross presented throughout an entire run in the centre of the screen (see *Stimuli and Stimuli Presentation*). Restricting the stimulus location to the left side of visual field was preferred in this first step, as it has been shown that parietal TMS can elicit different effects for contra- and ipsi-lateral stimuli (e.g. Hilgetag et al., 2001).

The task was performed under two different auditory contexts. In auditory runs, an auditory sound (see *Stimuli and Stimuli Presentation*) was presented synchronously with target onset, regardless of the presence/absence of the task-relevant visual input. Thus, in auditory runs the sound did not predict the presence of the visual stimulus. In the remaining runs no auditory sound was presented (see Fig. 3.1C). Therefore, considering all runs together resulted in four distinct sensory conditions: visual present trials presented with (AV) and without (V) a synchronously presented auditory sound and similarly, visual absent trials during which an auditory sound could be present (A) or absent (¬V). Participants were instructed to answer 'seen' only when completely sure and to report 'unseen' otherwise. Each participant was trained in a minimum of six runs prior to going inside the scanner.

Each trial started with the change of the fixation cross colour from grey to blue. After 100 ms the visual target was presented with 50% probability (Fig. 3.1B). Independently of the type of trial (V present, V absent), 4 TMS pulses were subsequently applied (see *Data Acquisition and TMS Procedures*; Fig. 3.1C). After 600 ms of trial begin, the fixation cross turned back to grey and remained like this for 2690 ms until the onset of the next trial. The interstimulus interval amounted thus to 3290 ms, equalling one TR of the EPI acquisition.

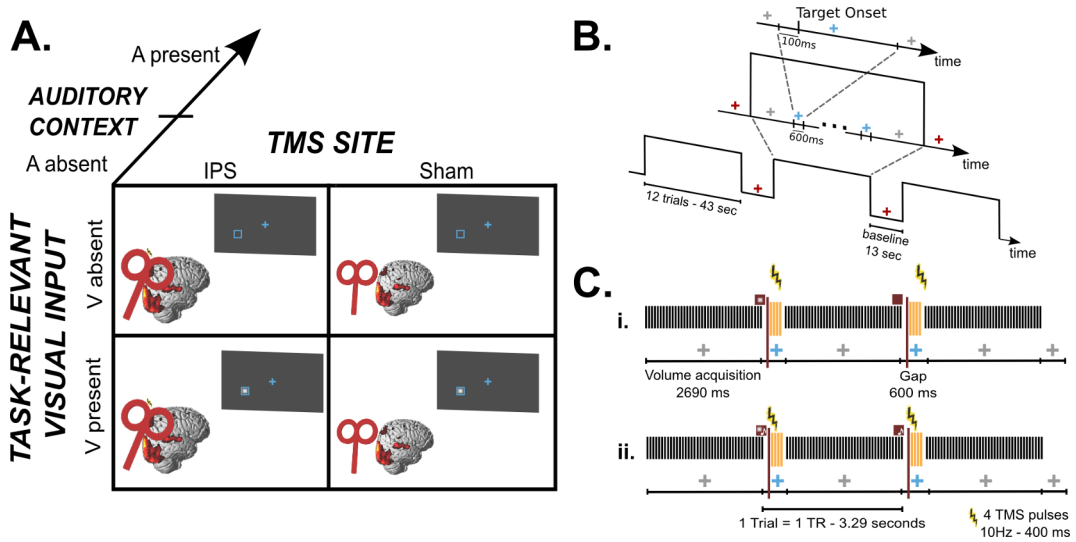

Figure 3.1 Experimental Design. (A) 2x2x2 factorial design manipulating (i) task-relevant visual input (V present, V absent), (ii) auditory context (A present, A absent) and (iii) TMS condition (right anterior IPS, Sham). **(B)** Timeline example of stimuli presentation. Blocks of 12 trials started and ended with a grey fixation cross and were interleaved with baseline periods, during which the fixation cross turned red. A trial began when the fixation cross turned blue. In target present trials, the visual stimulus was presented 100 ms after trial begin. After a total period of 600ms the fixation cross turned back to grey and remained like this until the next trial. **(C)** Illustration of the concurrent TMS-fMRI protocol and stimuli presentation timing for three scans (last scan corresponding to the end of the block) for i. auditory absent and ii. auditory present runs. Within a block the fixation cross was grey during volume acquisition and blue during the acquisition gaps. At 100 ms after trial begin, the task-relevant visual stimulus was either present (first depicted trial) or absent (second depicted trial). Bursts of 4 TMS pulses were applied during acquisiton gaps at 10 Hz and started 100 ms after the target onset time.

Trials were presented in blocks of twelve that started and ended with a grey fixation cross. These were interleaved with baseline periods of 13 seconds, which were made explicit via a red fixation cross. Hence, the colour of the fixation cross induced changes in the attentional settings of the participants: while blue or grey were accompanied by a high attentional load, red represented little attentional demands.

Each run consisted of seven blocks and there were eight runs per TMS condition. For each TMS condition, the auditory context was manipulated across runs following an ABBA design that was counterbalanced across participants. Hence, there were four runs per auditory context and a total of 168 trials per experimental condition.

The two TMS conditions (IPS/Sham) were performed in different sessions and the order was counterbalanced across participants. For each participant, the order of conditions (i.e. visual present/absent) was fully randomized within and across the eight runs that constituted a session. Across sessions, the same order of conditions was used.

Stimuli and Stimuli Presentation

The task-relevant visual stimulus consisted of a small (9x9 pixels, visual angle: 0.52°) square presented for one frame (i.e. 16 ms) on a grey background. When present, the visual stimulus

appeared in the centre of a blue placeholder (40x40 pixels, visual angle: 2.3º) that was continuously presented throughout an entire run and positioned 12º left and 5º down relative to the fixation cross. The grey level of the square was individually determined in a Quest Procedure (Watson and Pelli, 1983) inside the scanner aiming at a detection threshold of 70% and using the same parameters as the main experiment. The grey level was approximated by the use of dithering. Hence, instead of being a homogenous square, our stimulus was effectively a cloud of white pixels within the square. Importantly, identical grey levels were used across IPS and Sham stimulation.

To increase integration between auditory and visual stimuli, auditory stimuli were generated so as to be perceived at the approximate location of the visual target. Since auditory spatial localization is enhanced when stimuli have a broad range of frequency content, white noise is often used in auditory spatial localization paradigms. However, owing to scanner noise and TMS clicks, white noise was considered to not be salient enough in the context of this experiment. Therefore, an auditory stimulus was created by adding sinusoidal tones with base frequencies of 130.81 Hz, 164.81 Hz and 196 Hz and the following six terms of their respective geometric progressions (i.e. adding the terms 2^n*f, where f represents each of the three base frequencies and $1 \leq n \leq 6$). Hence, the auditory sound spanned a total of seven octaves and ranged from 130.81 Hz to 12543.58 Hz. This auditory signal was then convolved with spatially specific head-related transfer functions (HRTFs) to create a left localized stimulus. The HRTFs were pseudo-individualized by matching participants' head width, height, depth and circumference to the anthropometry of participants in the CIPIC database (Algazi et al., 2001). The duration of each auditory stimulus was 40 ms.

Visual and auditory stimuli were presented using Psychophysics Toolbox version 3.0.10 (Brainard, 1997; Kleiner et al., 2007) running on MATLAB 7.9 (MathWorks Inc, MA, USA) and a Macintosh laptop running OS-X 10.6.8 (Apple Inc, CA, USA). The visual stimulus was back-projected onto a frosted Plexiglas screen using a LCD projector (JVC Ltd., Yokohama, Japan; resolution: 800x600 pixels, refresh rate: 60Hz, viewing distance: 48 cm) visible to the participant through a mirror mounted on the MR-head coil. Auditory stimuli were presented via MR-compatible electrodynamic headphones at a sampling frequency of 44100 Hz (MR Confon GmbH). Furthermore, earplugs were used to attenuate both scanner and TMS noise.

Participants indicated their response (i.e. visual target seen or unseen) with their right hand using a MR-compatible custom-built button device connected to the stimulus computer.

TMS Sites

TMS was applied over the right anterior IPS as the experimental site and Sham TMS was included as a control condition.

The MNI coordinates (x = 42.3, y = -50.3, z = 64.4) reported by Oliver et al (2009) as a position over which TMS disrupted visuospatial processing were adopted for the parietal stimulation site. Individual stimulation coordinates were determined by inverse transforming the MNI coordinates from Oliver et al (2009) into native space using the parameters obtained from spatial normalization. *A posteriori* coil reconstruction of the coil position was based on custom-written MATLAB (MathWorks Inc, MA, USA) scripts and a water tube attached to the coil, which was clearly visible

on the MR images. Across participants, the target IPS coordinates were obtained with a mean deviance of 10 mm ± 6.2 (mean, SD). The mean reached coordinate in MNI space was (x = 34.1, y = -50.7, z = 64.3).

In the Sham condition, 2 cm thick plastic plates were fixed between the TMS coil and the skull. Given the quadratic decay of the TMS-induced magnetic field, this Sham condition precluded the effects of direct brain stimulation, while maintaining the auditory and somatosensory side effects. Indeed, when tested over the finger region of the motor cortex, this Sham condition did not induce muscular twitches on pre-activated finger muscles even at 100% of total output intensity. During the Sham condition the coil was placed over the right hemisphere as close as possible to the experimental stimulation condition, given the space constraints inside the MR coil.

Data Acquisition and TMS Procedures

A 3T TIM Trio System (Siemens, Erlangen, Germany) was used to acquire both high-resolution structural images (176 sagittal slices, TR = 2300 ms, TE = 2.98 ms, TI = 1100 ms, flip angle = 9°, FOV = 240 mm x 256 mm, image matrix = 240 x 256, voxel size = 1 mm x 1 mm x 1 mm, using a 12-channel head coil) and T2*-weighted axial echoplanar images (EPI) with blood oxygenation level dependent (BOLD) contrast (GE-EPI, TR = 3290 ms, TE = 35 ms, flip angle = 90°, FOV = 192 mm x 192 mm, image matrix 64 x 64, 40 axial slices acquired sequentially in ascending direction, slice thickness = 3 mm, interslice gap = 0.3 mm, voxel size = 3 mm x 3 mm x 3.3 mm, using a 1-channel Tx/Rx head coil). Each participant took part in a total of eight experimental runs per TMS condition. A total of 124 volume images were acquired for each run.

After each EPI run, a fast structural image (fast low-angle shot [FLASH], 100 axial slices, TR = 564 ms, TE = 2.46 ms, TI = 300ms, FOV = 256mm x 256 mm, image matrix = 256x256, voxel size = 1x1x3 mm) was acquired to enable *a posteriori* reconstruction of the TMS coil position inside the scanner, as described elsewhere (Leitão et al., 2013).

The EPI sequence was adapted for concurrent TMS-fMRI experiments by introducing gaps of 600 ms after every volume acquisition. Each gap was introduced to allow the delivery of four TMS pulses without interference with image quality (Bestmann, 2003; Moisa et al., 2009). Bursts of four pulses at 10 Hz were applied every trial, with the first pulse applied 2890 ms after begin of volume acquisition, i.e., 100 ms after stimulus onset (Fig. 3.1C). TMS pulses were applied after stimulus onset in order to minimize cross-modal interaction effects between our stimuli and the TMS induced auditory and somatosensory side effects (Duecker and Sack, 2013; Leitão et al., 2013). Similar TMS protocols have been used both in TMS studies outside the scanner (Chambers et al., 2004b; Oliver et al., 2009) and in concurrent TMS-fMRI studies investigating visuospatial processing (Ruff et al., 2006, 2008, 2009; Sack et al., 2007; Blankenburg et al., 2010; Heinen et al., 2011).

Biphasic stimuli were delivered using a MagPro X100 stimulator (MagVenture, Denmark) and a MR-compatible figure of eight TMS coil (MRi-B88), using the same coil-holding device as described in Moisa et al (2009).

During IPS stimulation, a fixed TMS intensity of 69% of total stimulator output was used for all participants. This corresponded to 125% of the mean resting motor threshold, as determined across

twenty-four participants in prior studies using the same coil (M Moisa, personal communication). To ensure similar somatosensory side effects between IPS- and Sham-TMS the TMS intensity was increased to 75% during the Sham condition based on the subjective report of two naïve participants that participated in a pilot test.

Extensive image quality tests of our setup are reported elsewhere (Moisa et al., 2009, 2010: Supplementary Material). For completeness, we acquired EPI data with a phantom using the same experimental design. After realignment, data were entered in a first level analysis using the same model as for the real participants. Computing all the relevant contrasts (height threshold: $p < 0.01$ uncorrected) yielded only spurious and randomly distributed activation patterns.

Behavioural Data Analysis

The proportion of correct responses for visual present and visual absent trials were computed separately for each auditory context and TMS conditions and were averaged across participants. To test for significant differences between TMS conditions and auditory contexts this index was entered in a two 3-way repeated measures analyses of variance (RM-ANOVA) with factors TMS condition (IPS, Sham) and auditory context (A present, A absent) and task-relevant visual input (V present, V absent).

Statistical analyses were also performed on reaction times data. Individual median reaction times were computed for each condition separately and averaged across participants. To evaluate how this behavioural index was modulated by each of the three factors in our experimental design, reaction time data was entered in a 3-way RM-ANOVA with factors TMS condition (IPS, Sham), auditory context (A present, A absent) and task-relevant visual input (V present, V absent).

fMRI Data Analysis

The fMRI data were analysed using SPM8 (Wellcome Department of Imaging Neuroscience, London; www.fil.ion.ucl.ac.uk/spm) (Friston et al., 1995). Scans from each subject were realigned using the first as a reference, unwarped, spatially normalized into MNI space, resampled to a spatial resolution of 2 x 2 x 2 mm^3, and spatially smoothed with a Gaussian kernel of 8 mm full-width at half-maximum. The time series of all voxels were high-pass filtered to 1/128 Hz. The first 3 volumes were discarded to allow for T1-equilibration effects.

The fMRI experiment was modeled as a mixed block-event-related design. Individual trials (visual present/absent) were modeled as events and entered into a design matrix after convolution with a canonical hemodynamic function and its first temporal derivative. The later was included as a variable-of-no-interest to capture variance caused by temporal deviations of the BOLD responses from the canonical response function. In addition to modeling these two conditions separately for each auditory context and TMS condition, our statistical model included block begin and end regressors (i.e. the periods during which the fixation was grey at the beginning and end of a block; see *Experimental Design*) as mini blocks of 2.69 s and 3.29 s duration, respectively. For each IPS- and Sham-TMS session the four runs acquired for each auditory context were concatenated with run-

specific means entered as separate regressors. Nuisance covariates included the realignment parameters to account for residual motion artifacts.

For each participant, condition specific effects were estimated according to the general linear model by creating contrast images of each condition relative to the arbitrary baseline (including only regressors based on the canonical hemodynamic response function). The following statistical comparisons were entered in independent second-level one-sample t-tests to allow for random effects analyses and inferences at the population level (Friston et al., 1999).

Overall Task Effects

Our experiment was modeled as a mixed block-event-related design. Hence, to assess overall task effects we separately computed the contrasts for events > baseline and block begin + block end > baseline pooled (i.e. summed) over TMS conditions.

Main Effects of TMS

To assess the overall effect of TMS condition, main effects of TMS were identified by comparing IPS > Sham and Sham > IPS pooled (i.e. summed) over visual and auditory conditions.

Effects of Task-relevant Visual Input

The effects of task-relevant visual input were analysed in two steps. First, we tested for main effects of task-relevant visual input by comparing visual present and visual absent trials [(AV + V) > (A + ¬V) and (A + ¬V) > (AV + V)] pooled (i.e. summed) over IPS and Sham stimulation. Second, interactions between TMS condition and visual input ($[(AV + V) > (A + \neg V)]_{IPS} > [(AV + V) > (A + \neg V)]_{Sham}$ and $[(A + \neg V) > (AV + V)]_{IPS} > [(A + \neg V) > (AV + V)]_{Sham}$) were evaluated to test for TMS modulations that depended on the current bottom-up visual input.

Effects of Auditory Context

Equivalent comparisons were performed to test for the main effects of auditory input [(AV + A) > (V + ¬V) and (V + ¬V) > (AV + A), pooled (i.e. summed) over IPS and Sham stimulation] and its interaction with TMS condition ($[(AV + A) > (V + \neg V)]_{IPS} > [(AV + A) > (V + \neg V)]_{Sham}$ and $[(V + \neg V) > (AV + A)]_{IPS} > [(V + \neg V) > (AV + A)]_{Sham}$).

Modulatory Effects of Auditory Context

Modulatory effects of auditory context on neural responses during performance of a visual detection task were evaluated in two steps. First, audiovisual interactions [(AV + ¬V) > (V + A) and (V + A) > (AV + ¬V), pooled over IPS and Sham stimulation] and interactions between visual input, auditory context and TMS condition ($[(AV + \neg V) > (V + A)]_{IPS} > [(AV + \neg V) > (V + A)]_{Sham}$ and $[(V + A) > (AV + \neg V)]_{IPS} > [(V + A) > (AV + \neg V)]_{Sham}$) were tested for within the entire brain.

Second, to specifically determine whether the activation pattern in regions that showed interaction effects between visual input and TMS (i.e. interaction effects between task-relevant bottom-up and

top-down signals) changed under different auditory contexts, we performed ROI analyses in those regions by extracting from each significant cluster the average parameter estimates for each condition and performing a direct comparison by means of analyses of variance (ANOVAs). Clusters were identified using an uncorrected auxiliary height threshold of $p = 0.01$ and no extent threshold. Please note that these analyses do not constitute a biased inference as the contrasts used for defining the regions of interest are orthogonal to those used for testing for modulatory effects of auditory context (Friston et al., 2006).

Search Volume Constraints

Except for the three-way interactions described above, effects were tested for within the entire brain and, based on our a priori hypothesis, in the auditory cortices. The region of interest for the auditory cortex was defined using the SPM Anatomy Toolbox (Eickhoff et al., 2005). The anatomical mask encompassed 975 voxels in the bilateral cytoarquitectonic maps TE 1.0, TE 1.1, and TE 1.2.
Unless stated otherwise, we report activation at $p < 0.05$ corrected at the cluster level for multiple comparisons (family-wise error rate) based on Gaussian Random Field theory within the entire brain and using an auxiliary uncorrected voxel threshold of $p = 0.01$ (Hayasaka and Nichols, 2003).

Eye monitoring (outside the scanner)

To ensure that the observed activation pattern did not result from eye movements, twitches, or startle effects, 8 additional participants took part in a supplementary experiment performed with equivalent parameters outside the scanner. One experimental run was acquired per participant for each TMS condition. To account for the absence of the high-current filter used in the concurrent TMS-MRI setup (Moisa et al., 2009), the TMS intensity was reduced to 63% of total output.
Horizontal and vertical eye movements were recorded using an iView XTM RED-III remote eyetracker system (SensoMotoric Instruments Inc., Needham/Boston, MA, USA) (50 Hz sampling rate). The eyetracking system was calibrated using a 13-point calibration. Eye position data were automatically corrected for blinks and converted to radial velocity.
For each trial the mean distance (degrees) from the fixation cross, the number of saccades (defined by a radial eye velocity threshold > 30°/s for a minimum of 60ms duration and radial amplitude larger than 5°), and the number of blinks were quantified for the period during which the fixation cross was blue (see *Experimental Design & Task*).
Across all participants saccades were almost completely absent, hence no further analyses were performed for this index. The two remaining indices were independently entered into a 3-way RM-ANOVA with the factors TMS condition (right IPS and Sham), auditory context (A present and A absent) and task-relevant visual input (V present and V absent).

Results

Behavioural Data

Participants performed a demanding visual detection task. In every trial, they had to report their percept (seen or unseen) of a visual stimulus that was present in half of the trials. For each participant, the behavioural indices were calculated for visual present and visual absent trials separately for each auditory context and TMS condition. Averaged percent correct responses and reaction time data for each individual condition are summarized in Table 3.1.

To test for significant differences between TMS conditions and auditory contexts, the proportion of correct responses for visual present and visual absent trials were entered in a 3-way RM-ANOVA. Apart from the expected main effect of visual input ($F_{(1,9)} = 27.142$; $p < 0.001$), there were no main effects of TMS ($F_{(1,9)} = 0.059$; $p = 0.814$) or auditory context ($F_{(1,9)} = 0.212$; $p = 0.656$), nor were there interactions between TMS and auditory context ($F_{(1,9)} = 0.108$; $p = 0.750$), TMS and visual input ($F_{(1,9)} = 0.006$; $p = 0.939$), auditory context and visual input ($F_{(1,9)} = 0.053$; $p = 0.824$), or between the three factors ($F_{(1,9)} = 0.859$; $p = 0.378$).

In addition, individual median reaction times were calculated for each condition separately. Reaction time data were entered in a 3-way RM-ANOVA with factors TMS condition (IPS, Sham), auditory context (A present, A absent) and task-relevant visual input (V present, V absent). This analysis did not reveal any significant main effects of TMS ($F_{(1,9)} = 0.240$; $p = 0.636$) or visual input ($F_{(1,9)} = 0.567$; $p = 0.471$), nor were there significant interactions between the TMS and auditory context ($F_{(1,9)} = 0.526$; $p = 0.487$), TMS and visual input ($F_{(1,9)} = 1.989$; $p = 0.192$) or between the three factors ($F_{(1,9)} = 0.065$; $p = 0.805$). However, there was a significant main effect of auditory context ($F_{(1,9)} = 6.145$; $p = 0.035$) and a significant interaction between auditory context and visual input ($F_{(1,9)} = 7.644$; $p = 0.022$).

To summarize, in line with other concurrent TMS-fMRI studies (Blankenburg et al., 2010; Moisa et al., 2012), our TMS manipulation did not elicit any behavioural changes. Hence, our TMS manipulation functioned as a purely physiological perturbation method that allowed examining influences on remote interconnected brain areas.

Table 3.1. Behavioural responses averaged across participants (± SD).

	Proportion Correct (%)				***Reaction Times (ms)***			
TMS Sites	*A Present*		*A Absent*		*A Present*		*A Absent*	
	V Present	*V Absent*	*V Present*	*V Absent*	*V Present*	*V Absent*	*V Present*	*V Absent*
IPS	75 ± 19	98 ± 1	74 ± 23	98 ± 1	704 ± 89	695 ± 79	710 ± 84	718 ± 63
Sham	75 ± 14	99 ± 1	75 ± 13	99 ± 1	699 ± 93	675 ± 98	712 ± 99	704 ± 89

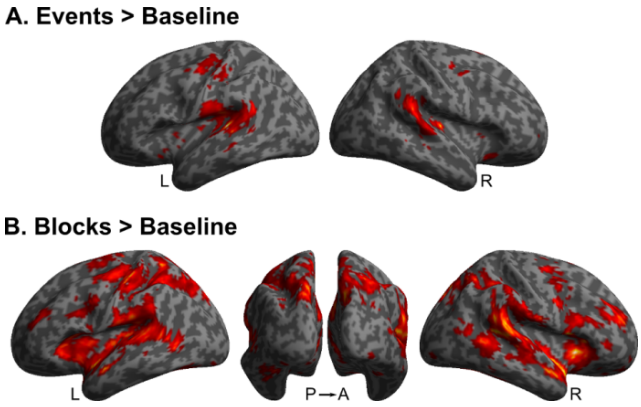

Figure 3.2. Overall Task Effects. Activations induced by contrasting **(A)** events and **(B)** blocks against the unmodelled baseline are rendered on an inflated SPM template of the entire brain. For illustrational purposes only, effects are displayed at a height threshold of $p = 0.01$ uncorrected and an extent threshold of 100 voxels.

Conversely, the auditory context had a modulatory effect on reaction time data. Specifically, for visual absent trials participants were in average 26 ms faster to respond when a sound was presented, whereas the difference in reaction times between auditory contexts during visual present trials was not as pronounced but still apparent (9 ms). Hence, in particular for visual absent trials, the auditory signal served as a precise temporal cue for target onset, which resulted in accelerated responses.

Neuroimaging Data

The neuroimaging data were analysed in five steps. First, the overall task effects were evaluated. Second, the main effects of TMS were tested for by directly comparing IPS- and Sham-TMS conditions. Third, the effects of task-relevant visual input were characterized by pooling over auditory contexts and computing main effects of visual input and interaction effects with TMS. Forth, the main effects of auditory context and interactions between auditory context and TMS conditions were similarly identified. Lastly, modulatory effects of auditory input were evaluated in the entire brain and within those regions that showed interaction effects between task-relevant visual input and TMS condition.

Overall Task Effects

We initially contrasted blocks and events against the resting baseline condition in order to evaluate the overall task effects. Events elicited significant activations in the bilateral auditory cortices likely as a result of the TMS clicks that were absent during baseline periods (Fig. 3.2A). Furthermore, significant effects were also observable in a motor network comprising the left motor cortex (Fig. 3.2A) and the right cerebellum (not shown), which is consistent with button-responses given with the right hand.

As expected, block periods increased activations in the attentional network that included bilateral frontoparietal regions and the bilateral insulae, plus areas of the occipital, motor and temporal cortices (Fig. 3.2B).

Main Effects of TMS

Main effects of TMS were identified by directly comparing IPS- and Sham-TMS conditions while pooling over auditory contexts and visual input. IPS- relative to Sham-TMS increased activations in the right parietal cortex. Precisely, significant activation clusters were found in the right superior parietal lobe, extending to the right postcentral gyrus and the right paracentral lobule (see Fig. 3.3A and Table 3.2). The average coil position for IPS stimulation is shown as a green circle in Fig. 3.3A. Note that IPS- relative to Sham-TMS did not activate the auditory and somatosensory cortices, suggesting that the Sham condition served as a good control for non-specific TMS effects in this study.

The comparison for Sham relative to IPS-TMS did not reveal any significant effects.

Effects of task-relevant visual input

Main Effects

Main effects of task-relevant visual input were calculated by pooling over auditory contexts and TMS conditions. The presence of targets increased activations in the right anterior insula, extending to the right inferior frontal gyrus (Fig. 3.3B.i, Table 3.2), a region that was often reported to be part of the salience network (Menon and Uddin, 2010). Notably, targets did not activate the primary visual cortex. This can be explained by the nature of our visual stimuli. Their size and duration, together with their peripheral location were probably not strong enough to produce BOLD activity in primary visual areas that could be reliably detected at the spatial resolution of our whole-brain EPI images.

However, deactivations in the left lingual and middle occipital gyri and the bilateral inferior occipital and fusiform gyri were observed for the comparison between visual absent and visual present trials (see Fig. 3.3B.i and Table 3.2). Specifically, independently of the TMS condition deactivations in these areas were increased for visual absent relative to visual present trials. Supplementary significant activations were also observed in the left orbitofrontal cortex and parahippocampal gyrus (Table 3.2).

Interaction Effects with TMS

Visual state-dependent TMS effects were characterized by testing for interactions between visual input and TMS conditions. The interaction contrast between (AV + V) > (A + ¬V) and IPS > Sham revealed significant activation clusters in the right fusiform gyrus extending to the right inferior and middle temporal gyri (lower part of Fig. 3.3B.ii, Table 3.3) and in the right posterior/middle insula extending laterally to the posterior part of BA44 (Fig. 3.3C, Table 3.3). In visual areas, parameter plots suggest that TMS over the IPS modulated activations in occipito-temporal visual regions by specifically increasing visual-evoked responses up to the level observed during visual absent trials.

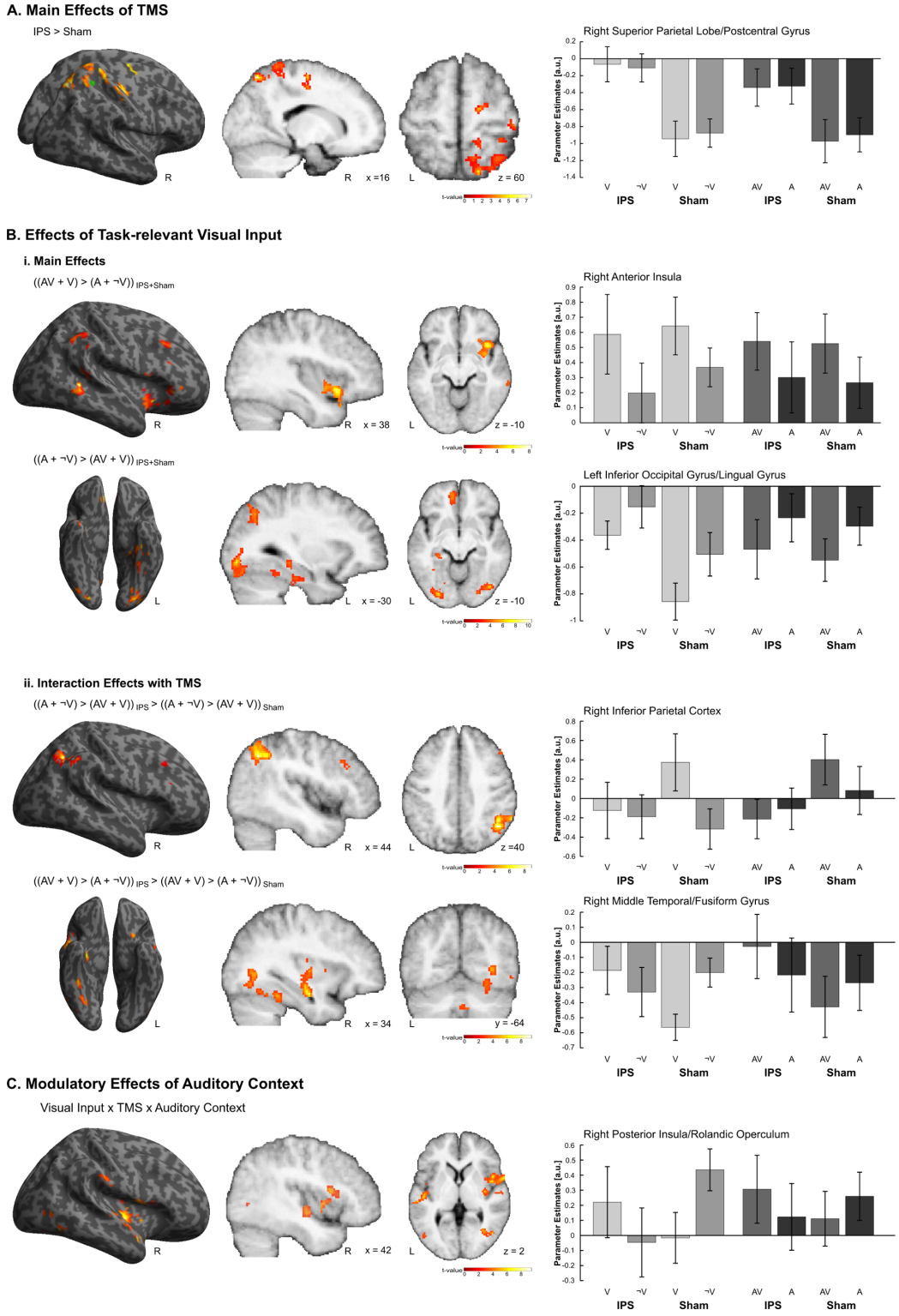

Figure 3.3. **(A)** Main Effects of TMS. Activations induced in the right parietal cortex by IPS- relative to Sham-TMS. The green circle marks the averaged reached position of the TMS coil during IPS stimulation. **(B)** Effects of Task-relevant Visual Input. *(i) Main Effects*. Activations induced in the right anterior insula by comparing visual present relative to visual absent and in the inferior occipital/lingual gyrus by comparing visual absent relative to visual present trials. *(ii) Interaction Effects with TMS*. Interaction effects between visual input and TMS conditions in the right inferior parietal cortex and in the right middle temporal/fusiform gyrus. **(C)** Modulatory Effects of Auditory Context. Activations in the right posterior insula showing interaction effects between TMS and visual input that were

In contrast, the interaction contrast between (AV + V) > (A + ¬V) and Sham > IPS showed effects in the right angular gyrus and inferior parietal lobe (upper part of Fig. 3.3B.ii, Table 3.3). Here, independently of the auditory context, IPS-TMS abolished visual-evoked activations observed during normal processing conditions.

Effects of Auditory Context

Main Effects

Main effects of auditory context were identified in an equivalent way to those of visual input. In particular, we evaluated auditory-evoked effects by pooling over the remaining conditions. Given the *a priori* hypotheses that auditory stimuli should activate auditory cortices, these effects were tested for within an anatomically defined mask comprising primary auditory areas (see *Search Volume Constraints*). Indeed, the presence of auditory stimuli increased activations in bilateral auditory cortices, with a significant activation cluster in the right Heschl's gyrus (Fig. 3.4A.i, Table 3.2). The absence of more reliable activations can be explained by the fact that the auditory cortex was already being strongly activated by the additional scanner noise and TMS clicks (see *Overall Task Effects*), which rendered the auditory stimuli too weak to elicit additional significant activations. The opposite comparison did not reveal any effects.

Interaction Effects with TMS

In addition, interaction effects between auditory context and TMS condition were tested for within the entire brain. Particularly, the interaction contrast between (AV + A) > (V + ¬V) and IPS > Sham revealed effects in the right middle temporal gyrus extending to the right angular and middle occipital gyri (Fig. 3.4A.ii, Table 3.3). This activation cluster did not survive multiple comparisons across the entire brain. However, it is referred here for completeness, as its location closely corresponds to areas of the posterior superior temporal sulcus that not only exhibit response overlaps to both visual and auditory stimulation in isolation (Driver and Noesselt, 2008) but have also been implicated in audiovisual temporal and object processing (Lewis et al., 2005; Noesselt et al., 2007).

---

modulated by the auditory context. All effects are rendered on an inflated SPM template of the entire brain and displayed on sagittal and axial slices of a mean image created by averaging the subjects' normalized structural images. For illustrational purposes only, effects are displayed at a height threshold of $p = 0.01$ uncorrected and an extent threshold of 100 voxels. Bar plots represent mean cluster parameter estimates (± standard error of the mean) at the respective locations displayed on the left, which were obtained by averaging across voxel-wise beta values extracted from each cluster for each individual condition. The bar graphs represent the size of the effect in non-dimensional units (corresponding to % whole-brain mean).

Modulatory Effects of Auditory Context

To examine how auditory context modulated the task-induced activation pattern, audiovisual interactions and 3-way interactions between all the three factors were tested for within the entire brain and within those regions showing visual state-dependent TMS effects.

Specifically, for each participant beta values were averaged within clusters that exhibited significant interactions between visual input and TMS condition. These clusters were localized in the right posterior/middle insula extending laterally to the posterior ventral lateral prefrontal cortex (VLPFC), the right fusiform/middle temporal gyrus and the right inferior parietal lobe (Table 3.3). For each cluster, individual averaged beta values were entered in 3-way RM-ANOVAs with factors TMS condition (right IPS, Sham), auditory context (A present and A absent) and visual input (V present and V absent). As expected, all clusters exhibited significant interactions between visual input and TMS (right insula: $F_{(1,9)} = 50.039$; $p < 0.001$; right fusiform: $F_{(1,9)} = 47.115$; $p < 0.001$; right inferior

Table 3.2. Main Effects

	MNI Coordinates (mm)			*Z Score*	*#Voxels in Cluster*	p_{FWE}*-value*
Brain Regions	x	y	z	*(peak)*		*(cluster)*
Main Effects of TMS						
IPS > Sham						
Right Superior Parietal Lobule	16	-68	58	4.15	737	0.009
Right Postcentral Gyrus	12	-40	70	3.99		
Right Paracentral Lobule	8	-44	68	3.96		
Main Effects of Visual Target Presence						
$(AV + V) > (A + \neg V)_{IPS + Sham}$						
Right Anterior Insula	38	16	-10	3.89	443	0.009
Right Inferior Frontal Gyrus	50	12	8	3.56		
$(A + \neg V) > (AV + V)_{IPS + Sham}$						
Left Inferior Occipital Gyrus	-30	-84	-8	4.04	410	0.032
Left Middle Occipital Gyrus	-28	-78	4	3.49		
Left Lingual Gyrus	-26	-86	-16	3.27		
Left Fusiform Gyrus	-30	-78	-18	3.06		
Left Hippocampus	-22	-24	-30	3.73	534	0.007
Left Parahippocampal Gyrus	-18	-26	-18	3.57		
Left Anterior Fusiform Gyrus	-36	-22	-28	3.34		
Left Mid Orbital Gyrus	-8	48	-8	3.30	397	0.038
Right Rectal Gyrus	10	36	-20	2.95		
Main Effects of Auditory Context						
$(AV + A) > (V + \neg V)_{IPS + Sham}$						
Right Heschl's Gyrus	46	-24	12	4.05	101*	0.025*
Right Superior Temporal Gyrus	50	-14	4	2.62		0.323*
Left Superior Temporal Gyrus	-48	-28	16	3.61	118*	0.266*

p-values are reported at the cluster level and corrected for multiple comparisons within the entire brain or at the peak level within the auditory cortex (*) using an auxiliary uncorrected voxel threshold of $p = 0.01$ and an extent threshold of 0 voxels. FWE = Family-wise error correction.

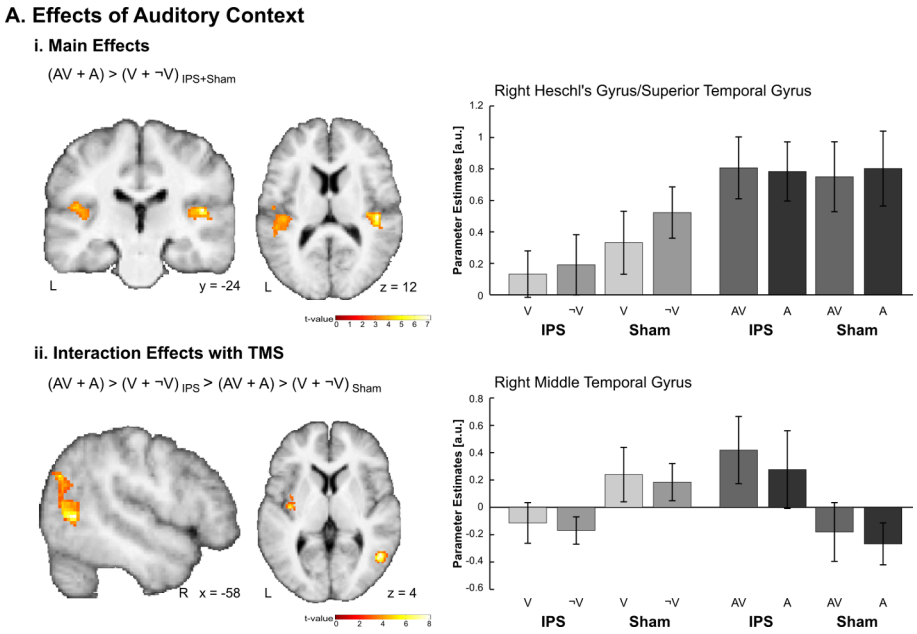

Figure 3.4. Effects of Auditory Context. (A) *(i) Main Effects*. Activations induced in auditory cortices by comparing auditory present relative to auditory absent trials. *(ii) Interaction Effects with TMS*. Activations in the right posterior middle temporal gyrus that resulted from the interaction between auditory context and TMS. All effects are displayed on coronal, sagittal and axial slices of a mean image created by averaging the subjects' normalized structural images. For illustrational purposes only, effects are displayed at a height threshold of $p = 0.01$ uncorrected and an extent threshold of 100 voxels. Bar plots represent mean cluster parameter estimates (± standard error of the mean) at the locations displayed on the left, which were obtained by averaging across voxel-wise beta values extracted from each cluster for each individual condition. The bar graphs represent the size of the effect in non-dimensional units (corresponding to % whole-brain mean).

parietal: $F_{(1,9)} = 40.982$; $p < 0.001$). Likewise, there was a significant main effect of visual input within the occipital and parietal clusters (occipital: $F_{(1,9)} = 5.644$; $p = 0.042$; parietal: $F_{(1,9)} = 5.618$; $p = 0.042$).

Crucially, there was also a significant three way interaction between visual input, auditory context and TMS condition in the insular cluster ($F_{(1,9)} = 8.350$; $p = 0.018$). In particular, in this region the auditory input reduced the interaction effects between visual input and TMS condition (Fig. 3.3C, right).

At the whole-brain level the analyses did not reveal significant effects when corrected at the cluster level for multiple comparisons.

Eyetracker Data

Two independent 3-way RM-ANOVAs with factors TMS condition (right IPS and Sham), auditory context (A present and A absent) and task-relevant visual input (V present and V absent) were performed for the mean distance from the fixation cross and the number of blinks.

For the number of blinks index, the analysis did not show main effects of TMS ($F_{(1,7)} = 0.112$; $p = 0.748$), visual input ($F_{(1,7)} = 0.028$; $p = 0.872$) or auditory context ($F_{(1,7)} = 0.385$; $p = 0.555$). There were also no significant interactions between TMS and auditory context ($F_{(1,7)} = 2.194$; $p = 0.182$),

TMS and visual input ($F_{(1,7)} = 1.823$; $p = 0.219$) or visual input and auditory context ($F_{(1,7)} = 1.057$; $p = 0.338$), nor was there a significant three way interaction between all factors ($F_{(1,7)} = 0.420$; $p = 0.538$).

For the mean distance from the fixation cross, there was no main effect of TMS ($F_{(1,7)} = 1.343$; $p = 0.285$), visual input ($F_{(1,7)} = 0.294$; $p = 0.604$) or a main effect of auditory context ($F_{(1,7)} = 0.164$; $p = 0.698$). The analysis did also not result in significant interactions between TMS and auditory context ($F_{(1,7)} = 0.175$; $p = 0.689$), TMS and visual input ($F_{(1,7)} = 0.553$; $p = 0.482$) or visual input and auditory context ($F_{(1,7)} = 0.345$; $p = 0.575$), nor was there a significant interaction between the three factors ($F_{(1,7)} = 0.633$; $p = 0.452$).

None of the RM-ANOVAs revealed any significant main effects or interactions demonstrating that differences in eye movements are unlikely to account for the observed activation profile in our fMRI data.

Table 3.3. State-dependent TMS effects

	MNI Coordinates (mm)			*Z Score*	*#Voxels in Cluster*	p_{FWE}-*value*
Brain Regions	x	y	z	*(peak)*		
Interactions between TMS and Visual						
$(AV + V) > (A + \neg V)_{IPS} > (AV + V) > (A + \neg V)_{Sham}$						
Right Posterior/Middle Insula	44	4	2	3.80	478	0.010
Right Rolandic Operculum	60	8	2	3.72		
Right Temporal Pole	54	4	-2	3.47		
Right Inferior Frontal Gyrus	42	18	10	2.65		
Right Inferior Temporal Gyrus	54	-58	-10	3.69	420	0.022
Right Middle Temporal Gyrus	46	-68	2	3.47		
Right Fusiform Gyrus	34	-42	-20	3.31		
Right Hippocampus	34	-10	-18	4.14	351	0.056
Right Insula	38	-12	-12	3.91		
Right Putamen	36	-10	2	3.57		
$(AV + V) > (A + \neg V)_{Sham} > (AV + V) > (A + \neg V)_{IPS}$						
Right Angular Gyrus	44	-58	40	4.43	444	0.016
Right Inferior Parietal Lobule	44	-52	40	3.92		
Interactions between TMS and Auditory Context						
$(AV + A) > (V + \neg V)_{IPS} > (AV + A) > (V + \neg V)_{Sham}$						
Right Middle Temporal Gyrus	50	-58	4	4.26	328	0.125
Right Angular Gyrus	50	-68	30	3.52		
Right Middle Occipital Gyrus	54	-68	24	3.23		

p-values are reported at the cluster level and corrected for multiple comparisons within the entire brain using an auxiliary uncorrected voxel threshold of $p = 0.01$ and an extent threshold of 0 voxels. FWE = Family-wise error correction.

Discussion

This concurrent TMS-fMRI study investigated the effects of IPS-TMS on task-related activity in a context of sustained attention to the left visual hemifield. To engage the attentional network, participants performed a demanding visual detection task that manipulated bottom-up visual input in a peripheral visual location. Moreover, since the detection of sensory stimuli can be influenced by co-occurring task-irrelevant sensory events, we further manipulated the bottom-up sensory context by introducing runs in which an auditory sound was presented at target-onset independently of the actual presence of the task-relevant visual input. Behaviourally, IPS-TMS did not interfere with normal task performance, thus ensuring that TMS-induced modulations on task-related activations were not confounded by behavioural changes. Conversely, the introduction of the bottom-up auditory context reduced the temporal uncertainty for task-relevant responses, as reflected by a diminishing effect of sound on reaction time data that was particularly evident for target absent trials. At the BOLD level, the acquisition of whole-brain EPI images revealed interactions between bottom-up and top-down signals induced by IPS-TMS in the right inferior parietal and occipito-temporal areas and in regions of the right posterior/middle insular cortex extending to the VLPFC. In the latter regions these interactions were further modulated by the additional auditory context.

To appropriately interact with the environment, the brain needs to be able to detect relevant sensory events even in cluttered surroundings. An influential model of attention control postulates the existence of two anatomically separate networks each undertaking distinct attentional functions (Corbetta and Shulman, 2002; Corbetta et al., 2008). According to this account, a dorsal frontoparietal network, comprising the superior parietal lobe, the IPS and the frontal eye fields, supports top-down endogenous attention by controlling factors such as prior knowledge, expectations and current goals. On the other hand, a mostly right lateralized ventral frontoparietal network, composed of the temporo-parietal junction (TPJ) and areas of the ventral frontal cortex that include the anterior insula, is involved in stimulus-driven control and responds to the detection of behaviourally relevant sensory events in the environment. Consistent with its role in the ventral attentional network, the anterior insula has likewise been considered a critical hub of the salience network that enables task-related information processing through the amplification of salient sensory events (Menon and Uddin, 2010). In line with previous research, our results show activation increases in the right anterior insula evoked by the presence of the task-relevant visual input (Fig. 3.3B.i). Interestingly, target-evoked increases in the right anterior insula were mirrored in bilateral occipito-temporal visual areas by target-evoked activation suppressions relatively to the level observed during target absent trials (Fig. 3.3B.i). This stimulus-driven anti-correlated activation pattern shared by a node of the ventral attentional/salience network and occipito-temporal visual areas raises the question of whether these effects in visual areas are purely driven by bottom-up sensory input or instead reflect an interaction between top-down and bottom-up factors.

In fact, numerous studies have shown that activity in extrastriate visual areas can be modulated by attention (e.g. Martínez et al., 1999; Hopfinger et al., 2000; Yantis and Serences, 2003). For

instance, Kastner et al. (1999) showed that activation in visual areas can increase even in the absence of visual stimulation by the mere anticipation of a behaviourally relevant stimulus. The authors propose that such increases might reflect top-down attentional biases prompted by covertly attending to the expected stimulus location. In this regard, the relative suppression induced by the task-relevant visual input in our study might similarly reflect the end of expectation for the visual stimulus following its detection in the right anterior insula.

As part of the dorsal attentional network, the IPS stands as a potential candidate for the source of these sensory-dependent top-down influences. In fact, alongside its role in top-down attention, the IPS has been shown to be sensitive to stimulus-driven aspects of attentional control (Geng and Mangun, 2009) and to integrate sensory and goal-directed information in order to form a priority or salience map of the environment (Gottlieb, 2007; Ptak, 2012). To investigate the role of this region in stimulus-dependent modulations during a demanding attentional context, we used TMS to disturb activity in the right anterior IPS during task performance. Relative to Sham-TMS, IPS stimulation induced activation increases in the right superior parietal lobes that were insensitive to the current bottom-up visual input (Fig. 3.3A). Yet, this TMS perturbation interacted with the task-relevant visual input in the inferior parietal lobe (IPL), in particular in the right angular gyrus (Fig. 3.3Bii). Although sometimes included as part of the TPJ in the ventral attentional network (Corbetta and Shulman, 2002; Chambers et al., 2004a), attention literature has more generally associated this region with sustaining attention during task-performance as well as with the detection of salient events in the environment (for a review see Singh-Curry and Husain, 2009). Moreover, in a recent attempt to identify a unified function that takes into account its involvement in a variety of cognitive tasks, it has been proposed that the angular gyrus integrates bottom-up information and top-down predictions in a context-dependent fashion through a complex interplay with other neural systems that are important for the task at hand (Seghier, 2013).

In accordance with these accounts, under normal processing conditions the IPL showed equivalent activation increases in response to task-relevant visual input. Conversely, disturbing IPS activity with TMS eliminated these relative increases (Fig. 3.3B.ii). More remarkably, these IPS-TMS modulations were accompanied by stimulus-evoked amplifications in right visual occipito-temporal areas up to the level observed for target-absent trials (Fig. 3.3B.ii). Thus, the seemingly stimulus-driven activation pattern observed in visual areas was actually influenced by perturbation of ongoing top-down signals. In keeping with the idea of expectation biases induced by covertly attending to the stimulus location, these results suggest that under normal processing conditions, the task-relevant visual input was detected by the IPL (possibly in combination with the anterior insula), thereby triggering the end of expectations in visual areas. However, the disruption of IPS activity interfered with the detection of task-relevant events in the IPL, which consequently abolished top-down expectation biases in visual cortices. Yet, more important than their exact interpretation, these effects reflect an interaction between bottom-up and top-down factors that were not directly exerted by the IPS, but involved different areas across sensory and attentional systems.

The previous observations considered interactions between task-relevant stimuli and top-down signals. However, in natural situations relevant events are embedded in a continuous stream of irrelevant sensory information. In circumstances in which a task-relevant stimulus is paired through

temporal or spatial constraints with signals from other sensory modalities, the additional sensory information might even influence task performance in a detrimental or beneficial way (Lippert et al., 2007; Fiebelkorn et al., 2011; Kim et al., 2012). We investigated the effects of different sensory contexts by introducing auditory stimuli as an additional contextual factor across runs. Behaviourally, the auditory contextual effect on task processing was evident from accelerated decisions, in particular in the absence of the task-relevant visual stimulus. Thus, whilst not informative of the correct response, the auditory sound contained task-relevant temporal information that influenced ongoing top-down processes.

In the brain, these influences were manifested by modulatory effects of auditory context in the right posterior/middle insula extending laterally to the posterior VLPFC. Specifically, interactions between TMS and task-relevant visual input in these regions were significantly attenuated during auditory runs (Fig. 3.3C). Contrasting its more anterior counterpart, the posterior/middle insula has been associated with sensorimotor integration (Kurth et al., 2010; Cauda et al., 2011; Deen et al., 2011). Furthermore, it has not only been shown to respond to stimuli from different sensory modalities (Downar et al., 2000) but also to substantiate audiovisual integration processes (Calvert et al., 2001; Naghavi et al., 2007). On the other hand, the posterior VLPFC has been associated with contextual sensory control and action selection (Koechlin and Summerfield, 2007; Verbruggen et al., 2010; Levy and Wagner, 2011). Thus, the interactions between TMS and the task-relevant visual input in these regions might reflect an exchange of control signals with the IPS to support the mapping of sensory stimuli into appropriate behavioural responses. Moreover, the auditory modulations emphasise the contextual nature of this exchange, whereby an auditory sound endowed with supplementary implicit timing information is able to reduce the need for top-down control from parietal regions.

To summarize, using concurrent TMS-fMRI this study provided causal evidence for interactions between task-relevant bottom-up input and top-down signals under a context of high attentional demands. Specifically, IPS-TMS abolished target-evoked activation increases in the right IPL, while having complementary effects in right occipito-temporal visual areas. This pattern suggests that processing of relevant sensory information during goal-directed behaviour involves a complex interplay between these regions. Moreover, in areas of the right posterior/middle insular cortex and the right VLPFC, interactions between TMS and visual input were modulated by the current auditory context. We propose that IPS-TMS influences in these regions reflect the exchange of control signals associated with the planning of an appropriate response, which is attenuated with the occurrence of an extra auditory sound loaded with implicit top-down information related to the task.

References

Algazi VR, Duda RO, Thompson DM, Avendano C (2001) The CIPIC HRTF database. Proc 2001 IEEE Work Appl Signal Process to Audio Acoust (Cat No01TH8575).

Bestmann S (2003) On the Synchrinzation of Transcranial Magnetic Stimulation and Functional Echo-Planar Imaging. J Magn Reson Imaging.

Blankenburg F, Ruff CC, Bestmann S, Bjoertomt O, Josephs O, Deichmann R, Driver J (2010) Studying the role of human parietal cortex in visuospatial attention with concurrent TMS-fMRI. Cereb Cortex 20:2702–2711.

Brainard DH (1997) The Psychophysics Toolbox. Spat Vis 10:433–436.

Calvert GA, Hansen PC, Iversen SD, Brammer MJ (2001) Detection of audio-visual integration sites in humans by application of electrophysiological criteria to the BOLD effect. Neuroimage 14:427–438.

Cauda F, D'Agata F, Sacco K, Duca S, Geminiani G, Vercelli A (2011) Functional connectivity of the insula in the resting brain. Neuroimage 55:8–23.

Chambers CD, Payne JM, Stokes MG, Mattingley JB (2004a) Fast and slow parietal pathways mediate spatial attention. Nat Neurosci 7:217–218.

Chambers CD, Stokes MG, Mattingley JB (2004b) Modality-specific control of strategic spatial attention in parietal cortex. Neuron 44:925–930.

Corbetta M, Patel G, Shulman GL (2008) The reorienting system of the human brain: from environment to theory of mind. Neuron 58:306–324.

Corbetta M, Shulman GL (2002) Control of goal-directed and stimulus-driven attention in the brain. Nat Rev Neurosci 3:201–215.

Deen B, Pitskel NB, Pelphrey K a (2011) Three systems of insular functional connectivity identified with cluster analysis. Cereb Cortex 21:1498–1506.

Downar J, Crawley AP, Mikulis DJ, Davis KD (2000) A multimodal cortical network for the detection of changes in the sensory environment. Nat Neurosci 3:277–283.

Driver J, Noesselt T (2008) Multisensory Interplay Reveals Crossmodal Influences on "Sensory-Specific" Brain Regions, Neural Responses, and Judgments. Neuron 57:11–23.

Duecker F, Sack AT (2013) Pre-stimulus sham TMS facilitates target detection. PLoS One 8:e57765.

Eickhoff SB, Stephan KE, Mohlberg H, Grefkes C, Fink GR, Amunts K, Zilles K (2005) A new SPM toolbox for combining probabilistic cytoarchitectonic maps and functional imaging data. Neuroimage 25:1325–1335.

Fiebelkorn IC, Foxe JJ, Butler JS, Molholm S (2011) Auditory facilitation of visual-target detection persists regardless of retinal eccentricity and despite wide audiovisual misalignments. Exp brain Res 213:167–174.

Friston KJ, Holmes AP, Price CJ, Büchel C, Worsley KJ (1999) Multisubject fMRI studies and conjunction analyses. Neuroimage 10:385–396.

Friston KJ, Holmes AP, Worsley KJ, Poline J-B, Frith CD, Frackowiak RSJ (1995) Statistical parametric maps in functional imaging: A general linear approach. Hum Brain Mapp 2:189–210.

Friston KJ, Rotshtein P, Geng JJ, Sterzer P, Henson RN (2006) A critique of functional localisers. Neuroimage 30:1077–1087.

Geng JJ, Mangun GR (2009) Anterior intraparietal sulcus is sensitive to bottom-up attention driven by stimulus salience. J Cogn Neurosci 21:1584–1601.

Gottlieb J (2007) From Thought to Action: The Parietal Cortex as a Bridge between Perception, Action, and Cognition. Neuron 53:9–16.

Hayasaka S, Nichols TE (2003) Validating cluster size inference: random field and permutation methods. Neuroimage 20:2343–2356.

Heinen K, Ruff CC, Bjoertomt O, Schenkluhn B, Bestmann S, Blankenburg F, Driver J, Chambers CD (2011) Concurrent TMS-fMRI reveals dynamic interhemispheric influences of the right parietal cortex during exogenously cued visuospatial attention. Eur J Neurosci 33:991–1000.

Hilgetag CC, Théoret H, Pascual-Leone a (2001) Enhanced visual spatial attention ipsilateral to rTMS-induced "virtual lesions" of human parietal cortex. Nat Neurosci 4:953–957.

Hopfinger JB, Buonocore MH, Mangun GR (2000) The neural mechanisms of top-down attentional control. Nat Neurosci 3:284–291.

Kastner S, Pinsk M a, De Weerd P, Desimone R, Ungerleider LG (1999) Increased activity in human visual cortex during directed attention in the absence of visual stimulation. Neuron 22:751–761.

Kastner S, Pinsk MA (2004) Visual attention as a multilevel selection process. Cogn Affect Behav Neurosci 4:483–500.

Kim R, Peters M a K, Shams L (2012) 0 + 1 > 1: How adding noninformative sound improves performance on a visual task. Psychol Sci 23:6–12.

Kleiner M, Brainard D, Pelli D, Ingling A, Murray R, Broussard C (2007) What ' s new in Psychtoolbox-3 ? Foreword ; -). Whats New 36:14.

Koechlin E, Summerfield C (2007) An information theoretical approach to prefrontal executive function. Trends Cogn Sci 11:229–235.

Kurth F, Zilles K, Fox PT, Laird AR, Eickhoff SB (2010) A link between the systems: functional differentiation and integration within the human insula revealed by meta-analysis. Brain Struct Funct:1–16.

Leitão J, Thielscher A, Werner S, Pohmann R, Noppeney U (2013) Effects of parietal TMS on visual and auditory processing at the primary cortical level -- a concurrent TMS-fMRI study. Cereb Cortex 23:873–884.

Levy BJ, Wagner AD (2011) Cognitive control and right ventrolateral prefrontal cortex: reflexive reorienting, motor inhibition, and action updating. Ann N Y Acad Sci 1224:40–62.

Lewis JW, Brefczynski JA, Phinney RE, Janik JJ, DeYoe EA (2005) Distinct cortical pathways for processing tool versus animal sounds. J Neurosci 25:5148–5158.

Lippert M, Logothetis NK, Kayser C (2007) Improvement of visual contrast detection by a simultaneous sound. Brain Res 1173:102–109.

Macaluso E, Doricchi F (2013) Attention and predictions: control of spatial attention beyond the endogenous-exogenous dichotomy. Front Hum Neurosci 7:685.

Martínez a, Anllo-Vento L, Sereno MI, Frank LR, Buxton RB, Dubowitz DJ, Wong EC, Hinrichs H, Heinze HJ, Hillyard S a (1999) Involvement of striate and extrastriate visual cortical areas in spatial attention. Nat Neurosci 2:364–369.

Menon V, Uddin LQ (2010) Saliency, switching, attention and control: a network model of insula function. Brain Struct Funct 214:655–667.

Moisa M, Pohmann R, Ewald L, Thielscher A (2009) New coil positioning method for interleaved transcranial magnetic stimulation (TMS)/functional MRI (fMRI) and its validation in a motor cortex study. J Magn Reson Imaging 29:189–197.

Moisa M, Pohmann R, Uludağ K, Thielscher A (2010) Interleaved TMS/CASL: Comparison of different rTMS protocols. Neuroimage 49:612–620.

Moisa M, Siebner HR, Pohmann R, Thielscher A (2012) Uncovering a Context-Specific Connectional Fingerprint of Human Dorsal Premotor Cortex. J Neurosci 32:7244–7252.

Naghavi HR, Eriksson J, Larsson A, Nyberg L (2007) The claustrum/insula region integrates conceptually related sounds and pictures. Neurosci Lett 422:77–80.

Noesselt T, Rieger JW, Schoenfeld MA, Kanowski M, Hinrichs H, Heinze H-J, Driver J (2007) Audiovisual temporal correspondence modulates human multisensory superior temporal sulcus plus primary sensory cortices. J Neurosci 27:11431–11441.

Oliver R, Bjoertomt O, Driver J, Greenwood R, Rothwell J (2009) Novel “hunting” method using transcranial magnetic stimulation over parietal cortex disrupts visuospatial sensitivity in relation to motor thresholds. Neuropsychologia 47:3152–3161.

Ptak R (2012) The Frontoparietal Attention Network of the Human Brain: Action, Saliency, and a Priority Map of the Environment. Neurosci 18:502–515.

Ruff CC, Bestmann S, Blankenburg F, Bjoertomt O, Josephs O, Weiskopf N, Deichmann R, Driver J (2008) Distinct causal influences of parietal versus frontal areas on human visual cortex: evidence from concurrent TMS-fMRI. Cereb Cortex 18:817–827.

Ruff CC, Blankenburg F, Bjoertomt O, Bestmann S, Freeman E, Haynes J-D, Rees G, Josephs O, Deichmann R, Driver J (2006) Concurrent TMS-fMRI and psychophysics reveal frontal influences on human retinotopic visual cortex. Curr Biol 16:1479–1488.

Ruff CC, Blankenburg F, Bjoertomt O, Bestmann S, Weiskopf N, Driver J (2009) Hemispheric differences in frontal and parietal influences on human occipital cortex: direct confirmation with concurrent TMS-fMRI. J Cogn Neurosci 21:1146–1161.

Sack AT, Kohler A, Bestmann S, Linden DEJ, Dechent P, Goebel R, Baudewig J (2007) Imaging the brain activity changes underlying impaired visuospatial judgments: simultaneous FMRI, TMS, and behavioral studies. Cereb Cortex 17:2841–2852.

Seghier ML (2013) The angular gyrus: multiple functions and multiple subdivisions. Neuroscientist 19:43–61.

Serences JT, Yantis S (2006) Selective visual attention and perceptual coherence. Trends Cogn Sci 10:38–45.

Singh-Curry V, Husain M (2009) The functional role of the inferior parietal lobe in the dorsal and ventral stream dichotomy. Neuropsychologia 47:1434–1448.

Swisher JD, Halko MA, Merabet LB, McMains SA, Somers DC (2007) Visual topography of human intraparietal sulcus. J Neurosci 27:5326–5337.

Verbruggen F, Aron AR, Stevens M a, Chambers CD (2010) Theta burst stimulation dissociates attention and action updating in human inferior frontal cortex. Proc Natl Acad Sci U S A 107:13966–13971.

Watson AB, Pelli DG (1983) QUEST: a Bayesian adaptive psychometric method. Percept Psychophys 33:113–120.

Yantis S, Serences JT (2003) Cortical mechanisms of space-based and object-based attentional control. Curr Opin Neurobiol 13:187–193.

Chapter 4

Using concurrent TMS-fMRI to unravel the differential effects of occipital and parietal TMS during a demanding visual detection task

Joana Leitão[1,2], Axel Thielscher[1,3,4], Johannes Tuennerhoff[1], Uta Noppeney[1,2]

[1]Max Planck Institute for biological Cybernetics, 72076 Tübingen, Germany

[2]Computational Neuroscience and Cognitive Robotics Centre, University of Birmingham, B15 2TT Birmingham, UK

[3]Department of Electrical Engineering, Technical University of Denmark, 2800 Lyngby, Denmark

[4]DRCMR, Copenhagen University Hospital Hvidovre, 2650 Hvidovre, Denmark

Author contributions

Leitão and Noppeney designed the experiment. Stimuli were programmed and designed by Leitão. Thielscher contributed with TMS expertise. Leitão collected the data with the support of Tuennerhoff. Leitão analysed the data with the help of Noppeney. Leitão wrote the manuscript with the help of Thielscher and Noppeney.

Acknowledgments

This work was supported by the European Research Council and the Max Planck Society. The authors would like to thank Julian Hofmeister and Simone Götze for helping with data acquisition, Mario Kleiner for technical assistance and the medical doctors Daniel Zaldivar, Johannes Schultz and Matthias Munk for their availability during data acquisition and participants' screening. The authors declare no competing financial interests.

Abstract

Accumulating evidence supports the existence of a distributed network of frontoparietal and sensory areas that is involved in the detection of environmental visual stimuli. Moreover, it is increasingly acknowledged that while distinct nodes in this network have its own specialized function, they interact in a dynamical and context-dependent manner in order to achieve an appropriate and flexible behaviour. Whereas offline TMS studies have provided invaluable insights about the functionally role of specific nodes, they preclude inferences from a network perspective. This study used concurrent TMS-fMRI to evaluate differential TMS effects over two distinct nodes within this network on task-related BOLD activations during a demanding attentional task. Specifically, we applied 4 bursts of TMS over right occipital (Occ) cortex (BA17/18) and the right anterior IPS, while participants reported their percept (seen/unseen) of a visual stimulus presented on 50% of the trials in their left lower visual field. TMS effects of each experimental stimulation site were evaluated by independently comparing them with a control Sham-TMS condition. Our results show an overlap of Occ- and IPS-TMS main effects in right parietal lobes. However, interaction effects between TMS and visual input in occipito-temporal areas were specific for IPS-TMS. Together, these results suggest two distinct mechanisms underlying TMS-induced activations in parietal cortices: while IPS-TMS effects emerge as a result of locally perturbed activity that influences activations in remote occipito-temporal areas, Occ-TMS effects likely reflect compensatory mechanisms to counteract perturbed activity in low-level visual areas.

Keywords: interleaved/concurrent TMS-fMRI, right anterior parietal cortex, right occipital cortex, bottom-up vs. top-down

Introduction

Perceptual and attentional processes rely on a highly distributed and dynamic network of regions supporting interactions between sensory structures and frontoparietal brain areas. Most of the evidence for these interactions comes from research on the visual system. In fact, whereas it was traditionally thought that visual information processing occurred in a strictly hierarchical feedforward manner, it is now evident that sensory encoding in early visual areas can likewise be modulated by signals arising from higher-order association areas (Büchel et al., 1998; Kastner et al., 1999; Hopfinger et al., 2000; Bullier et al., 2001; Cardin et al., 2011). Moreover, there is increasing evidence showing that this signal exchange between different cortical structures does not operate in a unidirectional and independent fashion but relies on a bidirectional and recurrent interchange of feedback and feedforward information (Mumford, 1992; Lamme and Roelfsema, 2000; Rauss and Pourtois, 2013).

By providing a focal and non-invasive way of interfering with neural activity in the stimulated region, transcranial magnetic stimulation (TMS) has frequently been employed to investigate the role of specific nodes within this network of frontoparietal and sensory regions during attentional and perceptual processes. For instance, numerous behavioural studies have reported performance disturbances during visuospatial tasks when TMS was applied to the parietal cortices (Pascual-Leone et al., 1994; Hilgetag et al., 2001; Thut et al., 2005; Oliver et al., 2009). When applied over the occipital cortex, single pulse TMS or short TMS bursts can interfere with normal visual perception (Amassian et al., 1989; Kastner et al., 1998; Kamitani and Shimojo, 1999; Kammer et al., 2005b; Thielscher et al., 2010) or elicit visual percepts designated as phosphenes (Boroojerdi et al., 2000; Cowey and Walsh, 2000; Stewart et al., 2001; Rauschecker et al., 2004; Kammer and Baumann, 2010), thereby providing valuable insights on the role of early visual areas in conscious visual processing.

Yet, while these studies are extremely useful in establishing causal structure-function relationships, they fall short in elucidating how TMS interacts with activity both in the locally targeted area and from a network perspective. One way to partially overcome this limitation is by applying dual-site TMS protocols to study interactions between two interconnected brain areas. In particular, when applied to the visual system, these protocols have demonstrated feedback modulations from higher to earlier visual areas (Pascual-Leone and Walsh, 2001; Silvanto et al., 2005a, 2006; Koivisto et al., 2010). For instance, targeting areas V1/V2 and V5 at different time windows during a motion detection task, Silvanto et al. (2005b) have shown that the two critical windows for inducing suppression effects in V1/V2 flanked the critical window for V5 stimulation, thus suggesting complex recurrent interactions between the two regions in order to promote conscious vision.

An alternative to dual-site protocols is to directly evaluate the effects of TMS on local and distal interconnected regions by concurrently measuring activity in these regions through imaging techniques, such as EEG, PET or fMRI (for reviews see: Reithler et al., 2011; Bestmann and Feredoes, 2013). In particular, the concurrent combination of TMS and fMRI has recently provided causal evidence for modulatory influences from parietal and frontal areas on visual cortices (Ruff et

al., 2006, 2008; Blankenburg et al., 2010; Feredoes et al., 2011; Leitão et al., 2013). Critically, these modulatory influences highly depend on the current state of the modulated area. For instance, in a previous study (Chapter 3) we investigated how TMS to the right anterior intraparietal sulcus (IPS) modulated task-related activations during a demanding visual detection task that involved covert attention to the left visual field. Our results revealed that IPS- relative to Sham-TMS abolished target-evoked activation increases in the right inferior parietal lobe, while having opposite effects in right occipito-temporal visual areas. This pattern of activations suggests that processing of relevant sensory information during goal-directed behaviour involves a complex interplay between these regions.

While several previous concurrent TMS-fMRI studies have applied TMS to higher-order frontal and parietal regions to investigate top-down influences on visual areas, there is an absence of studies using this methodology to examine the effects of occipital TMS on task-related activations. However, since the detection of environmental stimuli relies on a distributed network of dynamically interacting areas, it is important to evaluate the effects of stimulating low-level sensory areas and to examine in which way these differ from those provoked by stimulation of higher-order association cortices in identical experimental paradigms.

The present study aimed to investigate the differential effects of parietal and occipital stimulation on task-related BOLD activations during a spatially selective visual attention task. Participants maintained covert attention to the left lower visual field where a low contrast visual target was presented in 50% of the trials. Critically, the contrast of the target was adapted for each subject to be associated with approximately 70% detection rate. In two separate sessions, we applied 4 TMS pulses (10 Hz) starting 200 ms after trial begin (i.e. 100 ms after target onset in target present trials) to the right IPS or to the right occipital cortex (BA17/BA18). Since direct comparisons between experimental TMS conditions are difficult to interpret in the absence of a neutral control condition, we evaluated the main effects of TMS by comparing each of the experimental conditions (Occ/IPS) with an additional control Sham-TMS session. Similarly, to investigate state-dependent TMS effects, interactions between Occ/IPS-TMS and task-relevant visual input were assessed in an analogous fashion.

Materials and Methods

Participants

Eight participants (3 male; mean age: 30.9 years; standard deviation: 8.2; Edinburgh Handedness inventory score (mean ± SD) of 75±17.7) took part in the experiment. Participants were right-handed with no history of neurological illness, had normal or corrected-to-normal vision and reported normal hearing. All participants gave informed consent prior to participation and the study was approved by the Human Research Ethics Committee of the Medical Faculty at the University of Tübingen.

Experimental Design & Task

The 2x2x3 factorial design manipulated: (i) task-relevant visual input (V present, V absent) (ii) auditory context (A present, A absent) and (iii) TMS condition (right occipital cortex, right anterior IPS, Sham) (Fig. 4.1A). Note that the data sets for IPS stimulation have already been reported in our previous study that focused on the effects of IPS-TMS on a larger number of participants (Chapter 3).

In a visual detection paradigm, participants reported their percept (seen/unseen) of a visual stimulus presented in their left lower visual field, while at the same time fixating a cross presented throughout an entire run in the centre of the screen (see *Stimuli and Stimuli Presentation*). Restricting the stimulus location to the left side of visual field was preferred in this first step, as it has been shown that different effects for contra- and ipsi-lateral stimuli can be elicited when stimulating parietal and occipital cortices (e.g. Pascual-Leone et al., 1994; Hilgetag et al., 2001; Romei et al., 2010).

The task was performed under two different auditory contexts. In auditory runs, an auditory sound (see *Stimuli and Stimuli Presentation*) was presented synchronously with target onset, regardless of the presence/absence of the task-relevant visual input. Thus, in auditory runs the sound did not predict the presence of the visual stimulus. In the remaining runs, no auditory sound was presented (see Fig. 4.1C). Therefore, considering all runs together resulted in four distinct sensory conditions: visual present trials presented with (AV) and without (V) a synchronously presented auditory sound and similarly, visual absent trials during which an auditory sound could be present (A) or absent (¬V). Participants were instructed to answer 'seen' only when completely sure and to report 'unseen' otherwise. Each participant was trained in a minimum of six runs prior to going inside the scanner.

Each trial started with the change of the fixation cross colour from grey to blue. After 100 ms the visual stimulus was presented with 50% probability (Fig. 4.1B). Independently of the type of trial (V present, V absent), 4 TMS pulses were subsequently applied (see *Data Acquisition and TMS Procedures*; Fig. 4.1C). After 600 ms of trial begin, the fixation cross turned back to grey and remained like this for 2690 ms until the onset of the next trial. The interstimulus interval amounted thus to 3290 ms, equalling one TR of the EPI acquisition.

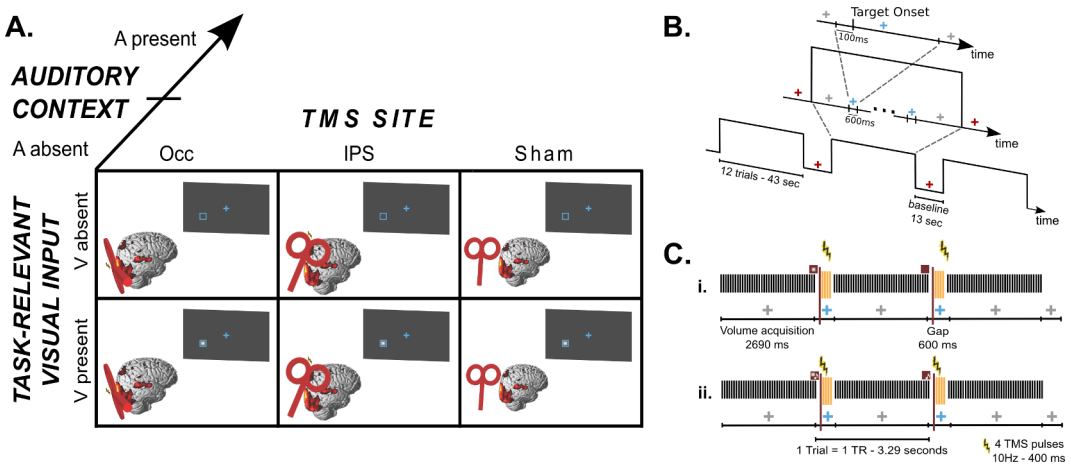

Figure 4.1. Experimental Design. (A) 2x2x3 factorial design manipulating (i) task-relevant visual input (V present, V absent), (ii) auditory context (A present, A absent) and (iii) TMS condition (Occ, IPS, Sham). **(B)** Timeline example of stimuli presentation. Blocks of 12 trials started and ended with a grey fixation cross and were interleaved with baseline periods, during which the fixation cross turned red. A trial began when the fixation cross turned blue. In target present trials, the visual stimulus was presented 100 ms after trial begin. After a total period of 600ms the fixation cross turned back to grey and remained like this until the next trial. **(C)** Illustration of the concurrent TMS-fMRI protocol and stimuli presentation timing for three scans (last scan corresponding to the end of the block) for i. auditory absent and ii. auditory present runs. Within a block the fixation cross was grey during volume acquisition and blue during the acquisition gaps. At 100 ms after trial begin, the task-relevant visual stimulus was either present (first depicted trial) or absent (second depicted trial). Bursts of 4 TMS pulses were applied during acquisiton gaps at 10 Hz and started 100 ms after the target onset time.

Trials were presented in blocks of twelve that started and ended with a grey fixation cross. These were interleaved with baseline periods of 13 seconds, which were made explicit via a red fixation cross. Hence, the colour of the fixation cross induced changes in the attentional settings of the participants: while blue or grey were accompanied by a high attentional load, red represented little attentional demands.

Each run consisted of seven blocks and there were eight runs per TMS condition. For each TMS condition, the auditory context was manipulated across runs following an ABBA design that was counterbalanced across participants. Hence, there were four runs per auditory context and a total of 168 trials per experimental condition.

The three TMS conditions (Occ, IPS, Sham) were performed in different sessions and the order was counterbalanced across participants. For each participant, the order of conditions (i.e. visual present/absent) was fully randomized within and across the eight runs that constituted a session. Across sessions, the same order of conditions was used.

Stimuli and Stimuli Presentation

The task-relevant visual stimulus consisted of a small (9x9 pixels, visual angle: 0.52°) square presented for one frame (i.e. 16ms) on a grey background. When present, the visual stimulus appeared in the centre of a blue placeholder (40x40 pixels, visual angle: 2.3°) that was continuously presented throughout an entire run and positioned 12° left and 5° down relative to the fixation cross.

The grey level of the square was individually determined in a Quest Procedure (Watson and Pelli, 1983) inside the scanner aiming at a detection threshold of 70% and using the same parameters as the main experiment. The grey level was approximated by the use of dithering. Hence, instead of being a homogenous square, our stimulus was effectively a cloud of white pixels within the square. Importantly, identical grey levels were used across TMS conditions.

To increase integration between auditory and visual stimuli, auditory stimuli were generated so as to be perceived at the approximate location of the visual target. Since auditory spatial localization is enhanced when stimuli have a broad range of frequency content, white noise is often used in auditory spatial localization paradigms. However, owing to scanner noise and TMS clicks, white noise was not salient enough in the context of this experiment. Therefore, an auditory stimulus was created by adding sinusoidal tones with frequencies of 130.81 Hz, 164.81 Hz and 196 Hz and the following six terms of their respective geometric progressions (i.e. 2^n*f, where f represents each of the three base frequencies and $1 \leq n \leq 6$). Hence, the auditory sound spanned a total of seven octaves and ranged from 130.81 Hz to 12543.58 Hz. This auditory signal was then convolved with spatially specific head-related transfer functions (HRTFs) to create a left localized stimulus. The HRTFs were pseudo-individualized by matching participants' head width, height, depth and circumference to the anthropometry of participants in the CIPIC database (Algazi et al., 2001). The duration of each auditory stimulus was 40 ms.

Visual and auditory stimuli were presented using Psychophysics Toolbox version 3.0.10 (Brainard, 1997; Kleiner et al., 2007) running on MATLAB 7.9 (MathWorks Inc, MA, USA) and a Macintosh laptop running OS-X 10.6.8 (Apple Inc, CA, USA). The visual stimulus was back-projected onto a frosted Plexiglas screen using a LCD projector (JVC Ltd., Yokohama, Japan; resolution: 800x600 pixels, refresh rate: 60Hz, viewing distance: 48 cm) visible to the participant through a mirror mounted on the MR-head coil. In addition, the lights in the scanner were switched off and the experiment was performed after a period of dark adaptation. Auditory stimuli were presented via MR-compatible electrodynamic headphones at a sampling frequency of 44100 Hz (MR Confon GmbH, Germany). Furthermore, earplugs were used to attenuate both scanner and TMS noise.

Participants indicated their response (i.e. target seen or unseen) with their right hand using a MR-compatible custom-built button device connected to the stimulus computer.

TMS Sites

TMS was applied over the right anterior IPS and the right occipital cortex (Occ) as experimental sites and Sham TMS was included as a control condition.

The MNI coordinates (x = 42.3, y = -50.3, z = 64.4) reported by Oliver et al (2009) as a position over which TMS disrupted visuospatial processing were adopted for the parietal stimulation site.

The choice of the occipital site followed the same criterion as the one used for the parietal site. Specifically, stimulation of the occipital site should be associated with interference of visuospatial perceptual processing. Thus, in order to determine an appropriate occipital coil position, a pilot hunting procedure with seven additional participants was performed outside the scanner.

In a previous study investigating the neural correlates of visual suppression, Thielscher et al. (2010) identified the MNI coordinates (x = -18; y = -102; z = 3) as the averaged centre of mass coordinates showing suppression effects for stimuli presented parafoveally in the right lower visual field. In our experiment, stimuli were presented more peripherally in the left lower visual field. To adjust for this stimulus location, a 3x3 grid of coil positions with an equidistant spacing of 1 cm was placed on the participants' skull over the right hemisphere and oriented parallel to the midline between both hemispheres. Moreover, given the retinotopic organization of the visual cortex and our lower stimulus position, the middle point in the last row of the grid corresponded to the MNI coordinates reported by Thielscher et al. mirrored along the x-axis and inverse transformed into native space using the parameters obtained from spatial normalization.

Using the same visual display and task as in the main experiment, the hunting procedure was performed in short runs over each grid position. In four participants an extra position over the left hemisphere was introduced to serve as a control position. To obtain more stable results in the hunting procedure the grey level of the visual stimulus was individually titrated prior to the experiment using a QUEST procedure that aimed at a baseline detection threshold of 90%. Participants were sitting in front of an LCD monitor (resolution: 800x600 pixels, refresh rate: 75Hz, background intensity of 85 cd/m^2) positioned 40 cm away from them. A chin rest was used to minimize head movements and the experiment was performed in a dimly lit room after an initial period of at least 15 min of dark adaptation. Participants wore earplugs throughout the experiment. Two to four repetitions for each grid position were completed per participant and performance (i.e. hit rates) was averaged across repetitions. The order of grid positions was randomized within and across participants.

The hunting procedure was performed using a single TMS pulse applied 100 ms after target onset. This TMS protocol was preferred for this procedure as it is an established protocol in the investigation of TMS-induced visual suppression effects (de Graaf et al., 2014) and is therefore more likely to result in an effective search process. To enable online monitoring of the coil position via a stereotactic neuronavigation system (LOCALITE GmbH, Sankt Augustin, Germany) during the grid search, a figure-of-eight coil (MC-B70) was used for this procedure, as the MR-compatible coil was not included in the neuronavigation software. Biphasic pulses were applied and the coil handle was pointing to the right (Corthout et al., 2001). Across participants an averaged intensity of 58% total output was used for this procedure.

The positions showing stronger behavioural decrements across participants were located in the middle row of the grid (from left to right hit rates (± SD) were 41 ± 26%, 43 ± 26% and 42 ±16%, respectively). To guarantee that the stimulated coordinates were located over primary visual areas on the right hemisphere and since performances along the middle row were equivalent across columns, the central grid position was deemed suitable for stimulation during the concurrent TMS-fMRI protocol. Hence, the MNI coordinates (x = 19.42, y = -102.35, z = 13.4) were used as a fixed occipital stimulation position for all participants that took part in the concurrent TMS-fMRI experiment. According to the SPM Anatomy Toolbox (Eickhoff et al., 2005), these coordinates are located above areas BA17/BA18. With the bursts of 4 pulses and the stimulation intensity used in the TMS-fMRI experiment (see *Data Acquisition and TMS Procedures*), this position did not induce

peripheral nerve stimulation that could cause discomfort to the participants. However, occipital stimulation inside the scanner inevitably involves lying on the TMS coil. While efforts were made to make the surface of the coil softer through the use of foam material, after a period of time lying on the coil induced pain and all participants had to come out of the scanner bore in the middle of the occipital session, i.e. after four runs were completed.

Individual stimulation coordinates for both experimental TMS sites were determined by inverse transforming the MNI coordinates for parietal and occipital targets into native space using the parameters obtained from spatial normalization. *A posteriori* coil reconstruction of the coil position was based on custom-written MATLAB (MathWorks Inc, MA, USA) scripts and a water tube attached to the coil, which was clearly visible on the MR images. Across participants, the target IPS coordinates were obtained with a mean deviance of 9 mm ± 2.5 (mean, SD). The mean reached coordinate in MNI space was (x = 34.7, y = -52.8, z = 63.5). The target Occ coordinates were obtained with a mean deviance of 5.1 mm ± 1.7 (mean, SD), whereas the mean attained coordinates in MNI space was (x = 18.8, y = -100.9, z = 11.4).

In the sham condition, 2 cm thick plastic plates were fixed between the TMS coil and the skull. Given the quadratic decay of the TMS-induced magnetic field, this sham condition precluded the effects of direct brain stimulation, while maintaining the auditory and somatosensory side effects. Indeed, when tested over the finger region of the motor cortex, this sham condition did not induce muscular twitches on pre-activated finger muscles even at 100% of total output intensity. During the Sham condition the coil was placed over the right hemisphere in a middle position between experimental locations.

Data Acquisition and TMS Procedures

A 3T TIM Trio System (Siemens, Erlangen, Germany) was used to acquire both high-resolution structural images (176 sagittal slices, TR = 2300 ms, TE = 2.98 ms, TI = 1100 ms, flip angle = 9°, FOV = 240 mm x 256 mm, image matrix = 240 x 256, voxel size = 1 mm x 1 mm x 1 mm, using a 12-channel head coil) and T2*-weighted axial echoplanar images (EPI) with blood oxygenation level dependent (BOLD) contrast (GE-EPI, TR = 3290 ms, TE = 35 ms, flip angle = 90°, FOV = 192 mm x 192 mm, image matrix 64 x 64, 40 axial slices acquired sequentially in ascending direction, slice thickness = 3 mm, interslice gap = 0.3 mm, voxel size = 3 mm x 3 mm x 3.3 mm, using a 1-channel Tx/Rx head coil). Each participant took part in a total of eight experimental runs per TMS condition and a total of 124 volume images were acquired for each run.

After each EPI run, a fast structural image (fast low-angle shot [FLASH], 100 axial slices, TR = 564 ms, TE = 2.46 ms, TI = 300ms, FOV = 256mm x 256 mm, image matrix = 256x256, voxel size = 1x1x3 mm) was acquired to enable *a posteriori* reconstruction of the TMS coil position inside the scanner, as described elsewhere (Leitão et al., 2013).

The EPI sequence was adapted for concurrent TMS-fMRI experiments by introducing gaps of 600 ms after every volume acquisition. Each gap was introduced to allow the delivery of four TMS pulses without interference with image quality (Bestmann, 2003; Moisa et al., 2009). Bursts of four pulses at 10 Hz were applied every trial, with the first pulse applied 2890 ms after begin of volume

acquisition, i.e., 100 ms after stimulus onset during target present trials (Fig. 4.1C). TMS pulses were applied after stimulus onset in order to minimize crossmodal interaction effects between our stimuli and the TMS induced auditory and somatosensory side effects (Duecker and Sack, 2013; Leitão et al., 2013).

Similar TMS protocols have been used over the parietal cortex in TMS studies outside the scanner (Chambers et al., 2004b; Oliver et al., 2009) and in concurrent TMS-fMRI studies (Ruff et al., 2006, 2008, 2009; Sack et al., 2007; Blankenburg et al., 2010; Heinen et al., 2011) investigating the effects of parietal TMS on visuospatial processing. However, the standard protocol used for stimulation over the occipital cortex differs from the one used here. In fact, occipital TMS studies are frequently performed using a single or double pulse TMS, in which an appropriate timing relative to stimulus onset (effective time window: 80-110 ms) is crucial in the generation of suppression effects (Amassian et al., 1989; Kammer et al., 2005b). Yet, to allow for comparisons between TMS conditions, bursts of 4 TMS pulses were employed for occipital stimulation instead, by applying the first pulse within the effective suppression time window reported in behavioural occipital TMS studies, whereas the remaining three pulses were not expected to significantly affect behaviour (though see de Graaf et al., 2014 for TMS-induced effects on higher-order visual processing during later time windows). Additionally, the TMS intensity used here (see below) was likely below the intensities necessary to induce effective suppression effects. Thus, rather than using TMS to actively impair performance, in this study occipital TMS served mainly to investigate changes in functional connectivity between the stimulated site and remote nodes of the involved network that might result from the perturbed neural activity.

Biphasic stimuli were delivered using a MagPro X100 stimulator (MagVenture, Denmark) and a MR-compatible figure of eight TMS coil (MRi-B88), using the same coil-holding device as described in Moisa et al (2009). During occipital stimulation the coil was directly placed on a cushion in the RF coil with the major axis oriented parallel to the scanner bore axis and the cable pointing to the right relative to participants' heads (Corthout et al., 2001).

During IPS and Occ stimulation, a fixed TMS intensity of 69% of total stimulator output was used for all participants. This corresponded to 125% of the mean resting motor threshold, as determined across twenty-four participants of prior studies using the same coil (M Moisa, personal communication). To ensure similar somatosensory side effects between experimental conditions and Sham-TMS the TMS intensity was increased to 75% during the Sham condition based on the subjective report of two naïve participants that participated in a pilot test.

Extensive image quality tests of our setup are reported elsewhere (Moisa et al., 2009, 2010: Supplementary Material). For completeness, we acquired EPI data with a phantom using the same experimental design. After realignment, data were entered in a first level analysis using the same model as for the real participants. Computing all the relevant contrasts (height threshold: $p < 0.01$ uncorrected) yielded only spurious and randomly distributed activation patterns.

Behavioural Data Analysis

The proportion of correct responses for target present and target absent trials were computed separately for each auditory and TMS conditions and were averaged across participants. These data were entered in a 3-way repeated measures analysis of variance (RM-ANOVA) with factors TMS condition (IPS, Occ, Sham) and auditory context (A present, A absent) and task-relevant visual input (V present, V absent) to test for significant differences between TMS conditions and auditory contexts.

Statistical analyses were also performed on reaction times data. Individual median reaction times were computed for each condition separately and averaged across participants. Reaction time data was entered in 3-way RM-ANOVAs with factors TMS condition (IPS, Occ, Sham), auditory context (A present and A absent) and task-relevant visual input (V present, V absent). Results are reported using the Greenhouse-Geisser correction.

Evaluation of Phosphene Perception

It is well established that in addition to being able to disrupt visual perception, TMS over the occipital cortex can elicit transient perceptions of light known as phosphenes. The ability to perceive phosphenes is quite variable across participants (Kamitani and Shimojo, 1999; Sparing et al., 2005; Deblieck et al., 2008) and strongly depends on the amount of attention given to them (Kammer et al., 2005b; Thielscher et al., 2010). On the other hand, the intensity needed to elicit phosphenes is generally lower than the one necessary to induce effective suppression effects (Kastner et al., 1998; Kammer et al., 2005a; Thielscher et al., 2010). As phosphenes are elicited contra-laterally to the stimulated hemisphere (Kastner et al., 1998; Kammer, 1999; Kammer et al., 2005a), they could have potentially interfered with task performance. To account for this, at the end of the Occ-TMS session participants were asked if they had perceived anything else apart from the standard visual display and were requested to draw what they saw. Only three participants reported having seen something, of which only two described image distortions in the vicinity of the placeholder. However, the reported distortions by one of these two participants were not specific to the vicinity of the placeholder but extended throughout the entire visual display comprising also the right visual field (i.e. ipsi-laterally to TMS stimulation), which suggests that the reported distortions were not authentic phosphenes. The remaining participant that saw visual distortions in the vicinity of the placeholder additionally reported that these distortions were clearly distinct from the task-relevant visual stimulus and therefore did not interfere with task performance. Hence, in total it is unlikely that phosphene perception influenced our results on the group level both behaviourally and for the BOLD measurements.

fMRI Data Analysis

The fMRI data were analysed using SPM8 (Wellcome Department of Imaging Neuroscience, London; www.fil.ion.ucl.ac.uk/spm) (Friston et al., 1995). Scans from each subject were realigned using the first as a reference, unwarped, spatially normalized into MNI space, resampled to a spatial

resolution of 2 x 2 x 2 mm^3, and spatially smoothed with a Gaussian kernel of 8 mm full-width at half-maximum. The time series of all voxels were high-pass filtered to 1/128 Hz. The first 3 volumes were discarded to allow for T1-equilibration effects.

The fMRI experiment was modeled as a mixed block-event-related design. Individual trials (visual present/absent) were modeled as events and entered into a design matrix after convolution with a canonical hemodynamic function and its first temporal derivative. The later was included as a variable-of-no-interest to capture variance caused by temporal deviations of the BOLD responses from the canonical response function. In addition to modeling these two conditions separately for each auditory context and TMS condition, our statistical model included block begin and end regressors (i.e. the periods during which the fixation cross was grey at the beginning and end of a block; see *Experimental Design*) as mini blocks of 2.69 s and 3.29 s duration, respectively. For each TMS session the four runs acquired for each auditory context were concatenated with run-specific means entered as separate regressors. Nuisance covariates included the realignment parameters to account for residual motion artifacts.

For each participant, condition specific effects were estimated according to the general linear model by creating contrast images of each effect relative to the unmodeled baseline of the respective TMS session (including only regressors based on the canonical hemodynamic response function). Hence, the baseline controls for the general positioning of the coil.

The following statistical comparisons were entered in independent second-level one-sample t-tests to allow for random effects analyses and inferences at the population level (Friston et al., 1999). Unless stated otherwise, we report activation at $p < 0.05$ corrected at the cluster level for multiple comparisons (family-wise error rate) based on Gaussian Random Field theory within the entire brain and using an auxiliary uncorrected voxel threshold of $p = 0.01$ (Hayasaka and Nichols, 2003).

Main Effects of Task-relevant Visual Input

Main effects of task-relevant visual input were tested separately for each of the two stimulation positions by comparing visual present and visual absent trials [(AV + V) > (A + ¬V) and (A + ¬V) > (AV + V)] pooled (i.e. summed) over TMS conditions.

Main Effects of TMS

Since TMS effects in the absence of a neutral control condition may result in interpretational ambiguities, comparisons between TMS conditions were implemented in a paired-wise fashion by comparing each experimental condition (IPS or Occ) with the control condition (Sham). While not the main focus of this study, comparisons between each experimental condition with each other were also computed for completeness. Hence, effects of IPS-TMS were identified by comparing IPS > Sham and Sham > IPS pooled (i.e. summed) over conditions. Equivalent contrasts were calculated for Occ-TMS and for direct comparisons between the two experimental conditions.

State-dependent TMS Effects: Interaction Effects between Visual Input and TMS

Likewise, interaction effects between visual input and TMS conditions were evaluated through direct comparisons between all possible combinations of TMS conditions. Consequently, interaction contrasts for $[(AV + V) > (A + \neg V)]_{IPS} > [(AV + V) > (A + \neg V)]_{Sham}$ and $[(A + \neg V) > (AV + V)]_{IPS} > [(A + \neg V) > (AV + V)]_{Sham}$) were estimated. Interaction effects between Occ- and IPS-TMS were directly evaluated in the same manner.

Effects of Auditory Context

The current study focused on the differential modulatory effects of occipital and parietal TMS during a demanding visual detection task. The effect of auditory context was not the focus of this study, but auditory runs were still included in the analyses to increase estimation power in hand of the small number of participants.

Nevertheless, main effects of auditory context [$(AV + A) > (V + \neg V)$ and $(V + \neg V) > (AV + A)$, pooled (i.e. summed) over TMS conditions Occ, IPS and Sham] and its interaction with TMS condition ($[(AV + A) > (V + \neg V)]_{IPS\ (or\ Occ)} > [(AV + A) > (V + \neg V)]_{Sham}$ and $[(V + \neg V) > (AV + A)]_{IPS\ (or\ Occ)} > [(V + \neg V) > (AV + A)]_{Sham}$) were still evaluated for completeness.

Eye monitoring (outside the scanner)

To ensure that the observed activation pattern did not result from eye movements, twitches, or startle effects, 8 additional participants took part in a supplementary experiment performed with equivalent parameters outside the scanner. For each TMS condition, one experimental run was acquired per participant. To account for the absence of the high-current filter used in the concurrent TMS-MRI setup (Moisa et al., 2009), the TMS intensity was reduced to 63% of total output.

Horizontal and vertical eye movements were recorded using an iView XTM RED-III remote eyetracker system (SensoMotoric Instruments Inc., Needham/Boston, MA, USA) (50 Hz sampling rate). The eyetracking system was calibrated using a 13-point calibration. Eye position data were automatically corrected for blinks and converted to radial velocity.

For each trial condition the mean distance (degrees) from the fixation cross, the number of saccades (defined by a radial eye velocity threshold > 30°/s for a minimum of 60ms duration and radial amplitude larger than 5°), and the number of blinks were quantified for the period during which the fixation cross was blue (see *Experimental Design & Task*).

Across all participants saccades were almost completely absent, hence no further analyses were performed for this index. The two remaining indices were independently entered into a 3-way RM-ANOVA with the factors TMS condition (Occ, IPS, Sham), auditory context (A present, A absent) and task-relevant visual input (V present, V absent).

Results

Behavioural Data

In a visual spatial attention task, participants reported whether or not they had detected a visual target that was presented on 50% of the trials. For each participant, the behavioural indices were calculated separately for visual present and visual absent trials separately for each auditory context and TMS condition. Averaged percent correct responses and reaction time data for each individual condition are summarized in table 4.1.

To test for significant differences between the individual conditions, the proportions of correct responses for visual present and visual absent trials were entered in a 3-way RM-ANOVA. Apart from the expected main effect of visual input ($F_{(1,7)}$ = 16.356; p = 0.005), these analyses did not reveal any other significant main effects (TMS: $F_{(1,7)}$ = 1.418; p = 0.275; Auditory Context: $F_{(1,7)}$ = 0.000; p = 0.988) nor interactions between the different factors (TMS and Auditory Context: $F_{(1,7)}$ = 2.233; p = 0.144; TMS and Visual Input: $F_{(1,7)}$ = 1.239; p = 0.320; Auditory Context and Visual Input: $F_{(1,7)}$ = 0.120; p = 0.739; Interaction between the three: $F_{(1,7)}$ = 1.598; p = 0.237).

Reaction time data was entered in a 3-way RM-ANOVA with factors TMS condition (IPS, Occ, Sham), auditory context (A present, A absent) and task-relevant visual input (V present, V absent). This analysis did not reveal any significant main effects of TMS ($F_{(1,7)}$ = 0.418; p = 0.642), visual input ($F_{(1,7)}$ = 0.342; p = 0.577) or auditory context ($F_{(1,7)}$ = 3.873; p = 0.090), nor were there significant interactions between the TMS and auditory context ($F_{(1,7)}$ = 0.169; p = 0.842), TMS and visual input ($F_{(1,7)}$ = 0.328; p = 0.683) or between the three factors ($F_{(1,7)}$ = 0.622; p = 0.524). However, there was a significant interaction between auditory context and visual ($F_{(1,7)}$ = 9.000; p = 0.020).

To summarize, in line with other concurrent TMS-fMRI studies (Blankenburg et al., 2010; Moisa et al., 2012), our TMS manipulation did not elicit any behavioural changes. Hence, our TMS manipulation functioned as a purely physiological perturbation method that allowed examining influences on remote interconnected brain areas.

Conversely, the auditory context had a modulatory effect on reaction time data. Specifically, the auditory signal served as a precise temporal cue for the target onset, as indexed by accelerated responses in particular in the absence of the task-relevant visual stimulus.

Table 4.1. Behavioural responses averaged across participants (± SD).

TMS Sites	***Proportion Correct (%)***				***Reaction Times (ms)***			
	A Present		*A Absent*		*A Present*		*A Absent*	
	V Present	*V Absent*	*V Present*	*V Absent*	*V Present*	*V Absent*	*V Present*	*V Absent*
IPS	75 ± 22	98 ± 2	75 ± 25	98 ± 1	708 ± 75	692 ± 76	707 ± 73	711 ± 63
Occ	68 ± 24	99 ± 1	67 ± 25	98 ± 1	707 ± 90	700 ± 85	716 ± 100	720 ± 90
Sham	77 ± 13	99 ± 1	79 ± 11	99 ± 1	695 ± 88	677 ± 103	701 ± 91	698 ± 94

Neuroimaging Data

The neuroimaging data were analysed in three steps. First, we evaluated the main effects of task-relevant visual input by pooling over auditory contexts and TMS conditions. Second, we examined the effects of IPS- and Occ-TMS by pooling over sensory conditions and performing paired-wise combinations between all TMS conditions. Third, interaction effects between visual input and TMS conditions were assessed by separately computing interaction contrast for each possible combination of TMS conditions. While not the main focus of this study, auditory effects (main effects and interactions with TMS conditions) were also evaluated for completeness.

Main Effects of Task-relevant Visual Input

We evaluated the main effects of task-relevant visual input by pooling over auditory contexts and TMS conditions. The presence of the target increased activations in the bilateral precuneus extending to the left superior parietal lobule and in the right supplementary motor area (SMA) extending to the right frontal and middle frontal gyri (Table 4.2). Furthermore, activations in the bilateral occipito-temporal areas that have been reported in our previous report were also observable albeit only at an uncorrected level (Table 4.2). Comparing visual present relative to visual absent did not reveal any significant effects.

Main Effects of TMS

We investigated the effects of IPS- and Occ-TMS by pooling over sensory conditions. Paired-wise comparisons were performed between all three TMS conditions.

Comparison between IPS and Sham

Activation increases in the right parietal cortex that were reported in our previous study (Chapter 3) with ten participants by comparing IPS- relative to Sham-TMS were maintained here with a more constrained number of participants (Fig. 4.2, Table 4.3). These activations extended anteriorly to the superior frontal gyrus. The opposite comparison did not reveal any effects.

Comparison between Occ and Sham

Interestingly, contrasting Occ- relative to Sham-TMS equally increased activations in the right parietal cortex. Specifically, this comparison revealed a significant activation cluster extending from the right precuneus to the right postcentral gyrus (Fig. 4.2, Table 4.3). The opposite comparison did not yield significant results.

Comparison between Occ and IPS

Occ- relative to IPS-TMS activated the left superior frontal gyrus, extending to the left superior medial gyrus and the left anterior cingulate cortex (Table 4.3). The opposite comparison did not show any effects.

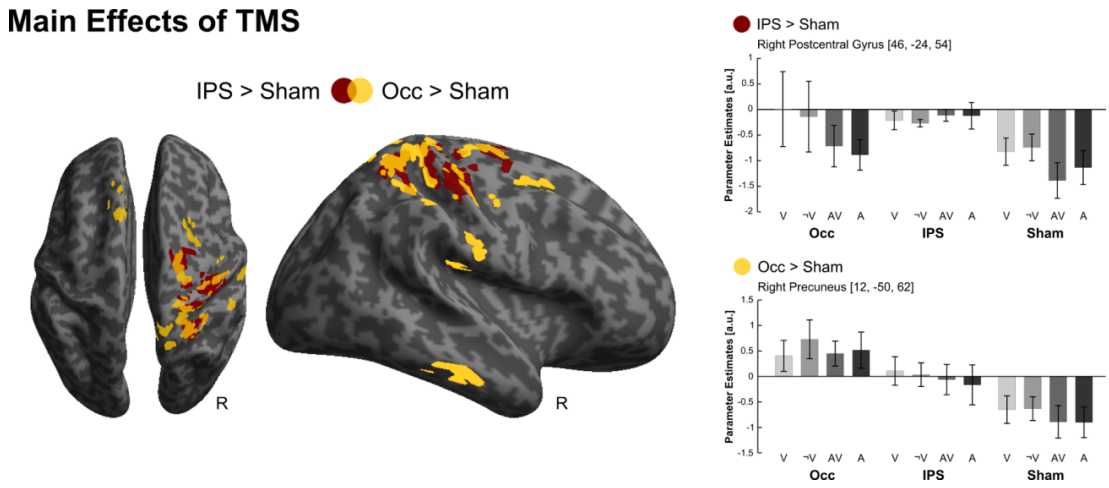

Figure 4.2. Main Effects of TMS. (*left panel*) Activations induced by IPS- relative to Sham-TMS (red) and Occ- relative to Sham-TMS (yellow) are rendered on an inflated SPM template of the entire brain. For illustrational purposes only, effects are displayed at a height threshold of $p = 0.01$ uncorrected and an extent threshold of 100 voxels. (*right panel*) Parameter estimates (mean ± standard error of the mean) are displayed at the given peak coordinates within the parietal cortex for IPS> Sham (*upper panel*) and Occ > Sham (*lower panel*). The bar graphs represent the size of the effect in non-dimensional units (corresponding to % whole-brain mean).

State-dependent TMS Effects: Interaction Effects between Visual Input and TMS

Interaction effects between the task-relevant visual input and TMS were evaluated separately for each possible combination of TMS conditions.

Comparison between IPS and Sham

As we had previously observed in our previous study (Chapter 3), the interaction between (AV + V) > (A + ¬V) and IPS > Sham revealed a significant activation cluster in the right insula lobe extending to the right temporal pole (Fig. 4.3, Table 4.3). Moreover, a cluster in the right fusiform gyrus was also observable albeit at an uncorrected level of significance (Fig. 4.3, Table 4.3). The opposite interaction showed significant effects in the right inferior parietal lobe (Table 4.3). The left inferior parietal lobe was also activated albeit only at an uncorrected level (Table 4.3).

Comparison between Occ and Sham

We did not observe significant interaction effects between (AV + V) > (A + ¬V) and Occ > Sham.

Comparison between Occ and IPS

The interaction between (AV + V) > (A + ¬V) and IPS > Occ revealed a significant activation cluster in the right fusiform gyrus extending to the right inferior temporal gyrus (Fig. 4.3, Table 4.3).

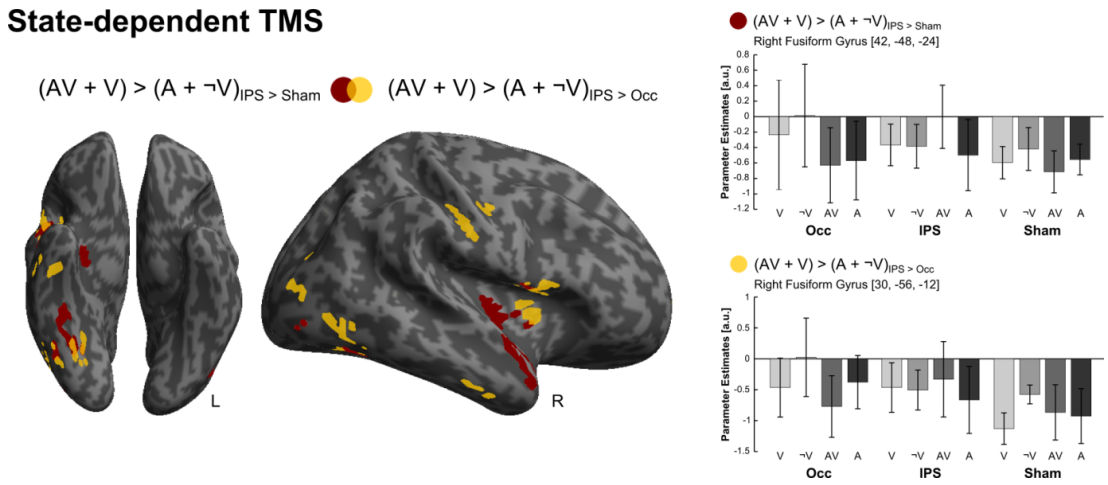

Figure 4.3. State-dependent TMS effects. (*left panel*) Activations induced the interaction between (AV + V) > (A + ¬V) and (red) IPS- relative to Sham-TMS or (yellow) and IPS- relative to Occ-TMS are rendered on an inflated SPM template of the entire brain. For illustrational purposes only, effects are displayed at a height threshold of $p = 0.01$ uncorrected and an extent threshold of 100 voxels. (*right panel*) Parameter estimates (mean ± standard error of the mean) are displayed at the given peak coordinates within the fusiform gyrus for the interaction between (AV + V) > (A + ¬V) and (upper panel) IPS > Sham and (lower panel) and IPS > Occ. The bar graphs represent the size of the effect in non-dimensional units (corresponding to % whole-brain mean).

Effects of Auditory Context

Main effects of auditory context and its interactions with TMS conditions were also evaluated for completeness. Albeit only at an uncorrected level, auditory-evoked effects were found in the auditory cortices (left auditory cortex: [-40 -26 2], $Z = 2.92$, $p_{peak} = 0.002$; right auditory cortex: [46 -28 12], $Z = 1.92$, $p_{peak} = 0.028$). Contrasting purely visual runs relative to auditory runs did not yield any results.

Table 4.2. Main Effects of Task-relevant Visual Input

Brain Regions	*MNI Coordinates (mm)*			*Z Score*	*#Voxels in Cluster*	p_{FWE}*-value*
	x	y	z	*(peak)*		*(cluster)*
Main Effects of Task-relevant Visual Input						
$(A + \neg V) > (AV + V)_{IPS + Sham}$						
Left Precuneus	-12	-60	42	4.06	722	0.001
Left Superior Parietal Lobule	-18	-60	42	3.22		
Right SMA	10	6	52	3.91	603	0.004
Right Superior Frontal Gyrus	20	14	54	3.82		
Right Middle Frontal Gyrus	22	12	46	3.77		
Left Fusiform Gyrus	-30	-84	-18	5.40	267	0.226
Left Cerebellum	-28	-80	-20	4.58		
Left Inferior Occipital Gyrus	-44	-80	-12	2.89		
Right Lingual Gyrus	24	-82	-8	3.79	219	0.414
Right Inferior Occipital Gyrus	38	-68	-10	3.76		
Right Fusiform Gyrus	28	-66	-12	2.97		

p-values are reported at the cluster level and corrected for multiple comparisons within the entire brain using an auxiliary uncorrected voxel threshold of $p = 0.01$ and an extent threshold of 0 voxels. FWE = Family-wise error correction.

The evaluation of the interaction effects between (AV + A) > (V + ¬V) and IPS > Sham revealed a significant activation cluster in the right posterior middle temporal gyrus (cluster size: 435; $p_{cluster}$ = 0.02; activation peak: [50 -58 0], Z = 4.09). The remaining comparisons did not show any effects.

Eyetracker Data

Two independent 3-way RM-ANOVAs with factors TMS condition (Occ, IPS, Sham), auditory context (A present, A absent) and task-relevant visual input (V present, V absent) and were performed for the mean distance from the fixation cross and the number of blinks.

Table 4.3. TMS effects

Brain Regions	*MNI Coordinates (mm)*			*Z Score*	*#Voxels in Cluster*	p_{FWE}-*value*
	x	y	z	*(peak)*		
Effects between TMS conditions						
IPS > Sham						
Right Superior Frontal Gyrus	22	-12	58	4.71	1290	< 0.001
Right Postcentral Gyrus	46	-24	54	4.59		
Right Precentral Gyrus	44	-22	60	3.82		
Right Superior Parietal Lobule	30	-48	56	3.43		
Right Intraparietal Sulcus	40	-40	50	3.21		
Occ > Sham						
Right Precuneus	12	-50	62	4.50	1017	0.002
Right Postcentral Gyrus	26	-44	66	4.14		
Right Superior Parietal Lobule	32	-54	66	3.99		
Occ > IPS						
Left Superior Frontal Gyrus	-16	32	38	4.41	1896	< 0.001
Left Superior Medial Gyrus	0	54	22	3.83		
Left Anterior Cingulate Cortex	-4	30	-6	3.77		
State-dependent TMS Effects						
$(AV + V) > (A + \neg V)_{IPS} > (AV + V) > (A + \neg V)_{Sham}$						
Right Insula Lobe	46	4	0	4.23	370	0.031
Right Temporal Pole	52	6	-16	3.66		
Right Fusiform Gyrus	42	-48	-24	3.69	295	0.095
$(AV + V) > (A + \neg V)_{Sham} > (AV + V) > (A + \neg V)_{IPS}$						
Right Inferior Parietal Lobule	46	-52	42	4.10	361	0.036
Right Angular Gyrus	44	-60	40	4.05		
Right Supramarginal Gyrus	60	-48	42	3.01		
Left Angular Gyrus	-42	-72	36	3.90	252	0.183
Left Inferior Parietal Lobule	-38	-78	44	3.36		
$(AV + V) > (A + \neg V)_{IPS} > (AV + V) > (A +$						
Right Fusiform Gyrus	30	-56	-12	3.66	440	0.015
Right Inferior Temporal Gyrus	50	-64	-12	3.27		
Right Putamen	34	4	4	3.82	290	0.120
Right Inferior Frontal Gyrus	50	14	2	3.77		

p-values are reported at the cluster level and corrected for multiple comparisons within the entire brain using an auxiliary uncorrected voxel threshold of p = 0.01 and an extent threshold of 0 voxels. FWE = Family-wise error correction.

For the number of blinks index, the analysis did not show main effects of TMS ($F_{(1,7)}$ = 0.171; p = 0.792), visual input ($F_{(1,7)}$ = 0.001; p = 0.972) or auditory context ($F_{(1,7)}$ = 0.337; p = 0.580). There were also no significant interactions between TMS and auditory context ($F_{(1,7)}$ = 2.120; p = 0.180), TMS and visual input ($F_{(1,7)}$ = 0.249; p = 0.682) or visual input and auditory context ($F_{(1,7)}$ = 1.224; p = 0.305), nor was there a significant three way interaction between all factors ($F_{(1,7)}$ = 0.320; p = 0.712).

For the mean distance from the fixation cross, there was no main effect of TMS ($F_{(1,7)}$ = 1.283; p = 0.305), visual input ($F_{(1,7)}$ = 0.340; p = 0.578) or a main effect of auditory context ($F_{(1,7)}$ = 1.735; p = 0.229). The analysis did also not result in significant interactions between TMS and auditory context ($F_{(1,7)}$ = 1.947; p = 0.204), TMS and visual input ($F_{(1,7)}$ = 0.193; p = 0.804) or visual input and auditory context ($F_{(1,7)}$ = 0.305; p = 0.598), nor was there a significant interaction between the three factors ($F_{(1,7)}$ = 0.455; p = 0.643).

None of the RM-ANOVAs revealed any significant main effects or interactions demonstrating that differences in eye movements are unlikely to account for the observed activation profile in our fMRI data.

Discussion

Concurrent TMS-fMRI allows examining local and distal consequences of TMS on ongoing neural activity. Most of the research that applied this methodology to investigate the neural correlates of visual processing has focused on the effects of higher-order association cortices on visual areas (Ruff et al., 2006, 2008; Blankenburg et al., 2010; Feredoes et al., 2011; Leitão et al., 2013), whereas the investigation of local and distal TMS effects induced by stimulating low-level visual areas has been sparse (Caparelli et al., 2010). This stands in strong contrast to offline TMS studies (Pascual-Leone and Walsh, 2001; Silvanto et al., 2005a, 2006; Koivisto et al., 2010) and TMS-EEG literature (Thut et al., 2003; Romei et al., 2008; Rosanova et al., 2009; Reichenbach et al., 2011), where TMS has frequently been applied over occipital areas to study the resulting changes in functional brain activity and behavioural performance.

The present study aimed at investigating how TMS over two distinct nodes of this distributed network involved in perceptual processing differentially modulates local and distal BOLD activations. Specifically, while participants performed a demanding visual detection task that involved covert attention to the left visual field, we stimulated the right occipital (Occ) cortex (BA17/18) and the right anterior IPS, whereas Sham-TMS was introduced as a control condition. The use of the same experimental design and participants allowed us to assess putative differential effects of each experimental site by independently comparing them with the Sham condition.

As we had previously observed in our previous IPS-TMS study that profited from a larger number of participants (Chapter 3), evaluating the main effects of IPS-TMS revealed significant activations underneath the directly stimulated region (Fig. 4.2, Table 4.3). Specifically, the comparison between IPS- and Sham-TMS showed a significant activation cluster that encompassed the right superior parietal lobe and extended rostrally toward the right superior frontal gyrus. Remarkably, the evaluation of the main effects of Occ-TMS equally revealed BOLD modulations in remote areas of the right parietal cortex. Indeed, comparing Occ- relative to Sham-TMS resulted in a significant activation cluster in the right superior parietal lobule, extending to the right postcentral gyrus (Fig. 4.2, Table 4.3).

It is very interesting that both Occ- and IPS-TMS main effects overlapped in the right parietal cortex. On the one hand, activations elicited by IPS-TMS are expected to emerge from perturbation of ongoing task-related activity underneath the coil. Interestingly, this perturbed IPS activity resulted in TMS-induced state-dependent effects in right occipito-temporal visual areas (Fig. 4.3, Table 4.3) that were accompanied by opposing state-dependent effects in the right inferior parietal cortex (Table 4.3). Conversely, Occ-TMS did not affect state-dependent activations in occipito-temporal visual areas. On the one hand, this suggests that Occ-TMS over early visual areas did not directly affect the information exchange with occipito-temporal cortices. However, these results also point to distinct neural mechanisms underlying Occ- and IPS-TMS induced parietal activations: whereas directly perturbed IPS activity modulated activations in occipito-temporal visual areas, indirectly induced parietal activations did not have any effect on these same cortical structures. This suggests that the latter possibly reflect compensatory mechanisms, by which additional attentional resources

were recruited to maintain task performance in response to perturbed activity in early visual areas. Although this represents the most likely hypothesis, our results are not suitable for drawing definitive conclusions about this suggestion, which should be directly tested for in future studies using, for example, a dual-site TMS approach. Irrespective of the exact mechanisms underlying these TMS-related activations, it is worth noting that the clear-cut differences seen for Occ- relative to IPS-TMS demonstrate the ability of the concurrent TMS-fMRI approach to dissect an overall task-related network into those sub-parts which are specifically linked to the tested target areas.

Another difference observed between both TMS conditions was the lack of local activation changes following Occ-TMS. This absence of activations underneath the coil is not unusual in concurrent TMS-fMRI studies (Blankenburg et al., 2008; Heinen et al., 2011; Moisa et al., 2012; Leitão et al., 2013). Moreover, studies stimulating the primary motor cortex (M1) revealed that whereas remote interconnected brain areas activated for both subthreshold and superthreshold TMS (i.e., TMS applied at intensities below and above the minimum intensity necessary to induce motor responses in the contralateral hand, respectively), the directly stimulated M1 showed significant activations only for superthreshold stimulation, whereby these later effects probably included afferent processing resulting from TMS-induced hand movements (Baudewig et al., 2001; Bestmann et al., 2003; Hanakawa et al., 2009). It is therefore possible that the intensity at which TMS was applied over the occipital cortex was not strong enough to elicit local activation changes, having in mind that it also did not produce behavioural changes or phosphene perception.

However, another possible explanation relates to the visual stimuli used in the current study. In fact, the visual stimuli were devised based on previous parietal (Hilgetag et al., 2001; Chambers et al., 2004a; Koch et al., 2005; Dambeck et al., 2006; Oliver et al., 2009; Bien et al., 2012) and occipital (Kastner et al., 1998; Kammer et al., 2005b; Romei et al., 2010; Thielscher et al., 2010; de Graaf et al., 2011; Railo and Koivisto, 2012) TMS studies that, in order to provoke behavioural deficits in the contralateral visual field, utilized rather small visual stimuli presented for a brief moment at peripheral visual locations. However, this stimulus size and duration might not have been ideal when testing for putative TMS-induced BOLD effects in visual areas, given that even its presence failed to be reliably detected at the spatial resolution of our whole-brain EPI images. Possibly, the use of stimuli that cover a larger part of the visual field while including within them trial-by-trial changes that have to be detected (Blankenburg et al., 2010; Reichenbach et al., 2011) might have proven more suitable to uncover Occ-TMS effects on bottom-up driven activations in visual areas during task performance.

An additional methodological issue relates to the TMS protocol used in this study. In fact, in order to allow for comparisons between the two experimental sites, certain compromises were made in this respect. In adherence to the protocol used for IPS-TMS, we used TMS to probe functional connectivity between the stimulated and remote interconnected regions by applying bursts of four TMS pulses (10 Hz) at an intensity that did not significantly affect behavioural performance (even though the first pulse was applied within the classical suppression window). An alternative would have been to follow the more frequently applied chronometric approach by employing one appropriately timed strong pulse to actively impair visual perception and assessing how these TMS-induced behavioural impairments correlate with TMS-induced changes in BOLD activations (Sack

et al., 2007; Heinen et al., 2011). In this regard, instead of using fixed coil positions and stimulation intensities as it is often done when stimulating over the parietal cortex (Sack et al., 2007; Ruff et al., 2008; Blankenburg et al., 2010; Leitão et al., 2013), participant specific parameters for the occipital site might be preferable in order to obtain more reliable behavioural effects. Yet, given the functional role of cortical oscillations at alpha frequency during perceptual and attentional visual processes, the fact that we used rTMS bursts close to this frequency might have potentially influenced our results.

Finally, it should also be mentioned that occipital TMS inside the scanner during task performance is subjected to additional practical complications associated with participants having to lie on the TMS coil. In fact, after a continuous and relatively long period of lying on the coil, participants started experiencing pain that required them to come out of the scanner even after measures were taken to render the coil surface as soft as possible, which is likely to have influenced the attentional state of the participants. Therefore, more effective measures are needed to reduce this type of problem associated with occipital TMS inside the scanner.

In conclusion, to the best of our knowledge this was the first study to investigate the differential effects of parietal and occipital TMS during an attentional demanding task that involved detection of external visual stimuli inside the scanner. While both experimental TMS conditions elicited significant activations in the right parietal cortex independently of the current visual input, state-dependent TMS effects were specific to IPS-TMS. These results suggest two distinct neural mechanisms for TMS-induced parietal activations. Whereas, IPS-TMS effects reflect locally perturbed neural activity, Occ-TMS induced parietal activations likely reflect compensatory mechanisms in response to activity disruption in remote early visual areas. In general, our study offers methodological considerations that might prove useful for future concurrent TMS-fMRI research over visual cortices.

References

Algazi VR, Duda RO, Thompson DM, Avendano C (2001) The CIPIC HRTF database. Proc 2001 IEEE Work Appl Signal Process to Audio Acoust (Cat No01TH8575).

Amassian VE, Cracco RQ, Maccabee PJ, Cracco JB, Rudell a, Eberle L (1989) Suppression of visual perception by magnetic coil stimulation of human occipital cortex. Electroencephalogr Clin Neurophysiol 74:458–462.

Baudewig J, Siebner HR, Bestmann S, Tergau F, Tings T, Paulus W, Frahm J (2001) Functional MRI of cortical activations induced by transcranial magnetic stimulation (TMS). Neuroreport 12:3543–3548.

Bestmann S (2003) On the Synchrinzation of Transcranial Magnetic Stimulation and Functional Echo-Planar Imaging. J Magn Reson Imaging.

Bestmann S, Baudewig J, Siebner HR, Rothwell JC, Frahm J (2003) Subthreshold high-frequency TMS of human primary motor cortex modulates interconnected frontal motor areas as detected by interleaved fMRI-TMS.

Bestmann S, Baudewig J, Siebner HR, Rothwell JC, Frahm J (2004) Functional MRI of the immediate impact of transcranial magnetic stimulation on cortical and subcortical motor circuits. Eur J Neurosci 19:1950–1962.

Bestmann S, Baudewig J, Siebner HR, Rothwell JC, Frahm J (2005) BOLD MRI responses to repetitive TMS over human dorsal premotor cortex. Neuroimage 28:22–29.

Bestmann S, Feredoes E (2013) Combined neurostimulation and neuroimaging in cognitive neuroscience: past, present, and future. Ann N Y Acad Sci 1296:1–20.

Bien N, Goebel R, Sack AT (2012) Extinguishing extinction: hemispheric differences in the modulation of TMS-induced visual extinction by directing covert spatial attention. J Cogn Neurosci 24:809–818.

Blankenburg F, Ruff CC, Bestmann S, Bjoertomt O, Eshel N, Josephs O, Weiskopf N, Driver J (2008) Interhemispheric effect of parietal TMS on somatosensory response confirmed directly with concurrent TMS-fMRI. J Neurosci 28:13202–13208.

Blankenburg F, Ruff CC, Bestmann S, Bjoertomt O, Josephs O, Deichmann R, Driver J (2010) Studying the role of human parietal cortex in visuospatial attention with concurrent TMS-fMRI. Cereb Cortex 20:2702–2711.

Boroojerdi B, Bushara KO, Corwell B, Immisch I, Battaglia F, Muellbacher W, Cohen LG (2000) Enhanced excitability of the human visual cortex induced by short-term light deprivation. Cereb Cortex 10:529–534.

Brainard DH (1997) The Psychophysics Toolbox. Spat Vis 10:433–436.

Büchel C, Josephs O, Rees G, Turner R, Frith CD, Friston KJ (1998) The functional anatomy of attention to visual motion. A functional MRI study. Brain 121 (Pt 7:1281–1294.

Bullier J, Hupé JM, James AC, Girard P (2001) The role of feedback connections in shaping the responses of visual cortical neurons. Prog Brain Res 134:193–204.

Caparelli EC, Backus W, Telang F, Wang G-J, Maloney T, Goldstein RZ, Anschel D, Henn F (2010) Simultaneous TMS-fMRI of the Visual Cortex Reveals Functional Network, Even in Absence of Phosphene Sensation. Open Neuroimag J 4:100–110.

Cardin V, Friston KJ, Zeki S (2011) Top-down modulations in the visual form pathway revealed with dynamic causal modeling. Cereb Cortex 21:550–562.

Chambers CD, Payne JM, Stokes MG, Mattingley JB (2004a) Fast and slow parietal pathways mediate spatial attention. Nat Neurosci 7:217–218.

Chambers CD, Stokes MG, Mattingley JB (2004b) Modality-specific control of strategic spatial attention in parietal cortex. Neuron 44:925–930.

Corthout E, Barker AT, Cowey A (2001) Transcranial magnetic stimulation: Which part of the current waveform causes the stimulation? Exp Brain Res 141:128–132.

Cowey A, Walsh V (2000) Magnetically induced phosphenes in sighted, blind and blindsighted observers. Neuroreport 11:3269–3273.

Dambeck N, Sparing R, Meister IG, Wienemann M, Weidemann J, Topper R, Boroojerdi B (2006) Interhemispheric imbalance during visuospatial attention investigated by unilateral and bilateral TMS over human parietal cortices. Brain Res 1072:194–199.

De Graaf T a, Herring J, Sack AT (2011) A chronometric exploration of high-resolution “sensitive TMS masking” effects on subjective and objective measures of vision. Exp Brain Res 209:19–27.

De Graaf T a, Koivisto M, Jacobs C, Sack AT (2014) The chronometry of visual perception: Review of occipital TMS masking studies. Neurosci Biobehav Rev 45C:295–304.

Deblieck C, Thompson B, Iacoboni M, Wu AD (2008) Correlation between motor and phosphene thresholds: A transcranial magnetic stimulation study. Hum Brain Mapp 29:662–670.

Duecker F, Sack AT (2013) Pre-stimulus sham TMS facilitates target detection. PLoS One 8:e57765.

Eickhoff SB, Stephan KE, Mohlberg H, Grefkes C, Fink GR, Amunts K, Zilles K (2005) A new SPM toolbox for combining probabilistic cytoarchitectonic maps and functional imaging data. Neuroimage 25:1325–1335.

Feredoes E, Heinen K, Weiskopf N, Ruff C, Driver J (2011) Causal evidence for frontal involvement in memory target maintenance by posterior brain areas during distracter interference of visual working memory. Proc Natl Acad Sci U S A 108:17510–17515.

Fierro B, Brighina F, Vitello G, Piazza A, Scalia S, Giglia G, Daniele O, Pascual-Leone A (2005) Modulatory effects of low- and high-frequency repetitive transcranial magnetic stimulation on visual cortex of healthy subjects undergoing light deprivation. J Physiol 565:659–665.

Friston KJ, Holmes AP, Price CJ, Büchel C, Worsley KJ (1999) Multisubject fMRI studies and conjunction analyses. Neuroimage 10:385–396.

Hanakawa T, Mima T, Matsumoto R, Abe M, Inouchi M, Urayama S-I, Anami K, Honda M, Fukuyama H (2009) Stimulus-response profile during single-pulse transcranial magnetic stimulation to the primary motor cortex. Cereb Cortex 19:2605–2615.

Heinen K, Ruff CC, Bjoertomt O, Schenkluhn B, Bestmann S, Blankenburg F, Driver J, Chambers CD (2011) Concurrent TMS-fMRI reveals dynamic interhemispheric influences of the right parietal cortex during exogenously cued visuospatial attention. Eur J Neurosci 33:991–1000.

Hilgetag CC, Théoret H, Pascual-Leone a (2001) Enhanced visual spatial attention ipsilateral to rTMS-induced "virtual lesions" of human parietal cortex. Nat Neurosci 4:953–957.

Hopfinger JB, Buonocore MH, Mangun GR (2000) The neural mechanisms of top- down attentional control. 3.

Indovina I, Macaluso E (2007) Dissociation of stimulus relevance and saliency factors during shifts of visuospatial attention. Cereb Cortex 17:1701–1711.

Kamitani Y, Shimojo S (1999) Manifestation of scotomas created by transcranial magnetic stimulation of human visual cortex. Nat Neurosci 2:767–771.

Kammer T (1999) Phosphenes and transient scotomas induced by magnetic stimulation of the occipital lobe: their topographic relationship. Neuropsychologia 37:191–198.

Kammer T, Baumann LW (2010) Phosphene thresholds evoked with single and double TMS pulses. Clin Neurophysiol 121:376–379.

Kammer T, Puls K, Erb M, Grodd W (2005a) Transcranial magnetic stimulation in the visual system. II. Characterization of induced phosphenes and scotomas. Exp Brain Res 160:129–140.

Kammer T, Puls K, Strasburger H, Hill NJ, Wichmann F a (2005b) Transcranial magnetic stimulation in the visual system. I. The psychophysics of visual suppression. Exp Brain Res 160:118–128.

Kastner S, Demmer I, Ziemann U (1998) Transient visual field defects induced by transcranial magnetic stimulation over human occipital pole. Exp Brain Res 118:19–26.

Kastner S, Pinsk M a, De Weerd P, Desimone R, Ungerleider LG (1999) Increased activity in human visual cortex during directed attention in the absence of visual stimulation. Neuron 22:751–761.

Kleiner M, Brainard D, Pelli D, Ingling A, Murray R, Broussard C (2007) What ' s new in Psychtoolbox-3 ? Foreword ; -). Whats New 36:14.

Koch G, Oliveri M, Torriero S, Caltagirone C (2005) Modulation of excitatory and inhibitory circuits for visual awareness in the human right parietal cortex. Exp Brain Res 160:510–516.

Koivisto M, Mäntylä T, Silvanto J (2010) The role of early visual cortex (V1/V2) in conscious and unconscious visual perception. Neuroimage 51:828–834.

Lamme V a, Roelfsema PR (2000) The distinct modes of vision offered by feedforward and recurrent processing. Trends Neurosci 23:571–579.

Leitão J, Thielscher A, Werner S, Pohmann R, Noppeney U (2013) Effects of parietal TMS on visual and auditory processing at the primary cortical level -- a concurrent TMS-fMRI study. Cereb Cortex 23:873–884.

Liu Y, Bengson J, Huang H, Mangun GR, Ding M (2014) Top-down Modulation of Neural Activity in Anticipatory Visual Attention: Control Mechanisms Revealed by Simultaneous EEG-fMRI. Cereb Cortex.

Mayhew SD, Hylands-White N, Porcaro C, Derbyshire SWG, Bagshaw AP (2013) Intrinsic variability in the human response to pain is assembled from multiple, dynamic brain processes. Neuroimage 75:68–78.

Moisa M, Pohmann R, Ewald L, Thielscher A (2009) New coil positioning method for interleaved transcranial magnetic stimulation (TMS)/functional MRI (fMRI) and its validation in a motor cortex study. J Magn Reson Imaging 29:189–197.

Moisa M, Pohmann R, Uludağ K, Thielscher A (2010) Interleaved TMS/CASL: Comparison of different rTMS protocols. Neuroimage 49:612–620.

Moisa M, Siebner HR, Pohmann R, Thielscher A (2012) Uncovering a Context-Specific Connectional Fingerprint of Human Dorsal Premotor Cortex. J Neurosci 32:7244–7252.

Mumford D (1992) On the computational architecture of the neocortex - II The role of cortico-cortical loops. Biol Cybern 66:241–251.

Oliver R, Bjoertomt O, Driver J, Greenwood R, Rothwell J (2009) Novel "hunting" method using transcranial magnetic stimulation over parietal cortex disrupts visuospatial sensitivity in relation to motor thresholds. Neuropsychologia 47:3152–3161.

Pascual-Leone A, Gomez tortosa E, Grafman J, Alway D, Nichelli P, Hallett M (1994) Induction of Visual Extinction by Rapid Rate Transcranial Magnetic Stimulation of Parietal Lobe. Neurology 44:494–498.

Pascual-Leone A, Walsh V (2001) Fast backprojections from the motion to the primary visual area necessary for visual awareness. Science 292:510–512.

Railo H, Koivisto M (2012) Two means of suppressing visual awareness: a direct comparison of visual masking and transcranial magnetic stimulation. Cortex 48:333–343.

Rauschecker AM, Bestmann S, Walsh V, Thilo K V. (2004) Phosphene threshold as a function of contrast of external visual stimuli. Exp Brain Res 157:124–127.

Rauss K, Pourtois G (2013) What is Bottom-Up and What is Top-Down in Predictive Coding? Front Psychol 4:276.

Reichenbach a, Whittingstall K, Thielscher a (2011) Effects of transcranial magnetic stimulation on visual evoked potentials in a visual suppression task. Neuroimage 54:1375–1384.

Reithler J, Peters JC, Sack a T (2011) Multimodal transcranial magnetic stimulation: using concurrent neuroimaging to reveal the neural network dynamics of noninvasive brain stimulation. Prog Neurobiol 94:149–165.

Romei V, Brodbeck V, Michel C, Amedi A, Pascual-Leone A, Thut G (2008) Spontaneous fluctuations in posterior alpha-band EEG activity reflect variability in excitability of human visual areas. Cereb Cortex 18:2010–2018.

Romei V, Gross J, Thut G (2010) On the role of prestimulus alpha rhythms over occipito-parietal areas in visual input regulation: correlation or causation? J Neurosci 30:8692–8697.

Rosanova M, Casali A, Bellina V, Resta F, Mariotti M, Massimini M (2009) Natural frequencies of human corticothalamic circuits. J Neurosci 29:7679–7685.

Ruff CC, Bestmann S, Blankenburg F, Bjoertomt O, Josephs O, Weiskopf N, Deichmann R, Driver J (2008) Distinct causal influences of parietal versus frontal areas on human visual cortex: evidence from concurrent TMS-fMRI. Cereb Cortex 18:817–827.

Ruff CC, Blankenburg F, Bjoertomt O, Bestmann S, Freeman E, Haynes J-D, Rees G, Josephs O, Deichmann R, Driver J (2006) Concurrent TMS-fMRI and psychophysics reveal frontal influences on human retinotopic visual cortex. Curr Biol 16:1479–1488.

Ruff CC, Blankenburg F, Bjoertomt O, Bestmann S, Weiskopf N, Driver J (2009) Hemispheric differences in frontal and parietal influences on human occipital cortex: direct confirmation with concurrent TMS-fMRI. J Cogn Neurosci 21:1146–1161.

Sack AT, Kohler A, Bestmann S, Linden DEJ, Dechent P, Goebel R, Baudewig J (2007) Imaging the brain activity changes underlying impaired visuospatial judgments: simultaneous FMRI, TMS, and behavioral studies. Cereb Cortex 17:2841–2852.

Silvanto J, Cowey A, Lavie N, Walsh V (2005a) Striate cortex (V1) activity gates awareness of motion. Nat Neurosci 8:143–144.

Silvanto J, Lavie N, Walsh V (2005b) Double dissociation of V1 and V5/MT activity in visual awareness. Cereb Cortex 15:1736–1741.

Silvanto J, Lavie N, Walsh V (2006) Stimulation of the human frontal eye fields modulates sensitivity of extrastriate visual cortex.

Sparing R, Dambeck N, Stock K, Meister IG, Huetter D, Boroojerdi B (2005) Investigation of the primary visual cortex using short-interval paired-pulse transcranial magnetic stimulation (TMS). Neurosci Lett 382:312–316.

Stewart LM, Walsh V, Rothwell JC (2001) Motor and phosphene thresholds: A transcranial magnetic stimulation correlation study. Neuropsychologia 39:415–419.

Taylor PCJ, Walsh V, Eimer M (2010) The neural signature of phosphene perception. Hum Brain Mapp 31:1408–1417.

Thielscher a, Reichenbach a, Uğurbil K, Uludağ K (2010) The cortical site of visual suppression by transcranial magnetic stimulation. Cereb Cortex 20:328–338.

Thut G, Nietzel A, Pascual-Leone A (2005) Dorsal posterior parietal rTMS affects voluntary orienting of visuospatial attention. Cereb Cortex 15:628–638.

Thut G, Northoff G, Ives JR, Kamitani Y, Pfennig A, Kampmann F, Schomer DL, Pascual-Leone A (2003) Effects of single-pulse transcranial magnetic stimulation (TMS) on functional brain activity: A combined event-related TMS and evoked potential study. Clin Neurophysiol 114:2071–2080.

Thut G, Veniero D, Romei V, Miniussi C, Schyns P, Gross J (2011) Rhythmic TMS causes local entrainment of natural oscillatory signatures. Curr Biol 21:1176–1185.

Watson AB, Pelli DG (1983) QUEST: a Bayesian adaptive psychometric method. Percept Psychophys 33:113–120.

Chapter 5

Right IPS-TMS abolishes neural signals of decisional uncertainty and response errors in bilateral prefrontal cortices

Joana Leitão[1,2], Axel Thielscher[1,3,4], Johannes Tuennerhoff[1], Uta Noppeney[1,2]

[1]Max Planck Institute for biological Cybernetics, 72076 Tübingen, Germany

[2]Computational Neuroscience and Cognitive Robotics Centre, University of Birmingham, B15 2TT Birmingham, UK

[3]Department of Electrical Engineering, Technical University of Denmark, 2800 Lyngby, Denmark

[4]DRCMR, Copenhagen University Hospital Hvidovre, 2650 Hvidovre, Denmark

Author contributions

Leitão and Noppeney designed the experiment. Stimuli were programmed and designed by Leitão. Thielscher contributed with TMS expertise. Leitão collected the data with the support of Tuennerhoff. Leitão analysed the data with the help of Noppeney. Leitão wrote the manuscript with the help of Thielscher and Noppeney.

Acknowledgments

This work was supported by the European Research Council and the Max Planck Society. The authors would like to thank Julian Hofmeister and Simone Götze for helping with data acquisition, Mario Kleiner for technical assistance and the medical doctors Daniel Zaldivar, Johannes Schultz and Matthias Munk for their availability during data acquisition and participants' screening. The authors declare no competing financial interests.

Abstract

In order to interact with the environment, the brain needs to appropriately map sensory information onto behavioural responses. This process is supported by a widespread network of brain areas that encompasses sensory and motor regions along with higher order association areas such as the prefrontal and parietal cortices, in particular the intraparietal sulcus (IPS). In order to investigate how disturbances to IPS activity influence the neural systems underlying perceptual decisions, this concurrent TMS-fMRI study applied bursts of 4 TMS pulses (10Hz) to the right anterior IPS and during a Sham condition while participants performed a demanding visual detection task. Participants were instructed to report their visual percept (seen/unseen) of a weak visual stimulus presented on half of the trials in their left lower visual hemifield, thus allowing the categorization of behavioural responses into hits, misses, false alarms and correct rejections. Our TMS manipulation did not alter behavioural performance. At the neural level, TMS-effects were assessed by comparing conditions with matched visual input but different behavioural response categories and vice versa. Our results show that IPS- relative to Sham-TMS extinguished activation increases for missed trials in the left posterior superior frontal and right precentral gyri. The duality between neural and behavioural effects suggests that these regions were not necessary for task performance. Instead, it might reflect TMS-induced influences on post-decisional implicit evaluations on task performance associated with missed trials.

Keywords: interleaved/concurrent TMS-fMRI, right anterior parietal cortex, perceptual decision making, metacognition, degeneracy

Introduction

Amid the stream of sensory signals that are constantly entering the brain it is inevitable that some information fails to be consciously perceived, in particular if it arises from a noisy environment. Experimentally, the study of visual perception relies on participants' subjective reports, which result from a decision process that selects between possible response options. Detection tasks, in which participants decide upon the presence or absence of a weak stimulus, are one of the simplest forms of perceptual decisions. According to signal-detection theory (SDT) (Green and Swets, 1966), the detection of the stimulus depends on an internal decision rule applied to noisy evidence, which can shift to adapt the response strategy to different task requirements. For instance, instructions to respond rapidly reduce the decision criterion resulting in less accurate responses, whereas the converse occurs when accuracy is emphasised (Bogacz et al., 2010), reflecting that the time needed to complete a decision is an important property of decision-making. Accordingly, sequential sampling models propose that perceptual decisions are formed by the temporal integration of noisy sensory evidence until a decision threshold is reached (Smith and Ratcliff, 2004).

Correspondingly, neurophysiological and neuroimaging studies have identified a widespread network of areas whose activity pattern is consistent with that of an evolving decision (Gold and Shadlen, 2007; Heekeren et al., 2008). Although specific task requirements have caused partly varying activation topographies, the intraparietal sulcus (IPS) has been consistently recruited during perceptual decisions (Churchland et al., 2008; Tosoni et al., 2008; Freedman and Assad, 2011). In particular, studies using microstimulation in monkeys (Hanks et al., 2006) and transcranial magnetic stimulation (TMS) in humans (Gould et al., 2012) have causally implicated this region in decision-making.

While TMS focally interferes with activity of the stimulated area, it may also influence other remote but functionally coupled regions. This distributed impact on ongoing neural activity can now be measured using concurrent TMS-fMRI (Ruff et al., 2006; Bestmann et al., 2008; Moisa et al., 2012; Leitão et al., 2013). This study used this methodology to investigate how IPS-TMS influences perceptual decisions at the neural level while participants performed a demanding visual detection task. Participants maintained covert attention to the left lower visual field and indicated their percept (seen/unseen) of a small visual stimulus presented there on 50% of the trials. Simultaneously, bursts of 4 TMS pulses (10 Hz) were applied to the right anterior IPS or during a Sham condition. This experimental configuration allowed for the categorization of participants' responses along SDT terms into hits, misses, false alarms and correct rejections. The assessment of TMS effects at the neural level followed two approaches. First, TMS effects on trials with matched visual input but different behavioural response were evaluated. Second, we tested for TMS effects on trials with matched behavioural response but different visual input. Due to a very low number of false alarms, we focused on comparing (i) misses vs. hits and (ii) misses vs. correct rejections. Together, these two perspectives amounted to the comparison between incorrect and correct trials.

Materials and Methods

In a previous account of our data we evaluated the effects of IPS-TMS on task-relevant bottom-up visual input per se, while engaging the attentional network with a demanding visual detection task (Chapter 3). Moreover, to assess the influence of task-irrelevant sensory stimuli on task-performance, we additionally manipulated the auditory context across runs. In this study we focused on the neural effects of IPS-TMS on participants' perceptual responses. Furthermore, to simplify the design we only considered runs without auditory stimulation. Hence, this study reanalysed part of previously reported data to investigate the effects of IPS-TMS on perceptual decisions in a purely visual context. Accordingly, the methods described in this section have been partially described before and are respectively reproduced here for completeness and to allow for an independent read of the individual chapters.

Participants

A total of ten right-handed participants (4 male; mean age: 31.5 years; standard deviation: 8.1; Edinburgh Handedness inventory score (mean ± SD) of 78±16.8) with no history of neurological illness took part in this concurrent TMS-fMRI experiment. Yet, to allow for more balanced comparisons between conditions (see below *Behavioural Data Analyses*) three participants were excluded due to insufficient number of missed trials, leaving a total of 7 participants who were included in further behavioural and fMRI analyses (2 male; mean age: 32.29 years; standard deviation: 9.25; Edinburgh Handedness inventory score (mean ± SD) of 75±17.7). Participants had normal or corrected-to-normal vision. All participants gave informed consent prior to participation and the study was approved by the Human Research Ethics Committee of the Medical Faculty at the University of Tübingen.

Experimental Design & Task

The 2x2x2 factorial design manipulated: (i) task-relevant visual input (V present, V absent), (ii) visual response (seen, unseen) and (iii) TMS condition (right anterior IPS, Sham) (Fig. 5.1A).
In a visual detection paradigm, participants reported their percept (seen/unseen) of a visual stimulus presented in their left lower visual field, while at the same time fixating on a cross presented throughout an entire run in the centre of the screen (see *Stimuli and Stimuli Presentation*). Restricting the stimulus location to the left side of the visual field was preferred in this first step, as it has been shown that parietal TMS can elicit different effects for contra- and ipsi-lateral stimuli (Hilgetag et al., 2001). Therefore, our paradigm involved covert attention to the left visual field, with manipulation of the bottom-up visual input. Participants were instructed to answer 'seen' only when completely sure and to report 'unseen' otherwise. Each participant was trained in the task prior to going inside the scanner.

Each trial started with the change of the fixation cross colour from grey to blue. After 100 ms the visual target was presented with 50% probability (Fig. 5.1B). Independently of the type of trial (V present, V absent), 4 TMS pulses were subsequently applied (see *Data Acquisition and TMS Procedures*; Fig. 5.1C). After 600 ms of trial begin, the fixation cross turned back to grey and remained like this for 2690 ms until the onset of the next trial. The interstimulus interval amounted thus to 3290 ms, equalling one TR of the EPI acquisition.

Trials were presented in blocks of twelve that started and ended with a grey fixation cross. These were interleaved with baseline periods of 13 seconds, which were made explicit via a red fixation cross. Hence, the colour of the fixation cross induced changes in the attentional settings of the participants: while blue or grey were accompanied by a high attentional load, red represented little attentional demands.

Each run consisted of seven blocks and there were four runs per TMS condition, giving a total of 168 trials per experimental condition. The two TMS conditions (IPS/Sham) were performed in different sessions and the order was counterbalanced across participants.

For each participant, the order of conditions was fully randomized within and across the four runs that constituted a session. Across sessions, the same order of conditions was used.

Stimuli and Stimuli Presentation

The task-relevant visual stimulus consisted of a small (9x9 pixels, visual angle: 0.52°) square presented for one frame (i.e. 16 ms) on a grey background. When present, the visual stimulus appeared in the centre of a blue placeholder (40x40 pixels, visual angle: 2.3º) that was continuously presented throughout an entire run and positioned 12º left and 5º down relative to the fixation cross.

The grey level of the square was individually determined in a Quest Procedure (Watson and Pelli, 1983) inside the scanner aiming at a detection threshold of 70% and using the same parameters as the main experiment. The grey level was approximated by the use of dithering. Hence, instead of being a homogenous square, our stimulus was effectively a cloud of white pixels within the square. Importantly, identical grey levels were used across IPS and Sham stimulation.

Visual stimuli were presented using Psychophysics Toolbox version 3.0.10 (Brainard 1997; Kleiner et al. 2007) running on MATLAB 7.9 (MathWorks Inc, MA, USA) and a Macintosh laptop running OS-X 10.6.8 (Apple Inc, CA, USA). The visual stimulus was back-projected onto a frosted Plexiglas screen using a LCD projector (JVC Ltd., Yokohama, Japan; resolution: 800x600 pixels, refresh rate: 60Hz, viewing distance: 48cm) visible to the participant through a mirror mounted on the MR-head coil. Participants indicated their response (i.e. visual target seen or not seen) with their right hand using a MR-compatible custom-built button device connected to the stimulus computer.

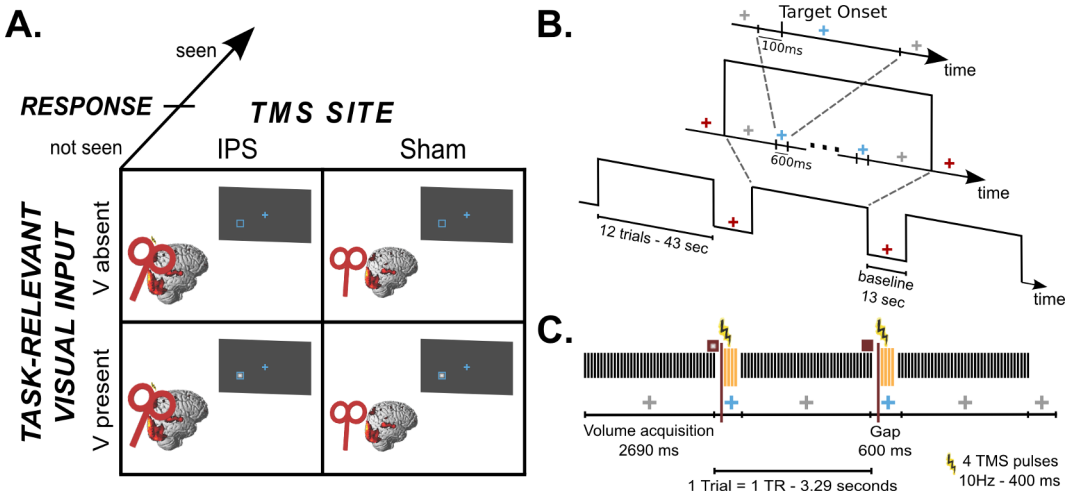

Figure 5.1. Experimental Design. (A) 2x2x2 factorial design manipulating (i) task-relevant visual input (V present, V absent), (ii) visual response (seen, unseen), (iii) TMS condition (IPS, Sham). **(B)** Timeline example of stimuli presentation. Blocks of 12 trials started and ended with a grey fixation cross and were interleaved with baseline periods, during which the fixation cross turned red. A trial began when the fixation cross turned blue. In target present trials, the visual stimulus was presented 100 ms after trial begin. After a total period of 600ms the fixation cross turned back to grey and remained like this until the next trial. **(C)** Illustration of the concurrent TMS-fMRI protocol and stimuli presentation timing for three scans (last scan corresponding to the end of the block). Within a block the fixation cross was grey during volume acquisition and blue during the acquisition gaps. At 100 ms after trial begin, the task-relevant visual stimulus was either present (first depicted trial) or absent (second depicted trial). Bursts of 4 TMS pulses were applied during acquisiton gaps at 10 Hz and started 100 ms after the target onset time.

TMS Sites

TMS was applied over the right anterior IPS as the experimental site and Sham TMS was included as a control condition.

The MNI coordinates (x = 42.3, y = -50.3, z = 64.4) reported by Oliver et al (2009) as a position over which TMS disrupted visuospatial processing were adopted for the parietal stimulation site. Individual stimulation coordinates were determined by inverse transforming the MNI coordinates from Oliver et al (2009) into native space using the parameters obtained from spatial normalization. *A posteriori* coil reconstruction of the coil position was based on custom-written MATLAB (MathWorks Inc, MA, USA) scripts and a water tube attached to the coil, which was clearly visible on the MR images. Across participants, the target IPS coordinates were obtained with a mean deviance of 10.6 mm ± 7.3 (mean, SD). The mean reached coordinate in MNI space was (x = 33.4, y = -49.2, z = 64.5).

In the Sham condition, 2 cm thick plastic plates were fixed between the TMS coil and the skull. Given the quadratic decay of the TMS-induced magnetic field, this Sham condition precluded the effects of direct brain stimulation, while maintaining the auditory and somatosensory side effects. Indeed, when tested over the finger region of the motor cortex, this Sham condition did not induce muscular twitches on pre-activated finger muscles even at 100% of total output intensity. During the Sham condition the coil was placed over the right hemisphere as close as possible to the experimental stimulation condition, given the space constraints inside the MR coil.

Data Acquisition and TMS Procedures

A 3T TIM Trio System (Siemens, Erlangen, Germany) was used to acquire both high-resolution structural images (176 sagittal slices, TR = 2300 ms, TE = 2.98 ms, TI = 1100 ms, flip angle = 9°, FOV = 240 mm x 256 mm, image matrix = 240 x 256, voxel size = 1 mm x 1 mm x 1 mm, using a 12-channel head coil) and T2*-weighted axial echoplanar images (EPI) with blood oxygenation level dependent (BOLD) contrast (GE-EPI, TR = 3290 ms, TE = 35 ms, flip angle = 90°, FOV = 192 mm x 192 mm, image matrix 64 x 64, 40 axial slices acquired sequentially in ascending direction, slice thickness = 3 mm, interslice gap = 0.3 mm, voxel size = 3 mm x 3 mm x 3.3 mm, using a 1-channel Tx/Rx head coil). Each participant took part in a total of eight experimental runs per TMS condition, from which only four are reported in the current study. A total of 124 volume images were acquired for each run.

After each EPI run, a fast structural image (fast low-angle shot [FLASH], 100 axial slices, TR = 564 ms, TE = 2.46 ms, TI = 300ms, FOV = 256mm x 256 mm, image matrix = 256x256, voxel size = 1x1x3 mm) was acquired to enable *a posteriori* reconstruction of the TMS coil position inside the scanner, as described elsewhere (Leitão et al., 2013).

The EPI sequence was adapted for concurrent TMS-fMRI experiments by introducing gaps of 600 ms after every volume acquisition. Each gap was introduced to allow the delivery of four TMS pulses without interference with image quality (Bestmann, 2003; Moisa et al., 2009). Bursts of four pulses at 10 Hz were applied every trial, with the first pulse applied 2890 ms after begin of volume acquisition, i.e., 100 ms after stimulus onset (Fig. 5.1C).

TMS pulses were applied after stimulus onset in order to minimize crossmodal interaction effects between our stimuli and the TMS induced auditory and somatosensory side effects (Duecker and Sack, 2013; Leitão et al., 2013). Similar TMS protocols have been used both in TMS studies outside the scanner (Chambers et al., 2004; Oliver et al., 2009) and in concurrent TMS-fMRI studies (Ruff et al., 2006, 2008, 2009; Sack et al., 2007; Blankenburg et al., 2010; Heinen et al., 2011) investigating visuospatial processing.

Biphasic stimuli were delivered using a MagPro X100 stimulator (MagVenture, Denmark) and a MR-compatible figure of eight TMS coil (MRi-B88), using the same coil-holding device as described in Moisa et al (2009).

During IPS stimulation, a fixed TMS intensity of 69% of total stimulator output was used for all participants. This corresponded to 125% of the mean resting motor threshold, as determined across twenty-four participants of prior studies using the same coil (M Moisa, personal communication). To ensure similar somatosensory side effects between IPS- and Sham-TMS the TMS intensity was increased to 75% during the Sham condition based on the subjective report of two naïve participants that participated in a pilot test.

Extensive image quality tests of our setup are reported elsewhere (Moisa et al., 2009, 2010: Supplementary Material). For completeness, we acquired EPI data with a phantom using the same experimental design. After realignment, data were entered in a first level analysis using the same model as for the real participants. Computing all the relevant contrasts (height threshold: $p < 0.01$ uncorrected) yielded only spurious and randomly distributed activation patterns.

Behavioural Data Analysis

Behavioural responses were categorized in hits, false alarms, misses and correct rejections (CR). Hit and CR rates were computed separately for IPS-TMS and Sham-TMS and averaged across participants. Paired t-tests were performed to test for significant differences between TMS conditions. Analyses on the CR rates revealed that under both TMS conditions, false alarm rate was very low and thus this response category was excluded from further behavioural analyses.

TMS effects were thus assessed under two different perspectives. First, we investigated the TMS effects between trials that elicited different behavioural responses but were matched in terms of visual input. In other words, TMS effects on visual percept during the presence of the task-relevant visual input (comparison between Hits and Misses) were evaluated. Second, we tested for TMS effects between trials with matched behavioural response but different visual input. Expressly, the effects of TMS on task-relevant visual input during trials labelled as unseen (comparison between CR and Misses) were investigated. Therefore, to allow for more balanced comparisons only participants with a minimum of 10% missed trials in each of the two TMS conditions (IPS/Sham) were included in the analyses.

Statistical analyses were also performed on reaction times data. As the median is a biased estimator of the population median, it should not be used on reaction time data when comparing conditions with different number of trials. Hence, individual mean reaction times were computed for hits, misses and CR separately for IPS-TMS and Sham-TMS and averaged across participants. The calculation of the individual mean reaction times excluded very slow reaction times (under 200ms) and reaction times that were two standard deviations longer than the mean. Reaction time data was entered in a 2-way repeated measures analysis of variance (RM-ANOVA) with factors TMS condition (IPS, Sham) and response category (Hits, Misses, CR). Post-hoc paired t-tests were computed to test for the simple main effects of response category by pooling over TMS conditions. Results are reported using the Greenhouse-Geisser correction.

fMRI Data Analysis

The fMRI data were analysed using SPM8 (Wellcome Department of Imaging Neuroscience, London; www.fil.ion.ucl.ac.uk/spm) (Friston et al. 1995). Scans from each subject were realigned using the first as a reference, unwarped, spatially normalized into MNI space, resampled to a spatial resolution of 2 x 2 x 2 mm^3, and spatially smoothed with a Gaussian kernel of 8 mm full-width at half-maximum. The time series of all voxels were high-pass filtered to 1/128 Hz. The first 3 volumes were discarded to allow for T1-equilibration effects.

The fMRI experiment was modeled as a mixed block-event-related design. Individual response categories (Hits, Misses, False alarms and CR) were modeled as events locked to the stimulus onset and entered into a design matrix after convolution with a canonical hemodynamic function and its first temporal derivative. The later was included as a variable-of-no-interest to capture variance caused by temporal deviations of the BOLD responses from the canonical response function. In addition to modeling these conditions separately for each IPS-TMS and Sham-TMS session, our statistical model included block begin and block end regressors (i.e. the periods during which the

fixation was grey at the beginning and end of a block; see *Experimental Design*) as mini blocks of 2.69 s and 3.29 s duration, respectively. The four runs acquired for each IPS- and Sham-TMS session were concatenated with run-specific means entered as separate regressors. Nuisance covariates included the realignment parameters to account for residual motion artifacts.

While all response categories were modelled at the first level, false alarms were not included in further analyses (see *Behavioural Data Analysis*). For each participant, the remaining condition specific effects were estimated according to the general linear model by creating contrast images of each effect relative to the implicit baseline.

As mentioned above, we examined the effects of TMS on (i) conscious visual percept during target present trials (Hits vs. Misses) and on (ii) task-relevant visual input in the absence of conscious visual percept (CR vs. Misses). These effects were analysed in three steps. First, we identified main effects of TMS by comparing IPS > Sham and Sham > IPS pooled (i.e. summed) over all response categories. Second, we tested for the effects of a conscious visual percept by comparing (i) Hits > Misses and Misses > Hits and (ii) CR > Misses and Misses > CR, while pooling (i.e. summing) over IPS and Sham stimulation. Lastly, state-dependent TMS effects were evaluated by computing the interactions between TMS and response category. Specifically, the contrasts (i) $[(\text{Misses} > \text{Hits})_{\text{IPS}} > (\text{Misses} > \text{Hits})_{\text{Sham}}]$ and $[(\text{Misses} > \text{Hits})_{\text{Sham}} > (\text{Misses} > \text{Hits})_{\text{IPS}}]$ and (ii) $[(\text{Misses} > \text{CR})_{\text{IPS}} > (\text{Misses} > \text{CR})_{\text{Sham}}]$ and $[(\text{Misses} > \text{CR})_{\text{Sham}} > (\text{Misses} > \text{CR})_{\text{IPS}}]$ were evaluated. All the evaluated statistical comparisons included only regressors based on the canonical hemodynamic response function.

To allow for a random effects analysis and inferences at the population level, these contrast images were entered into independent second-level one-sample t-tests (Friston et al. 1999).

Unless stated otherwise, we report activation at $p < 0.05$ corrected at the cluster level for multiple comparisons (family-wise error rate) based on Gaussian Random Field theory within the entire brain and using an auxiliary uncorrected voxel threshold of $p = 0.01$ (Hayasaka and Nichols, 2003).

Effects of RT covariate

A frequent concern in neuroimaging studies is that differences in reaction times between two conditions may constitute a confound in functional imaging data. Accordingly, this behavioural measure is frequently covaried out and involvement of a specific area is only taken into account if it cannot be explained by differences in reaction times. Yet, it has been argued that reaction times and hemodynamic changes are two dependent variables and thereby represent different indices of the same perceptual processes (Henson, 2005). Consequently, correlations between reaction times and differential activations would be anticipated in regions that are involved in the process under investigation. In fact, this is the standard assumption in behavioural studies, where differences in reaction times between two conditions are frequently considered to indicate different underlying processing mechanisms. In a attempt to reconcile these two approaches, a recent study proposed that whether or not differential activations should be independent of reaction time data is contingent on whether different conditions are thought to engage a certain region or are instead thought to induce different levels of processing effort in these regions (Taylor et al., 2014). Specifically, the authors

propose that whereas conditions that differentially engage a certain region should be independent of reaction times, conditions that involve different levels of processing effort, even when correlating with reaction times, are still of interest for the investigated task. As argued by the authors, these dissociations can be assessed by modeling the data with and without reaction time regressors.
Accordingly, we performed an additional analysis by expanding our initial general linear model by one additional regressor per TMS condition that modeled trial-specific reaction times from all three response categories. Specifically, for each TMS condition we constructed an onset vector that was amplitude modulated by trial-specific reaction times values. After mean-correction, these vectors were convolved with the hemodynamic response function and were inserted as user-defined regressors in the new design matrix. Note that the introduction of the reaction time regressors only accounts for the partition of variance that cannot be explained by the condition effects.

Eye monitoring (outside the scanner)

Eight additional participants took part in a supplementary TMS experiment performed outside the scanner to ensure that the observed activation pattern did not result from eye movements, twitches, and startle effects. For each TMS condition, one experimental run was acquired per participant using an equivalent experimental paradigm. To account for the absence of the high-current filter used in the concurrent TMS-MRI setup (Moisa et al., 2009), the TMS intensity was reduced to 63% of total output.
Horizontal and vertical eye movements were recorded in 8 additional participants using an iView XTM RED-III remote eyetracker system (SensoMotoric Instruments Inc., Needham/Boston, MA, USA) (50 Hz sampling rate). The eyetracking system was calibrated using a 13-point calibration. Eye position data were automatically corrected for blinks and converted to radial velocity.
For each response category (Hits, Misses, CR) the mean distance (degrees) from the fixation cross, the number of saccades (defined by a radial eye velocity threshold > 30°/s for a minimum of 60ms duration and radial amplitude larger than 5°), and the number of blinks were quantified for the period during which the fixation cross was blue (see *Experimental Design & Task*).
Across all participants saccades were almost completely absent, hence no further analyses were performed for this index. The two remaining indices were independently entered into a 2-way repeated measures analysis of variance (RM-ANOVA) with the factors TMS condition (IPS, Sham) and response category (Hits, Misses, CR). Results are reported using the Greenhouse-Geisser correction.

Results

Behavioural Data

Participants performed a demanding visual detection task. In every trial, they had to report their percept (seen or unseen) of a visual stimulus that was present in half of the trials. Responses were thus categorized in hits, false alarms, misses and correct rejections (CR).

Participants detected on average 64 ± 20% (± SD) of the task-relevant visual stimuli and correctly rejected 99 ± 1% (± SD) of the trials during IPS stimulation. During the Sham condition, there were 71 ± 12% (± SD) hits and 99 ± 1% (± SD) correct rejections, indicating that on average the quest procedure worked out as desired. Paired t-tests confirmed that there was no effect of TMS on the hit rate ($t_{(6)} = -0.994$, $p = 0.358$) nor on the CR rate ($t_{(6)} = 0.27$, $p = 0.979$). As can be deducted from the elevated CR rate, participants had almost no false alarms, which were thus excluded from further analyses.

For each of the remaining response categories the mean reaction time was calculated for each participant. Across participants the average reaction time during IPS stimulation was 730 ± 95 ms (± SD) for hits, 830 ± 83 ms (± SD) for misses and 747 ± 57 ms (± SD) for CR. During Sham stimulation, mean reaction times amounted to 726 ± 117 ms (± SD), 849 ± 145 ms (± SD) and 731 ± 95 ms (± SD) for hits, misses and CR, respectively. Reaction times data were entered in a 2-way RM-ANOVA with factors TMS condition (IPS, Sham) and response category (Hits, Misses, CR). There was no main effect of TMS ($F_{(1,6)} = 0.000$; $p = 0.987$) nor was there an interaction between the two factors ($F_{(1,6)} = 1.085$; $p = 0.345$). However, there was a significant main effect of response category ($F_{(1,6)} = 11.729$; $p = 0.007$). Pooling over IPS and Sham conditions, post-hoc paired t-tests on all three pair combinations confirmed that there was a significant effect for the pairs Hits vs. Misses ($t_{(6)} = -4.047$, $p = 0.007$) and CR vs. Misses ($t_{(6)} = -6.065$, $p < 0.001$), whereas no significant effect was observed for the pair Hits vs. CR ($t_{(6)} = -0.653$, $p = 0.538$).

In summary, participants took significantly longer to respond during missed trials compared to both hits and correct rejections. Given that participants were instructed to answer ‘seen’ only when completely sure about their percept, this suggests that missed trials were coupled with increased decisional uncertainty and thereby required additional processing effort. Importantly, however, IPS- relative to Sham-TMS did not result in any behavioural changes, which guarantees that the TMS effects on the BOLD signals reported here are not confounded by behavioural differences (Bestmann et al., 2010; Blankenburg et al., 2010; Moisa et al., 2012).

Neuroimaging Data

The data were separately analysed for the effects on visual percept (i.e. the comparison between Hits and Misses trials) and the effects on task-relevant visual input in the absence of a visual percept (i.e.

the comparison between Misses trials and CR). Common to both approaches is the comparison of incorrect (Misses) with correct (Hits, CR) trials.
First, we identified the main effects of TMS by comparing IPS- with Sham-TMS independently of the response category. Second, we tested for the effects of response category by comparing response categories (Misses vs. Hits and Misses vs. CR) while pooling over both TMS conditions. Third, we characterized state-dependent TMS effects by testing for the interaction between response category and TMS condition. All effects were tested for the entire brain.

Main Effects of TMS

Main effects of TMS were identified by directly comparing IPS and Sham TMS conditions and pooling over all response categories. Comparing Sham- relative to IPS-TMS activated the left dorsal lateral prefrontal cortex. Specifically, significant activation clusters were localized in the left superior and middle frontal gyri (see Table 5.1). However, this region also showed interaction effects (see below) and therefore these main effects will not be considered further.
In a prior study that included the same data we modelled visual input present (i.e. hits and misses) as well as visual input absent trials (i.e. correct rejections and false alarms) as two regressors (Chapter 2). Comparing IPS- relative to Sham-TMS in this analysis increased activations in the right parietal cortex close to the stimulated site. The present model was less efficient in detecting these main effects, as the variance from each run was distributed amongst four rather than two different regressors. However, activation clusters underneath the coil were still detectable at an uncorrected level of significance (Table 5.1). Consequently, our TMS protocol functioned as an effective perturbation method at the neuronal level in the locally targeted region.

Effects of Response Category

We investigated the effects of response processing per se by pooling over TMS conditions. Missed relative to hit trials increased activations in the left posterior cingulate cortex (PCC), extending to the bilateral visual cortex and the precuneus (see Fig. 5.2 and Table 5.2). Inspection of the parameter estimates suggests that, independently of the TMS condition, stronger activations were observable for missed trials relative the other two response categories in this region.
Furthermore, both comparison approaches between incorrect (Misses) and correct (Hits or CR) trials overlapped in a significant activation cluster in the superior medial and frontal gyri, extending to the anterior cingulate cortex (see Fig. 5.2 and Table 5.2). Even though the effects in this region only emerged as (simple) main effects rather than interactions (see next paragraph), inspection of the parameter estimate plots suggests that IPS-TMS had a modulatory effect in this area by increasing activations for correct responses.
The remaining comparisons did not reveal any significant effects.

Interaction Effects

To test for state-dependent TMS effects, we computed interactions between TMS conditions and response categories (Misses > Hits and Misses > CR, respectively).

Testing for the interaction between Misses > Hits and Sham > IPS revealed effects in the right precentral and middle frontal gyri (Fig. 5.3 and Table 5.1). The interaction contrast between Misses > CR and Sham > IPS resulted in a significant cluster in the posterior prefrontal cortex (BA8). In particular, this comparison showed activations in the left posterior middle/superior frontal gyrus extending to the right superior medial gyrus (Fig. 5.3 and Table 5.2). Under normal processing circumstances, these prefrontal areas showed higher activations during missed trials relative to hits and CR. This discrimination between incorrect and correct trials disappeared when activity in the IPS was perturbed. The remaining interactions were not significant.

Effects of RT covariate

To evaluate the effects of different reaction times between the conditions in our experiment, we extended our initial general linear model to include trial-specific reaction times regressors for each TMS condition. Areas that were positively predicted by reaction times included the bilateral frontoparietal cortices, the bilateral anterior insulae/frontal opercula and inferior frontal gyri, the left motor and somatosensory cortices and the anterior cingulate/middle prefrontal cortex extending to the supplementary motor area. Conversely, areas that were negatively correlated with reaction times included the left precuneus, the left angular gyrus and the left middle/superior frontal gyri.

Table 5.1. Effects of TMS

Brain Regions	*MNI Coordinates (mm)*			*Z Score*	*#Voxels in Cluster*	p_{FWE}*-value*
	x	y	z	*(peak)*		*(cluster)*
Main TMS Effects						
Sham > IPS $_{(Hits+Misses+CR)}$						
Left Superior Frontal Gyrus	-16	28	40	4.53	494	0.006
Left Middle Frontal Gyrus	-20	26	48	4.12		
IPS > Sham $_{(Hits+Misses+CR)}$						
Right Superior Parietal Lobule	34	-52	62	2.85	22	0.002*
Right Postcentral Gyrus	32	-34	72	2.63	18	0.004*
Right Precuneus	12	-48	74	4.14	57	<0.001*
State-dependent TMS Effects						
Hits >Misses $_{(IPS>Sham)}$						
Right Middle Frontal Gyrus	38	14	48	4.17	412	0.028
Right Precentral Gyrus	48	6	44	4.04		
CR >Misses $_{(IPS>Sham)}$						
Left Middle Frontal Gyrus	-22	20	50	4.39	863	<0.001
Left Superior Frontal Gyrus	-16	24	50	4.13		
Right Superior Frontal Gyrus	26	30	46	3.37		

p-values marked with * are reported at an uncorrected peak-level. All the remaining *p*-values are corrected for multiple comparisons within the entire brain

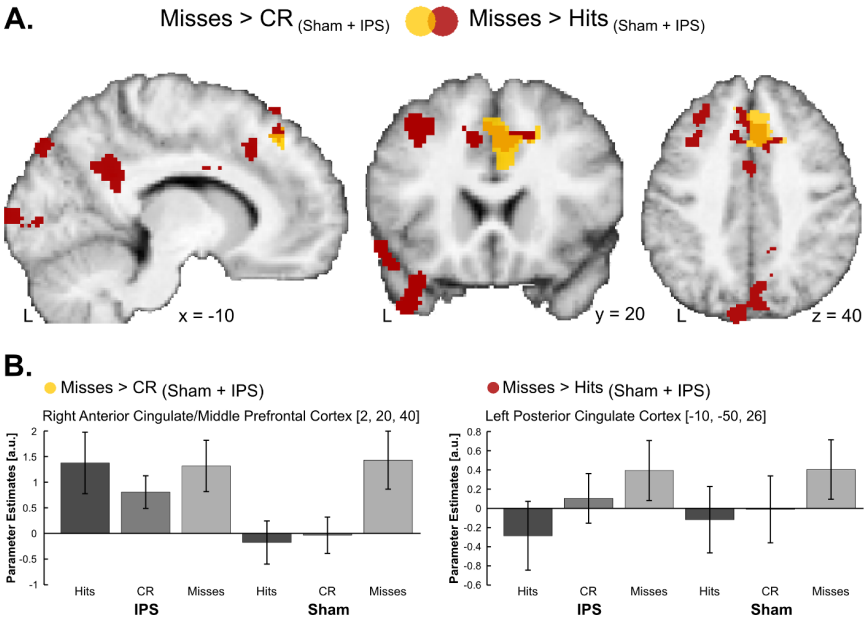

Figure 5.2. Effects of Response Category. (A) Activations induced by the comparisons between (i) Misses and Hits (red) and (ii) Misses and CR (yellow) trials are displayed on sagittal, coronal and axial slices of a mean image created by averaging the subjects' normalized structural images. For illustrational purposes only, effects are displayed at a height threshold of $p = 0.01$ uncorrected and an extent threshold of 250 voxels. **(B)** Parameter estimates (mean ± standard error of the mean) are displayed at the given coordinates in the right anterior cingulate/middle prefrontal cortex (for Misses vs. CR) and in the left posterior cingulate cortex (for Misses vs. Hits). The bar graphs represent the size of the effect in non-dimensional units (corresponding to % whole-brain mean).

Crucially, apart from the effects of response category in the anterior cingulate/middle prefrontal cortex (ACC/mPFC) all the other effects reported above persisted even after inclusion of the reaction time regressors. Given that missed trials were associated in increased decisional uncertainty it is unsurprising that the introduction of the reaction time regressors removed differential activations between the different conditions in the ACC/mPFC (see *fMRI Data Analysis*), which is an area that has been previously associated with decisional uncertainty (Volz et al., 2004; Huettel et al., 2005; Grinband et al., 2006; Yoshida and Ishii, 2006; Pochon et al., 2008). Yet, also as expected, state-dependent TMS effects were independent of any behavioural differences between response categories.

Eyetracker Data

Two independent 2-way repeated measures analysis of variance (RM-ANOVA) with the factors TMS condition (right IPS and Sham) and response category (Hits, Misses, CR) were performed for the mean distance from the fixation cross and the number of blinks.

For the number of blinks index, the analysis did not show main effects of TMS ($F_{(1,7)} = 1.532$; $p = 0.256$) nor response category ($F_{(1,7)} = 3.406$; $p = 0.098$), nor was there a significant interaction between the two ($F_{(1,7)} = 2.617$; $p = 0.128$). Similarly, for the mean distance for the fixation, there was no main effect of TMS ($F_{(1,7)} = 1.338$; $p = 0.285$) nor a main effect of response category ($F_{(1,7)} =$

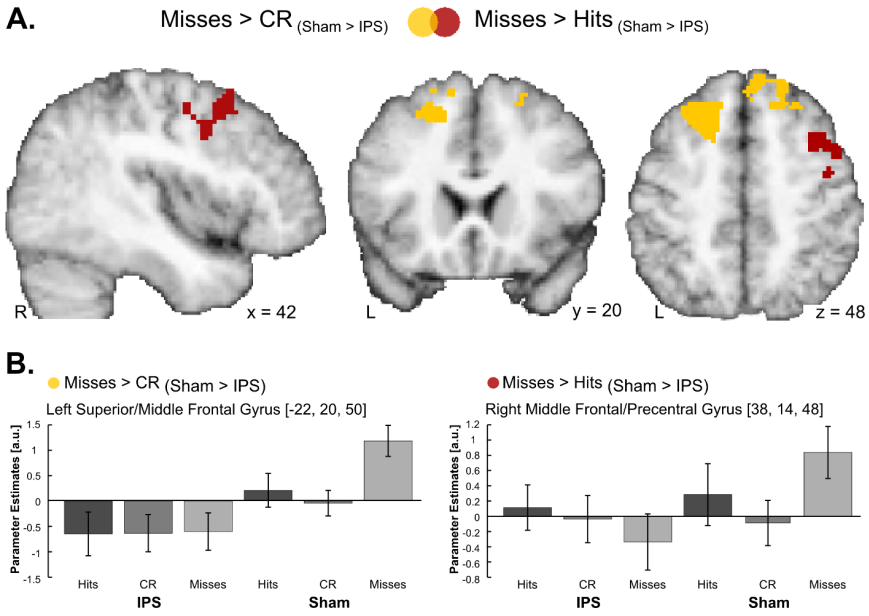

Figure 5.3. Interaction Effects. (A) Activations induced by the interaction between TMS and (i) Misses vs. Hit (red) and (ii) Misses vs. CR (yellow) are displayed on sagittal, coronal and axial slices of a mean image created by averaging the subjects' normalized structural images. For illustrational purposes only, effects are displayed at a height threshold of $p = 0.01$ uncorrected and an extent threshold of 250 voxels. **(B)** Parameter estimates (mean ± standard error of the mean) are displayed at the given coordinates within the left superior/middle frontal gyrus (for Misses vs. CR) and the right middle frontal/precentral gyrus (for Misses vs. Hits). The bar graphs represent the size of the effect in non-dimensional units (corresponding to % whole-brain mean).

Table 5.2. Effects of Response Category

Brain Regions	*MNI Coordinates (mm)*			*Z Score*	*#Voxels in*	p_{FWE}*-value*
	x	y	z	*(peak)*	*Cluster*	*(cluster)*
Effects of Response Category						
Misses >Hits $_{(IPS+Sham)}$						
Left Superior Medial Gyrus	-8	36	44	4.86	533	0.005
Left Superior Frontal Gyrus	-10	36	48	4		
Left Anterior Cingulate Cortex	-6	4	30	3.44		
Left Posterior Cingulate Cortex	-10	-50	26	4.46	2285	<0.001
Right Lingual Gyrus	18	-84	-10	3.70		
Left Superior Occipital Gyrus	-10	-102	6	3.64		
Left Calcarine Gyrus	2	-98	0	3.54		
Right Precuneus	8	-66	36	3.51		
Misses > CR $_{(IPS+Sham)}$						
Right Middle Cingulate Cortex	2	20	40	3.99	722	<0.001
Right Anterior Cingulate Cortex	6	16	28	3.49		
Left Superior Medial Gyrus	-10	38	42	3.26		
Left Superior Frontal Gyrus	-14	34	48	3.25		

p-values are corrected for multiple comparisons within the entire brain

1.866; $p = 0.208$), nor a significant interaction between the two ($F_{(1,7)} = 2.595$; $p = 0.140$).
None of the RM-ANOVAs revealed any significant main effects or interactions suggesting that differences in eye movements are unlikely to account for the observed activation profile in our fMRI data.

Table 5.3. Simple Main Effects

Brain Regions	*MNI Coordinates (mm)*			*Z Score (peak)*	*#Voxels in Cluster*	p_{FWE}-*value (cluster)*
	x	y	z			
Effects of TMS						
CR $_{(IPS > Sham)}$						
Left Lingual Gyrus	-20	-66	0	3.63	702	0.001
Left Inferior Occipital Gyrus	-30	-76	-8	3.62		
Left Cerebellum	-36	-72	-30	3.58		
Left Fusiform	-30	-70	-18	3.23		
Hits $_{(IPS > Sham)}$						
Left Inferior Occipital Gyrus	-46	-72	-10	4.27	604	0.002
Left Lingual Gyrus	-18	-72	-10	3.66		
Left Fusiform Gyrus	-28	-58	-10	3.65		
Right Middle Temporal Gyrus	44	-64	-2	4.02	621	0.002
Right Lingual Gyrus	22	-76	-10	3.67		
Right Fusiform Gyrus	34	-68	-14	3.43		
Misses $_{(Sham > IPS)}$						
Left Middle Frontal Gyrus	-22	26	50	4.83	483	0.007
Left Superior Frontal Gyrus	-14	26	48	4.18		
Effects of Response Category						
Hits >Misses $_{IPS}$						
Left Putamen	-22	4	-2	4.67	355	0.052
Left Caudate Nucleus	-8	14	12	3.43		
Misses >CR $_{Sham}$						
Left Middle Frontal Gyrus	-28	22	44	4.90	2579	<0.001
Left Superior Medial Gyrus	-10	34	46	3.94		
Right Superior Frontal Gyrus	22	30	60	3.76		
Misses >Hits $_{Sham}$						
Right Middle Cingulate Cortex	4	-2	32	4.44	479	0.01
Left Inferior Frontal Gyrus	-54	22	6	4.43	394	0.031
Left Calcarine Gyrus	-8	-100	0	4.42	882	< 0.001
Left Superior Occipital Gyrus	-22	-96	22	3.64		
Left Middle Occipital Gyrus	-20	-98	14	3.57		
Right Superior Frontal Gyrus	16	34	52	4.23	352	0.055
Left Precentral Gyrus	-48	-6	48	3.80	349	0.057
Left Postcentral Gyrus	-40	-20	44	2.96		
Left Middle Frontal Gyrus	-20	0	48	2.69		

p-values are corrected for multiple comparisons within the entire brain

Discussion

Decisions about sensory events in the surroundings are ubiquitous in our daily lives. Perceptual decisions involve a series of cognitive and non-cognitive processes, ranging from the gathering and accumulation of sensory evidence, the detection of perceptual uncertainty signalling (among other things) the need for more attentional resources and finally the categorization into a behavioural response that is followed by the corresponding motor output. At the neural level, these different processing modules are supported by a widespread network of areas that include sensory, frontal and parietal cortices, as well motor and premotor regions (Kim and Shadlen, 1999; Heekeren et al., 2004, 2006; de Lafuente and Romo, 2006; Pleger et al., 2006; Thielscher and Pessoa, 2007; Ho et al., 2009; Noppeney et al., 2010). In particular, neuroimaging and neurophysiological studies have shown that the parietal cortex is recruited during perceptual decisions (Churchland et al., 2008; Tosoni et al., 2008; Rorie et al., 2010; Freedman and Assad, 2011; White et al., 2012). This is further supported by off-line TMS studies that provided causal evidence for an involvement of the right parietal cortex during visual detection tasks by reporting TMS-induced behavioural disturbances (Pascual-Leone et al., 1994; Hilgetag et al., 2001; Thut et al., 2005). Particularly, using signal detection measures, Oliver et al. (2009) reported an optimal region in the right anterior IPS at which TMS reduced the visual sensitivity (i.e. d') for peripheral target-gaps presented in the left visual hemifield. However, while off-line TMS studies are invaluable in the determination of causal structure-function relationships, they are restricted to inferences at the stimulated area. In this study we used concurrent TMS-fMRI to investigate how stimulating this location at the right IPS affected processing in other remote brain areas during a similar visual detection task.

Behaviourally, participants' reports about their visual percept were not altered by our TMS manipulation. This is beneficial when investigating TMS effects at the neural level using fMRI, as these might otherwise be contaminated by behavioural changes that would result in interpretational difficulties (see Price et al., 2006 for related issues with neurological patients).

Yet, analyses on reaction time data showed that, independently of the TMS condition, participants took significantly longer to respond during missed trials compared to both hits and correct rejections. This suggests that missed trials were associated with more uncertainty as indexed by longer response times, thus reflecting task instructions given prior to the experiment. Indeed, participants were instructed to answer 'seen' only when completely sure about their percept. This induced a very high decisional criterion, under which missed trials are likely to include both truly undetected stimuli and trials in which participants were unsure about their visual percept and responded 'unseen' so as not to incur in any false alarms. At the neural level, this uncertainty might be associated with a noisy neural representation already at the level of visual cortices. Alternatively, it might reflect weaker attentional selection mechanisms at a higher-order processing stage, where short lapses of attention result in ambivalent trials. While it is not possible to disentangle between these two alternatives, noisy representations during missed trials are likely to be accompanied with additional neural processing, in particular at the decisional level.

Indeed, under normal processing circumstances, missed (i.e. incorrect) relative to both hit and correctly rejected (i.e. correct) trials elicited increased activations in the anterior cingulate/middle prefrontal cortex (AC/mPFC) (Fig. 5.2). This region has been previously associated with decision uncertainty (Volz et al., 2004; Huettel et al., 2005; Grinband et al., 2006; Yoshida and Ishii, 2006; Pochon et al., 2008), an interpretation that is consistent with the decision ambivalence associated with missed trials in this study.

Even though response category effects in the AC/mPFC only emerged as simple main effects, an inspection of the parameter estimates plot suggests that IPS-TMS had a modulatory effect in this region (Fig. 5.2). This modulatory effect was significant in areas of the bilateral prefrontal cortex that strongly interact with this area (MacDonald, 2000; Badre and Wagner, 2004; Domenech and Dreher, 2010). In fact, state-dependent TMS effects were found in the posterior superior frontal gyri (SFG) and in the right precentral and posterior middle frontal gyri (MFG). In these regions, the common response enhancement for missed trials during normal processing conditions was abolished when TMS was applied at the IPS (Fig. 5.3). In the left prefrontal cortex in particular, significant post-hoc comparisons testing for simple main effects of TMS (Table 5.3) suggest that these state-dependent TMS effects were specifically driven by IPS-TMS modulations during missed trials.

The areas showing state-dependent TMS effects in this study overlap considerably with areas previously implicated in perceptual decision-making (Heekeren et al., 2004; Ruff et al., 2010). In particular, Heekeren et al. (2004) reported increased activations for easy relative to difficult decisions in the SFG, whereas activations in the posterior MFG exhibited the opposite pattern. However, in this study both areas consistently showed increased activations for uncertain/incorrect trials relative to correct trials during Sham-TMS, which in accordance to Heekeren et al. suggests that these regions might also be signalling the need for additional attentional resources in situations of high decisional uncertainty. Consequently, TMS-induced decreases in these areas would respectively indicate an abolishment of this signalling.

It is thus surprising that such state-dependent TMS effects on hemodynamic responses were mirrored by an absence of TMS-induced behavioural changes. Taking the notion of degeneracy in consideration (Edelman and Gally, 2001; Price and Friston, 2002; Noppeney et al., 2004), this dichotomy might reflect the existence of different sets of areas involved in decision-making, such as the insula, the dorsolateral prefrontal cortex or subcortical structures, that can complete similar task requirements as reflected by behavioural measures. These compensatory mechanisms would reflect a flexible and resilient system that is able to adapt to ever-changing circumstances. In our study, it is plausible that a function that under normal processing conditions is preferentially performed by a particular set of areas was shifted to other regions following disturbances to the system. Potentially, the modulatory effects of IPS-TMS in the AC/mPFC, that were characterized by an increase of activation for correct trials up to the level observed for missed trials, might reflect the recruitment of this alternative source of control.

Yet, the absence of consistent compensatory activations suggests an alternative account, by which prefrontal activations might instead reflect processing that is incidental to task performance. In fact, it has been shown that functional imaging can detect implicit activations like for instance hemodynamic changes in response to unaware emotional facial expressions during an unaffected

naming-task (Morris et al., 1998). In decision-making, secondary processing often takes place in form of metacognitive evaluations about task performance, such as error monitoring and confidence judgments about the chosen response (Maniscalco and Lau, 2012; Fleming and Lau, 2014). Based on evidence showing that participants can spontaneously detect incorrect decisions and correct them when given a chance to do so, it has been proposed that these evaluations occur at a post-decisional stage that uses accumulated evidence from both afore and after the decisional response (Pleskac and Busemeyer, 2010; Yeung and Summerfield, 2012).

Studies with human and non-human primates have associated metacognitive abilities with a number of different areas that include the parietal cortex, the frontal eye fields, the cingulate and prefrontal cortices, amongst other regions (Kiani and Shadlen, 2009; Rounis et al., 2010; Fleming et al., 2012; Middlebrooks and Sommer, 2012; Charles et al., 2013; Teichert et al., 2014). This dispersed account across different studies suggests that different metacognitive abilities might be supported by distinct neural mechanisms that are determined by existing task specificities (Baird et al., 2013; McCurdy et al., 2013; Fleming et al., 2014). In this respect, our results might reflect a distributed network of frontoparietal regions that implements post-decisional evaluations about task performance. Yet, since the current study was not directly designed to evaluate this type of metacognitive processes, this hypothesis remains conjectural and should be explicitly investigated in future studies.

In conclusion, our study demonstrated that IPS-TMS abolished activation increases for decisional uncertainty and response errors in the bilateral prefrontal cortices without eliciting any behavioural changes. Neural effects were state-dependent, emerging primarily via specific activation decreases during missed trials. These specific neural effects and the simultaneous lack of behavioural impairments suggest that the modulated areas were not necessary for objective task performance. Instead, we propose that this dichotomy reflects influences of IPS-TMS on post-decisional evaluations about task performance associated with incorrect responses.

References

Badre D, Wagner AD (2004) Selection, integration, and conflict monitoring; assessing the nature and generality of prefrontal cognitive control mechanisms. Neuron 41:473–487.

Baird B, Smallwood J, Gorgolewski KJ, Margulies DS (2013) Medial and lateral networks in anterior prefrontal cortex support metacognitive ability for memory and perception. J Neurosci 33:16657–16665.

Bestmann S (2003) On the Synchrinzation of Transcranial Magnetic Stimulation and Functional Echo-Planar Imaging. J Magn Reson Imaging.

Bestmann S, Ruff CC, Blankenburg F, Weiskopf N, Driver J, Rothwell JC (2008) Mapping causal interregional influences with concurrent TMS-fMRI. Exp Brain Res 191:383–402.

Bestmann S, Swayne O, Blankenburg F, Ruff CC, Teo J, Weiskopf N, Driver J, Rothwell JC, Ward NS (2010) The role of contralesional dorsal premotor cortex after stroke as studied with concurrent TMS-fMRI. J Neurosci 30:11926–11937.

Blankenburg F, Ruff CC, Bestmann S, Bjoertomt O, Josephs O, Deichmann R, Driver J (2010) Studying the role of human parietal cortex in visuospatial attention with concurrent TMS-fMRI. Cereb Cortex 20:2702–2711.

Bogacz R, Wagenmakers E-J, Forstmann BU, Nieuwenhuis S (2010) The neural basis of the speed-accuracy tradeoff. Trends Neurosci 33:10–16.

Chambers CD, Stokes MG, Mattingley JB (2004) Modality-specific control of strategic spatial attention in parietal cortex. Neuron 44:925–930.

Charles L, Van Opstal F, Marti S, Dehaene S (2013) Distinct brain mechanisms for conscious versus subliminal error detection. Neuroimage 73:80–94.

Churchland AK, Kiani R, Shadlen MN (2008) Decision-making with multiple alternatives. Nat Neurosci 11:693–702.

De Lafuente V, Romo R (2006) Neural correlate of subjective sensory experience gradually builds up across cortical areas. Proc Natl Acad Sci U S A 103:14266–14271.

Domenech P, Dreher J-C (2010) Decision threshold modulation in the human brain. J Neurosci 30:14305–14317.

Duecker F, Sack AT (2013) Pre-stimulus sham TMS facilitates target detection. PLoS One 8:e57765.

Edelman GM, Gally J a (2001) Degeneracy and complexity in biological systems. Proc Natl Acad Sci U S A 98:13763–13768.

Fleming SM, Huijgen J, Dolan RJ (2012) Prefrontal contributions to metacognition in perceptual decision making. J Neurosci 32:6117–6125.

Fleming SM, Lau HC (2014) How to measure metacognition. Front Hum Neurosci 8:1–9.

Fleming SM, Ryu J, Golfinos JG, Blackmon KE (2014) Domain-specific impairment in metacognitive accuracy following anterior prefrontal lesions. Brain.

Freedman DJ, Assad J a (2011) A proposed common neural mechanism for categorization and perceptual decisions. Nat Neurosci 14:143–146.

Gold JI, Shadlen MN (2007) The neural basis of decision making. Annu Rev Neurosci 30:535–574.

Gould IC, Nobre AC, Wyart V, Rushworth MFS (2012) Effects of decision variables and intraparietal stimulation on sensorimotor oscillatory activity in the human brain. J Neurosci 32:13805–13818.

Green DM, Swets JA (1966) Signal detection theory and psychophysics.

Grinband J, Hirsch J, Ferrera VP (2006) A neural representation of categorization uncertainty in the human brain. Neuron 49:757–763.

Hanks TD, Ditterich J, Shadlen MN (2006) Microstimulation of macaque area LIP affects decision-making in a motion discrimination task. Nat Neurosci 9:682–689.

Hayasaka S, Nichols TE (2003) Validating cluster size inference: random field and permutation methods. Neuroimage 20:2343–2356.

Heekeren HR, Marrett S, Bandettini P a, Ungerleider LG (2004) A general mechanism for perceptual decision-making in the human brain. Nature 431:859–862.

Heekeren HR, Marrett S, Ruff D a, Bandettini P a, Ungerleider LG (2006) Involvement of human left dorsolateral prefrontal cortex in perceptual decision making is independent of response modality. Proc Natl Acad Sci U S A 103:10023–10028.

Heekeren HR, Marrett S, Ungerleider LG (2008) The neural systems that mediate human perceptual decision making. Nat Rev Neurosci 9:467–479.

Heinen K, Ruff CC, Bjoertomt O, Schenkluhn B, Bestmann S, Blankenburg F, Driver J, Chambers CD (2011) Concurrent TMS-fMRI reveals dynamic interhemispheric influences of the right parietal cortex during exogenously cued visuospatial attention. Eur J Neurosci 33:991–1000.

Henson R (2005) What can functional neuroimaging tell the experimental psychologist? Q J Exp Psychol A 58:193–233.

Hilgetag CC, Théoret H, Pascual-Leone a (2001) Enhanced visual spatial attention ipsilateral to rTMS-induced "virtual lesions" of human parietal cortex. Nat Neurosci 4:953–957.

Ho TC, Brown S, Serences JT (2009) Domain general mechanisms of perceptual decision making in human cortex. J Neurosci 29:8675–8687.

Huettel S a, Song AW, McCarthy G (2005) Decisions under uncertainty: probabilistic context influences activation of prefrontal and parietal cortices. J Neurosci 25:3304–3311.

Kiani R, Shadlen MN (2009) Representation of confidence associated with a decision by neurons in the parietal cortex. Science 324:759–764.

Kim JN, Shadlen MN (1999) Neural correlates of a decision in the dorsolateral prefrontal cortex of the macaque. Nat Neurosci 2:176–185.

Leitão J, Thielscher A, Werner S, Pohmann R, Noppeney U (2013) Effects of parietal TMS on visual and auditory processing at the primary cortical level -- a concurrent TMS-fMRI study. Cereb Cortex 23:873–884.

MacDonald a. W (2000) Dissociating the Role of the Dorsolateral Prefrontal and Anterior Cingulate Cortex in Cognitive Control. Science (80-) 288:1835–1838.

Maniscalco B, Lau H (2012) A signal detection theoretic approach for estimating metacognitive sensitivity from confidence ratings. Conscious Cogn 21:422–430.

McCurdy LY, Maniscalco B, Metcalfe J, Liu KY, de Lange FP, Lau H (2013) Anatomical coupling between distinct metacognitive systems for memory and visual perception. J Neurosci 33:1897–1906.

Middlebrooks PG, Sommer MA (2012) Neuronal Correlates of Metacognition in Primate Frontal Cortex. Neuron 75:517–530.

Moisa M, Pohmann R, Ewald L, Thielscher A (2009) New coil positioning method for interleaved transcranial magnetic stimulation (TMS)/functional MRI (fMRI) and its validation in a motor cortex study. J Magn Reson Imaging 29:189–197.

Moisa M, Pohmann R, Uludağ K, Thielscher A (2010) Interleaved TMS/CASL: Comparison of different rTMS protocols. Neuroimage 49:612–620.

Moisa M, Siebner HR, Pohmann R, Thielscher A (2012) Uncovering a Context-Specific Connectional Fingerprint of Human Dorsal Premotor Cortex. J Neurosci 32:7244–7252.

Morris JS, Ohman A, Dolan RJ (1998) Conscious and unconscious emotional learning in the human amygdala. Nature 393:467–470.

Noppeney U, Friston KJ, Price CJ (2004) Degenerate neuronal systems sustaining cognitive functions. J Anat 205:433–442.

Noppeney U, Ostwald D, Werner S (2010) Perceptual decisions formed by accumulation of audiovisual evidence in prefrontal cortex. J Neurosci 30:7434–7446.

Oliver R, Bjoertomt O, Driver J, Greenwood R, Rothwell J (2009) Novel "hunting" method using transcranial magnetic stimulation over parietal cortex disrupts visuospatial sensitivity in relation to motor thresholds. Neuropsychologia 47:3152–3161.

Pascual-Leone A, Gomez tortosa E, Grafman J, Alway D, Nichelli P, Hallett M (1994) Induction of Visual Extinction by Rapid Rate Transcranial Magnetic Stimulation of Parietal Lobe. Neurology 44:494–498.

Pleger B, Ruff CC, Blankenburg F, Bestmann S, Wiech K, Stephan KE, Capilla A, Friston KJ, Dolan RJ (2006) Neural coding of tactile decisions in the human prefrontal cortex. J Neurosci 26:12596–12601.

Pleskac TJ, Busemeyer JR (2010) Two-stage dynamic signal detection: a theory of choice, decision time, and confidence. Psychol Rev 117:864–901.

Pochon J-B, Riis J, Sanfey AG, Nystrom LE, Cohen JD (2008) Functional imaging of decision conflict. J Neurosci 28:3468–3473.

Price CJ, Crinion J, Friston KJ (2006) Design and analysis of fMRI studies with neurologically impaired patients. J Magn Reson Imaging 23:816–826.

Price CJ, Friston KJ (2002) Degeneracy and cognitive anatomy. Trends Cogn Sci 6:416–421.

Rorie AE, Gao J, McClelland JL, Newsome WT (2010) Integration of sensory and reward information during perceptual decision-making in lateral intraparietal cortex (LIP) of the macaque monkey. PLoS One 5:e9308.

Rounis E, Maniscalco B, Rothwell JC, Passingham RE, Lau H (2010) Theta-burst transcranial magnetic stimulation to the prefrontal cortex impairs metacognitive visual awareness. Cogn Neurosci 1:165–175.

Ruff CC, Bestmann S, Blankenburg F, Bjoertomt O, Josephs O, Weiskopf N, Deichmann R, Driver J (2008) Distinct causal influences of parietal versus frontal areas on human visual cortex: evidence from concurrent TMS-fMRI. Cereb Cortex 18:817–827.

Ruff CC, Blankenburg F, Bjoertomt O, Bestmann S, Freeman E, Haynes J-D, Rees G, Josephs O, Deichmann R, Driver J (2006) Concurrent TMS-fMRI and psychophysics reveal frontal influences on human retinotopic visual cortex. Curr Biol 16:1479–1488.

Ruff CC, Blankenburg F, Bjoertomt O, Bestmann S, Weiskopf N, Driver J (2009) Hemispheric differences in frontal and parietal influences on human occipital cortex: direct confirmation with concurrent TMS-fMRI. J Cogn Neurosci 21:1146–1161.

Ruff D a, Marrett S, Heekeren HR, Bandettini P a, Ungerleider LG (2010) Complementary roles of systems representing sensory evidence and systems detecting task difficulty during perceptual decision making. Front Neurosci 4:190.

Sack AT, Kohler A, Bestmann S, Linden DEJ, Dechent P, Goebel R, Baudewig J (2007) Imaging the brain activity changes underlying impaired visuospatial judgments: simultaneous FMRI, TMS, and behavioral studies. Cereb Cortex 17:2841–2852.

Smith PL, Ratcliff R (2004) Psychology and neurobiology of simple decisions. Trends Neurosci 27:161–168.

Taylor JSH, Rastle K, Davis MH (2014) Interpreting response time effects in functional imaging studies. Neuroimage 99:419–433.

Teichert T, Yu D, Ferrera VP (2014) Performance monitoring in monkey frontal eye field. J Neurosci 34:1657–1671.

Thielscher A, Pessoa L (2007) Neural correlates of perceptual choice and decision making during fear-disgust discrimination. J Neurosci 27:2908–2917.

Thut G, Nietzel A, Pascual-Leone A (2005) Dorsal posterior parietal rTMS affects voluntary orienting of visuospatial attention. Cereb Cortex 15:628–638.

Tosoni A, Galati G, Romani GL, Corbetta M (2008) Sensory-motor mechanisms in human parietal cortex underlie arbitrary visual decisions. Nat Neurosci 11:1446–1453.

Volz KG, Schubotz RI, von Cramon DY (2004) Why am I unsure? Internal and external attributions of uncertainty dissociated by fMRI. Neuroimage 21:848–857.

Watson AB, Pelli DG (1983) QUEST: a Bayesian adaptive psychometric method. Percept Psychophys 33:113–120.

White CN, Mumford J a, Poldrack R a (2012) Perceptual criteria in the human brain. J Neurosci 32:16716–16724.

Yeung N, Summerfield C (2012) Metacognition in human decision-making: confidence and error monitoring. Philos Trans R Soc Lond B Biol Sci 367:1310–1321.

Yoshida W, Ishii S (2006) Resolution of uncertainty in prefrontal cortex. Neuron 50:781–789.

6 General Conclusions

Cognitive functions rely on a distributed network of interconnected brain areas that dynamically interact in order to generate outputs that are suitably adjusted to existing circumstances. By allowing direct monitoring of local and distal effects of TMS on ongoing task-related activations, concurrent TMS-fMRI constitutes a promising tool for studying this interconnected nature of the brain. In a series of studies we employed this methodology to investigate the underlying mechanisms of auditory and visual processing during different experimental contexts. In particular, due to its involvement in a number of distinct cognitive functions and its connectivity with visual and auditory cortices (Hyvärinen, 1982; Maunsell and van Essen, 1983; Boussaoud et al., 1990; Lewis and Van Essen, 2000), special focus was given to the role of the right intraparietal sulcus (IPS) during these processes.

In **Chapter 2** we investigated how TMS to the right IPS influenced visual and auditory processing from a multisensory perspective. In fact, previous studies have demonstrated that activations in sensory cortices are increased for signals from the preferred sensory modality but decreased for non-preferred sensory inputs (Haxby et al., 1994; Kawashima et al., 1995; Laurienti et al., 2002). These crossmodal deactivations may be mediated by top-down modulation from higher-order association areas such as the IPS, thereby reflecting competition for common attentional resources (Shomstein and Yantis, 2004; Johnson and Zatorre, 2005; Werner and Noppeney, 2010, 2011). Hence, we hypothesized that IPS-TMS might jointly amplify auditory-induced activation decreases and visual-evoked activation increases in visual areas.

Our results showed that high-intensity (relative to no or low-intensity) TMS resulted in increased activations in auditory cortices irrespectively of the current sensory context, an outcome that is commonly associated with non-specific side effects caused by the accompanying TMS clicks without being further evaluated. Yet, directly comparing IPS- relative to Vertex-TMS proposed a second mechanism, whereby activation increases in auditory cortices might have been directly induced by top-down modulatory effects from the IPS.

Conversely, IPS-TMS effects in visual cortices were state-dependent. Indeed, high-intensity IPS-TMS deactivated the visual cortex under auditory stimulation but amplified the BOLD responses to visual stimulation, which is in apparent support of our hypothesis. However, auditory-induced deactivations were also observed during no stimulation and Vertex-TMS, thus suggesting that crossmodal deactivations emerged primarily from audiovisual interactions resulting from TMS side effects on activations in auditory cortices. Yet, despite not having modulated crossmodal deactivations directly, our IPS stimulation selectively increased visual-evoked responses. Similarly to TMS-induced effects in auditory cortices, we propose two different mechanisms for these TMS-induced modulations. First, from a unisensory perspective, IPS may have increased visual activations by determining the gain of stimulus-evoked responses in visual cortices in reminiscence of attentional control mechanisms within the visual system. Alternatively, from a multisensory

perspective, IPS-TMS may have specifically modulated the effect of concurrent auditory TMS clicks on the BOLD responses in the visual cortex via crossmodal mechanisms.
Collectively, this study highlights the importance of interpreting TMS effects on BOLD activations in a multisensory framework and in the context of other control sites. Indeed, under a multisensory perspective our results show that BOLD effects due to TMS side effects in auditory cortices might emerge outside auditory areas in a manner that can non-linearly depend on the current sensory context. Exclusively resorting to parametric TMS protocols to control for non-specific TMS effects might thus result in interpretational ambiguities even when investigating neural processes in a single sensory modality.

The first study presented rare but salient auditory and visual targets, which were mainly introduced in order to maintain participants' attention and were therefore not considered in the evaluation of parietal TMS effects. Nevertheless, the detection of relevant sensory events can equally be influenced by top-down modulatory signals arising from higher-order association cortices such as the IPS. In fact, alongside its role in top-down attention, the IPS has been shown to be sensitive to stimulus-driven aspects of attentional control (Geng and Mangun, 2009) and to integrate sensory and goal-directed information in order to form a priority or salience map of the environment (Gottlieb, 2007; Ptak, 2012). Consequently, in **Chapter 3** we explicitly evaluated how TMS at the right IPS influenced task-related activations while engaging the attentional network in a demanding visual detection task that manipulated the presence of small and peripherally presented visual stimuli. Furthermore, since the detection of sensory stimuli can be influenced by co-occurring task-irrelevant sensory events, we further manipulated the bottom-up sensory context by introducing runs in which an auditory sound was presented at target-onset independently of the actual presence of the task-relevant visual input.
Our results show that the disruption of IPS activity abolished activation increases for task-relevant events in the inferior parietal cortex, while simultaneously amplifying stimulus-evoked responses in right visual occipito-temporal areas. In line with the idea of expectation biases induced by covertly attending to the stimulus location (Kastner et al., 1999), these results suggest that IPS-TMS interfered with the detection of task-relevant events in the inferior parietal cortex, which consequently abolished top-down expectation biases in visual cortices. More generally, this pattern suggests that processing of relevant sensory information during goal-directed behaviour involves a complex interplay between these regions.
In addition, interactions between TMS and visual input were equally observed in areas of the right posterior/middle insular cortex and the right ventral lateral prefrontal cortex. However, interactions in these areas were further significantly attenuated during the auditory context, which similarly affected the behavioural task performance, as reflected by accelerated decisions relative to the purely visual context. We propose that IPS-TMS influences in these regions reflect the exchange of control signals associated with the planning of an appropriate response, which is attenuated with the occurrence of an extra auditory sound loaded with implicit top-down information related to the task.

Given the recurrent interchange of feedback and feedforward information between different structures in the cortical hierarchy during visual processing, in **Chapter 4** we evaluated the effects

of stimulating low-level visual areas. In particular, we examined in which way occipital (Occ) TMS-induced effects differed from those elicited by stimulating parietal areas during a demanding visual detection task.

Our results showed an overlap of Occ- and IPS-TMS main effects in right parietal lobes. Moreover, while directly perturbed parietal activity additionally modulated activations in right occipito-temporal visual areas in a state-dependent fashion, activations induced indirectly by Occ-TMS in parietal cortices did not have any effect on these same cortical structures. Hence, while IPS-TMS activations in parietal cortices unsurprisingly reflect locally perturbed activity, activations induced by Occ-TMS most likely indicate compensatory mechanisms that arise in response to perturbed activity in early visual areas. Altogether, given that Occ-TMS during external visual stimulation was never applied inside the scanner before, the methodological considerations discussed in this study might prove useful for future concurrent TMS-fMRI research over visual cortices.

Finally, in **Chapter 5** we investigated the causal role of the right IPS during perceptual decisions. Indeed, among the widespread aggregate of areas that has been implicated in perceptual decision-making, the IPS has been consistently recruited in a large number of studies (Hanks et al., 2006; Churchland et al., 2008; Tosoni et al., 2008; Rorie et al., 2010; Freedman and Assad, 2011; Gould et al., 2012; White et al., 2012). Hence, we categorized participants' responses on a visual detection task into hits, misses, false alarms and correct rejections and assessed the effects of IPS-TMS by comparing conditions with matched visual input but different behavioural response categories and vice versa.

Comparing IPS- relative to Sham-TMS revealed state-dependent effects in the bilateral superior frontal gyri and the right precentral gyrus, which are areas that have previously been associated with perceptual decision-making. Specifically, in these regions IPS-TMS abolished the common response enhancement for missed trials that was observed during normal processing conditions. These state-dependent TMS effects on hemodynamic responses were mirrored by an absence of TMS-induced behavioural changes. We propose two possible explanations for this neural-behavioural dichotomy. First, consistent with the concept of degenerate brain systems, this dichotomy might reflect the existence of an alternative set of areas that is recruited to accomplish task requirements following disturbances to the system. Yet, the absence of consistent compensatory activations might suggest an alternative account. Specifically, instead of being necessary for the behavioural outcome of the current task, these regions might be involved in implicit post-decisional evaluations on task performance.

In summary, our results provide causal evidence for the involvement of the right IPS in different stages of sensory processing. In Chapters 2 and 3 we showed that top-down modulations from the IPS on visual areas are highly dependent on current sensory and cognitive contexts. Additionally, during an attentional demanding context, these modulations likely involve other brain areas in the inferior parietal cortex. In Chapter 4 we showed that stimulation of occipital areas elicits activations in right parietal lobes, probably reflecting compensatory mechanisms in order to maintain similar task performance. Finally, at a decisional stage over sensory input, IPS abolished response enhancement for missed trials in bilateral prefrontal cortices. At a more general level, our results

emphasise that cognitive and sensory processes rely on a contextual collaborative interplay between different brain regions.

6.1 Future Directions

Taken together, the studies comprised in this dissertation have provided causal evidence for the context-dependent cooperative dynamics of the brain. However, some open questions remain. For instance, in Chapter 4 we showed that Occ-TMS elicited activations in the right parietal lobe, which we interpreted as reflecting compensatory mechanisms that developed in order to maintain task performance despite perturbed activity in early visual areas. Along similar lines, one of the ideas we proposed to explain the neural-behavioural dichotomy observed in Chapter 5 was based on the notion of degenerate brain systems. Although in this case the absence of reliable compensatory activations did not offer strong support for this hypothesis, our present approach does not allow us to unequivocally exclude this possibility, in the same way that it cannot address the existence of compensatory mechanisms in Chapter 4.

It has been proposed that a full understanding of degenerate brain function can only be achieved by following a multi-lesion approach (Price and Friston, 2002; Friston and Price, 2011). In this respect, possible follow-up experiments could involve simultaneous stimulation of a second brain region (e.g. the parietal cortex in Chapter 4 and the anterior cingulate/medial prefrontal cortex in Chapter 5) in order to assess resulting changes in behavioural performance and brain activation patterns. Yet, although dual-site TMS protocols are frequently used outside the scanner, it is questionable whether they could be implemented inside the scanner. In fact, whereas the combination of two TMS coils inside the scanner is, in principle, technically feasible (Bohning et al., 1997), it is unlikely that it is practically achievable with current technology, if nothing else because of space restrictions in the placement of the coils.

However, a possible alternative would be to combine an offline repetitive TMS (rTMS) protocol with an online protocol inside the scanner. Indeed, offline rTMS protocols are currently already used in combination with fMRI in order to evaluate compensatory changes in response to stimulation (O'Shea et al., 2008). Likewise offline and online TMS protocols outside the scanner have also been successfully combined before. For instance, Devare et al. (2010) showed that applying offline theta-burst TMS over the anterior IPS modified subsequent interactions between the primary motor and ventral premotor cortices as measured by paired-pulse TMS. Moreover, modulations induced by offline TMS were specific to the performance of a grasping task and were absent during the rest condition. Hence, experiments that factorially manipulate offline rTMS protocols (real TMS vs. control) and single coil TMS protocols inside the scanner (TMS vs. control) might be able to provide some useful insights on the degenerate organization of brain function.

Yet, in order to fully benefit from this or other procedures that combine TMS with fMRI, it is essential to have a better understanding of how different protocols affect neural activity and in particular hemodynamic responses. A step towards this goal could be achieved through the systematic comparison between different TMS protocols. While some important steps have been made in this direction by studies investigating the motor system (e.g. Bohning et al., 2003c;

Hanakawa et al., 2009; Moisa et al., 2010), this systematic approach is completely missing for other brain regions. Finally, another interesting approach towards this goal would be to combine/compare (resting state) functional connectivity analyses with connectivity as assessed with TMS, as it was recently proposed by Fox et al. (2012).

7 Bibliography

Abbruzzese G, Trompetto C, Schieppati M (1996) The excitability of the human motor cortex increases during execution and mental imagination of sequential but not repetitive finger movements.

Ackermann H, Scholz E, Koehler W, Dichgans J (1991) Influence of posture and voluntary background contraction upon compound muscle action potentials from anterior tibial and soleus muscle following transcranial magnetic stimulation. Electroencephalogr Clin Neurophysiol 81:71–80.

Alais D, Burr D (2004) Ventriloquist Effect Results from Near-Optimal Bimodal Integration. Curr Biol 14:257–262.

Alho K, Teder W, Lavikainen J, Naatanen R (1994) Strongly focused attention and auditory event-related potentials. Biol Psychol 38:73–90.

Allen EA, Pasley BN, Duong T, Freeman RD (2007) Transcranial magnetic stimulation elicits coupled neural and hemodynamic consequences. Science 317:1918–1921.

Amedi A, Jacobson G, Hendler T, Malach R, Zohary E (2002) Convergence of visual and tactile shape processing in the human lateral occipital complex. Cereb Cortex 12:1202–1212.

Anderson ML, Kinnison J, Pessoa L (2013) Describing functional diversity of brain regions and brain networks. Neuroimage 73:50–58.

Ansari D (2007) Does the parietal cortex distinguish between "10," "ten," and ten dots? Neuron 53:165–167.

Antal A, Nitsche MA, Kincses TZ, Lampe C, Paulus W (2004) No correlation between moving phosphene and motor thresholds: a transcranial magnetic stimulation study. Neuroreport 15:297–302.

Avillac M, Ben Hamed S, Duhamel J-R (2007) Multisensory integration in the ventral intraparietal area of the macaque monkey. J Neurosci 27:1922–1932.

Aydin-Abidin S, Moliadze V, Eysel UT, Funke K (2006) Effects of repetitive TMS on visually evoked potentials and EEG in the anaesthetized cat: dependence on stimulus frequency and train duration. J Physiol 574:443–455.

Baudewig J, Paulus W, Frahm J (2000) Artifacts Caused by Transcranial Magnetic Stimulation Coils and EEG Electrodes in T2*-Weighted Echo-Planar Imaging. Magn Reson Imaging:479–484.

Beauchamp MS, Pasalar S, Ro T (2010) Neural substrates of reliability-weighted visual-tactile multisensory integration. Front Syst Neurosci 4:25.

Bestmann S, Baudewig J, Frahm J (2003a) On the synchronization of transcranial magnetic stimulation and functional echo-planar imaging. J Magn Reson Imaging 17:309–316.

Bestmann S, Baudewig J, Siebner HR, Rothwell JC, Frahm J (2003b) Subthreshold high-frequency TMS of human primary motor cortex modulates interconnected frontal motor areas as detected by interleaved fMRI-TMS.

Bestmann S, Baudewig J, Siebner HR, Rothwell JC, Frahm J (2004) Functional MRI of the immediate impact of transcranial magnetic stimulation on cortical and subcortical motor circuits. Eur J Neurosci 19:1950–1962.

Bestmann S, Baudewig J, Siebner HR, Rothwell JC, Frahm J (2005) BOLD MRI responses to repetitive TMS over human dorsal premotor cortex. Neuroimage 28:22–29.

Bien N, Goebel R, Sack AT (2012) Extinguishing extinction: hemispheric differences in the modulation of TMS-induced visual extinction by directing covert spatial attention. J Cogn Neurosci 24:809–818.

Blankenburg F, Ruff CC, Bestmann S, Bjoertomt O, Eshel N, Josephs O, Weiskopf N, Driver J (2008) Interhemispheric effect of parietal TMS on somatosensory response confirmed directly with concurrent TMS-fMRI. J Neurosci 28:13202–13208.

Blankenburg F, Ruff CC, Bestmann S, Bjoertomt O, Josephs O, Deichmann R, Driver J (2010) Studying the role of human parietal cortex in visuospatial attention with concurrent TMS-fMRI. Cereb Cortex 20:2702–2711.

Bogacz R, Wagenmakers E-J, Forstmann BU, Nieuwenhuis S (2010) The neural basis of the speed-accuracy tradeoff. Trends Neurosci 33:10–16.

Bohning DE, Denslow S, Bohning P., Walker J., George M. (2003a) A TMS coil positioning/holding system for MR image-guided TMS interleaved with fMRI. Clin Neurophysiol 114:2210–2219.

Bohning DE, Denslow S, Bohning PA, Lomarev MP, George MS (2003b) Interleaving fMRI and rTMS. Suppl Clin Neurophysiol:42–54.

Bohning DE, Pecheny AP, Epstein CM, Speer AM, Vincent DJ, Dannels W, George MS (1997) Mapping transcranial magnetic stimulation (TMS) fields in vivo with MRI. Neuroreport 8:2535–2538.

Bohning DE, Shastri A, Lomarev MP, Lorberbaum JP, Nahas Z, George MS (2003c) BOLD-fMRI response vs. transcranial magnetic stimulation (TMS) pulse-train length: testing for linearity. J Magn Reson Imaging 17:279–290.

Bohning DE, Shastri A, Nahas Z, Lorberbaum JP, Andersen SW, Dannels WR, Haxthausen EU, Vincent DJ, George MS (1998) Echoplanar BOLD fMRI of brain activation induced by concurrent transcranial magnetic stimulation. Neuroreport 33:943–948.

Bohning DE, Shastri A, Wassermann EM, Ziemann U, Lorberbaum JP, Nahas Z, Lomarev MP, George MS (2000) BOLD-f MRI response to single-pulse transcranial magnetic stimulation (TMS).

Boroojerdi B, Meister IG, Foltys H, Sparing R, Cohen LG, Töpper R (2002) Visual and motor cortex excitability: a transcranial magnetic stimulation study.

Boussaoud D, Ungerleider LG, Desimone R (1990) Pathways for motion analysis: Cortical connections of the medial superior temporal and fundus of the superior temporal visual areas in the macaque. J Comp Neurol 296:462–495.

Bremmer F, Schlack A, Shah NJ, Zafiris O, Kubischik M, Hoffmann K, Zilles K, Fink GR, Zoologie A (2001) Polymodal Motion Processing in Posterior Parietal and Premotor Cortex : A Human fMRI Study Strongly Implies Equivalencies between Humans and Monkeys. 29:287–296.

Bressler SL (1995) Large-scale cortical networks and cognition. Brain Res Rev 20:288–304.

Bressler SL, Tognoli E (2006) Operational principles of neurocognitive networks. Int J Psychophysiol 60:139–148.

Büchel C, Price C, Friston K (1998) A multimodal language region in the ventral visual pathway. Nature 394:274–277.

Bullmore E, Sporns O (2009) Complex brain networks: graph theoretical analysis of structural and functional systems. Nat Rev Neurosci 10:186–198.

Bungert A, Chambers CD, Phillips M, Evans CJ (2012) Reducing image artefacts in concurrent TMS/fMRI by passive shimming. Neuroimage 59:2167–2174.

Burton H, Abend NS, MacLeod AMK, Sinclair RJ, Snyder AZ, Raichle ME (1999) Tactile attention tasks enhance activation in somatosensory regions of parietal cortex: A positron emission tomography study. Cereb Cortex 9:662–674.

Calvert GA, Hansen PC, Iversen SD, Brammer MJ (2001) Detection of audio-visual integration sites in humans by application of electrophysiological criteria to the BOLD effect. Neuroimage 14:427–438.

Calvert GA, Spence C, Stein BE (2004) The Handbook of Multisensory Processing. Cambrige, MA: MIT Press.

Caparelli EC, Backus W, Telang F, Wang G-J, Maloney T, Goldstein RZ, Anschel D, Henn F (2010) Simultaneous TMS-fMRI of the Visual Cortex Reveals Functional Network, Even in Absence of Phosphene Sensation. Open Neuroimag J 4:100–110.

Cappe C, Rouiller EM, Barone P (2009) Multisensory anatomical pathways. Hear Res 258:28–36.

Catani M, Ffytche DH (2005) The rises and falls of disconnection syndromes. Brain 128:2224–2239.

Chambers CD, Stokes MG, Mattingley JB (2004) Modality-specific control of strategic spatial attention in parietal cortex. Neuron 44:925–930.

Chawla D, Rees G, Friston KJ (1999) The physiological basis of attentional modulation in extrastriate visual areas. Nat Neurosci 2:671–676.

Chen Y-C, Huang P-C, Yeh S-L, Spence C (2011) Synchronous sounds enhance visual sensitivity without reducing target uncertainty. Seeing Perceiving 24:623–638.

Churchland AK, Kiani R, Shadlen MN (2008) Decision-making with multiple alternatives. Nat Neurosci 11:693–702.

Clark VP, Parasuraman R, Keil K, Kulansky R, Fannon S, Maisog JM, Ungerleider LG, Haxby J V. (1997) Selective attention to face identity and color studied with fMRI. In: Human Brain Mapping, pp 293–297.

Cohen Kadosh R, Walsh V (2009) Numerical representation in the parietal lobes: abstract or not abstract? Behav Brain Sci 32:313–28; discussion 328–73.

Cohen YE, Russ BE, Gifford GW (2005) Auditory processing in the posterior parietal cortex. Behav Cogn Neurosci Rev 4:218–231.

Colby CL, Duhamel JR, Goldberg ME (1993) Ventral intraparietal area of the macaque: anatomic location and visual response properties. J Neurophysiol 69:902–914.

Cole MW, Reynolds JR, Power JD, Repovs G, Anticevic A, Braver TS (2013) Multi-task connectivity reveals flexible hubs for adaptive task control. Nat Neurosci 16:1348–1355.

Corbetta M, Kincade JM, Ollinger JM, McAvoy MP, Shulman GL (2000) Voluntary orienting is dissociated from target detection in human posterior parietal cortex. Nat Neurosci 3:292–297.

Corbetta M, Miezin FM, Dobmeyer S, Shulman GL, Petersen SE (1990) Attentional modulation of neural processing of shape, color, and velocity in humans. Science 248:1556–1559.

Corbetta M, Shulman GL (2002) Control of goal-directed and stimulus-driven attention in the brain. Nat Rev Neurosci 3:201–215.

Cowey A (2005) The Ferrier Lecture 2004 what can transcranial magnetic stimulation tell us about how the brain works? Philos Trans R Soc Lond B Biol Sci 360:1185–1205.

Davare M, Rothwell JC, Lemon RN (2010) Causal connectivity between the human anterior intraparietal area and premotor cortex during grasp. Curr Biol 20:176–181.

De Graaf TA, Goebel R, Sack AT (2012) Feedforward and quick recurrent processes in early visual cortex revealed by TMS? Neuroimage 61:651–659.

De Labra C, Rivadulla C, Grieve K, Mariño J, Espinosa N, Cudeiro J (2007) Changes in visual responses in the feline dLGN: selective thalamic suppression induced by transcranial magnetic stimulation of V1. Cereb Cortex 17:1376–1385.

De Lafuente V, Romo R (2006) Neural correlate of subjective sensory experience gradually builds up across cortical areas. Proc Natl Acad Sci U S A 103:14266–14271.

Deblieck C, Thompson B, Iacoboni M, Wu AD (2008) Correlation between motor and phosphene thresholds: A transcranial magnetic stimulation study. Hum Brain Mapp 29:662–670.

Dehaene S, Molko N, Cohen L, Wilson AJ (2004) Arithmetic and the brain. Curr Opin Neurobiol 14:218–224.

Denslow S, Bohning DE, Bohning PA, Lomarev MP, George MS (2005a) An increased precision comparison of TMS-induced motor cortex BOLD fMRI response for image-guided versus function-guided coil placement.

Denslow S, Lomarev M, George MS, Bohning DE (2005b) Cortical and subcortical brain effects of transcranial magnetic stimulation (TMS)-induced movement: an interleaved TMS/functional magnetic resonance imaging study. Biol Psychiatry 57:752–760.

Di Lazzaro V, Profice P, Ranieri F, Capone F, Dileone M, Oliviero a, Pilato F (2012) I-wave origin and modulation. Brain Stimul 5:512–525.

Diederich A, Colonius H (2004) Bimodal and trimodal multisensory enhancement: effects of stimulus onset and intensity on reaction time. Percept Psychophys 66:1388–1404.

Driver J, Noesselt T (2008) Multisensory Interplay Reveals Crossmodal Influences on "Sensory-Specific" Brain Regions, Neural Responses, and Judgments. Neuron 57:11–23.

Egner T, Monti JMP, Trittschuh EH, Wieneke CA, Hirsch J, Mesulam M-M (2008) Neural integration of top-down spatial and feature-based information in visual search. J Neurosci 28:6141–6151.

Ekstrom A (2010) How and when the fMRI BOLD signal relates to underlying neural activity: the danger in dissociation. Brain Res Rev 62:233–244.

Ekstrom LB, Roelfsema PR, Arsenault JT, Bonmassar G, Vanduffel W (2008) Bottom-up dependent gating of frontal signals in early visual cortex. Science 321:414–417.

Epstein R, Kanwisher N (1998) A cortical representation of the local visual environment. Nature 392:598–601.

Ernst MO, Bülthoff HH (2004) Merging the senses into a robust percept. Trends Cogn Sci 8:162–169.

Ettinger GJ, Leventon ME, Grimson WE, Kikinis R, Gugino L, Cote W, Sprung L, Aglio L, Shenton ME, Potts G, Hernandez VL, Alexander E (1998) Experimentation with a transcranial magnetic stimulation system for functional brain mapping. Med Image Anal 2:133–142.

Fairhall SL, Ishai A (2007) Effective connectivity within the distributed cortical network for face perception. Cereb Cortex 17:2400–2406.

Falchier A, Clavagnier S, Barone P, Kennedy H (2002) Anatomical evidence of multimodal integration in primate striate cortex. J Neurosci 22:5749–5759.

Feredoes E, Heinen K, Weiskopf N, Ruff C, Driver J (2011) Causal evidence for frontal involvement in memory target maintenance by posterior brain areas during distracter interference of visual working memory. Proc Natl Acad Sci U S A 108:17510–17515.

Fiebelkorn IC, Foxe JJ, Butler JS, Molholm S (2011) Auditory facilitation of visual-target detection persists regardless of retinal eccentricity and despite wide audiovisual misalignments. Exp brain Res 213:167–174.

Filimon F, Philiastides MG, Nelson JD, Kloosterman N a, Heekeren HR (2013) How embodied is perceptual decision making? Evidence for separate processing of perceptual and motor decisions. J Neurosci 33:2121–2136.

Finger S (1994a) The Era of Cortical Localization. In: Origins of Neuroscience. A History of Explorations into Brain Function, pp 32:50.

Finger S (1994b) Holism and the Critics of Cortical Localization. In: Origins of Neuroscience. A History of Explorations into Brain Function, pp 51:62.

Fleming SM, Lau HC (2014) How to measure metacognition. Front Hum Neurosci 8:1–9.

Forster B, Cavina-Pratesi C, Aglioti SM, Berlucchi G (2002) Redundant target effect and intersensory facilitation from visual-tactile interactions in simple reaction time. Exp Brain Res 143:480–487.

Fox MD, Halko M a, Eldaief MC, Pascual-Leone A (2012) Measuring and manipulating brain connectivity with resting state functional connectivity magnetic resonance imaging (fcMRI) and transcranial magnetic stimulation (TMS). Neuroimage 62:2232–2243.

Foxe JJ, Morocz IA, Murray MM, Higgins BA, Javitt DC, Schroeder CE (2000) Multisensory auditory-somatosensory interactions in early cortical processing revealed by high-density electrical mapping. Cogn Brain Res 10:77–83.

Freedman DJ, Assad J a (2011) A proposed common neural mechanism for categorization and perceptual decisions. Nat Neurosci 14:143–146.

Friston KJ, Büchel C (2000) Attentional modulation of effective connectivity from V2 to V5/MT in humans. Proc Natl Acad Sci U S A 97:7591–7596.

Friston KJ, Price CJ (2011) Modules and brain mapping. Cogn Neuropsychol 28:241–250.

Fritz JB, Elhilali M, David S V, Shamma SA (2007) Auditory attention--focusing the searchlight on sound. Curr Opin Neurobiol 17:437–455.

Gazzaley A, Rissman J, D'Esposito M (2004) Functional connectivity during working memory maintenance. Cogn Affect Behav Neurosci 4:580–599.

Geng JJ, Mangun GR (2009) Anterior intraparietal sulcus is sensitive to bottom-up attention driven by stimulus salience. J Cogn Neurosci 21:1584–1601.

Ghazanfar AA, Schroeder CE (2006) Is neocortex essentially multisensory? Trends Cogn Sci 10:278–285.

Giard MH, Peronnet F (1999) Auditory-visual integration during multimodal object recognition in humans: a behavioral and electrophysiological study. J Cogn Neurosci 11:473–490.

Gitelman DR, Nobre AC, Parrish TB, LaBar KS, Kim YH, Meyer JR, Mesulam MM (1999) A large-scale distributed network for covert spatial attention. Further anatomical delineation based on stringent behavioural and cognitive controls. Brain 122:1093–1106.

Gottlieb J (2007) From Thought to Action: The Parietal Cortex as a Bridge between Perception, Action, and Cognition. Neuron 53:9–16.

Gould IC, Nobre AC, Wyart V, Rushworth MFS (2012) Effects of decision variables and intraparietal stimulation on sensorimotor oscillatory activity in the human brain. J Neurosci 32:13805–13818.

Green DM, Swets JA (1966) Signal detection theory and psychophysics.

Hanakawa T, Mima T, Matsumoto R, Abe M, Inouchi M, Urayama S-I, Anami K, Honda M, Fukuyama H (2009) Stimulus-response profile during single-pulse transcranial magnetic stimulation to the primary motor cortex. Cereb Cortex 19:2605–2615.

Hanks TD, Ditterich J, Shadlen MN (2006) Microstimulation of macaque area LIP affects decision-making in a motion discrimination task. Nat Neurosci 9:682–689.

Haxby J V, Horwitz B, Ungerleider LG, Maisog JM, Pietrini P, Grady CL (1994) The functional organization of human extrastriate cortex: a PET-rCBF study of selective attention to faces and locations. J Neurosci 14:6336–6353.

Hecht D, Reiner M, Karni A (2008) Multisensory enhancement: Gains in choice and in simple response times. Exp Brain Res 189:133–143.

Heekeren HR, Marrett S, Bandettini P a, Ungerleider LG (2004) A general mechanism for perceptual decision-making in the human brain. Nature 431:859–862.

Heekeren HR, Marrett S, Ruff D a, Bandettini P a, Ungerleider LG (2006) Involvement of human left dorsolateral prefrontal cortex in perceptual decision making is independent of response modality. Proc Natl Acad Sci U S A 103:10023–10028.

Heinen K, Feredoes E, Weiskopf N, Ruff CC, Driver J (2013) Direct Evidence for Attention-Dependent Influences of the Frontal Eye-Fields on Feature-Responsive Visual Cortex. Cereb Cortex.

Heinen K, Ruff CC, Bjoertomt O, Schenkluhn B, Bestmann S, Blankenburg F, Driver J, Chambers CD (2011) Concurrent TMS-fMRI reveals dynamic interhemispheric influences of the right parietal cortex during exogenously cued visuospatial attention. Eur J Neurosci 33:991–1000.

Heinze HJ, Mangun GR, Burchert W, Hinrichs H, Scholz M, Münte TF, Gös A, Scherg M, Johannes S, Hundeshagen H (1994) Combined spatial and temporal imaging of brain activity during visual selective attention in humans. Nature 372:543–546.

Helbig HB, Ernst MO (2007) Optimal integration of shape information from vision and touch. Exp Brain Res 179:595–606.

Hershenson M (1962) Reaction time as a measure of intersensory facilitation. J Exp Psychol 63:289–293.

Hillyard SA, Hink RF, Schwent VL, Picton TW (1973) Electrical Signs of Selective Attention in the Human Brain. Science (80-) 182:177–180.

Hopf J, Boehler CN, Luck SJ, Tsotsos JK, Heinze H, Schoenfeld MA (2005) Direct neurophysiological evidence for spatial suppression surrounding the focus.

Hopfinger JB, Buonocore MH, Mangun GR (2000) The neural mechanisms of top-down attentional control. Nat Neurosci 3:284–291.

Hsiao SS, O'Shaughnessy DM, Johnson KO (1993) Effects of selective attention on spatial form processing in monkey primary and secondary somatosensory cortex. J Neurophysiol 70:444–447.

Hubel DH, Henson CO, Rupert A, Galambos R (1959) Attention units in the auditory cortex. Science 129:1279–1280.

Hyvärinen J (1982) Posterior parietal lobe of the primate brain. Physiol Rev 62:1060–1129.

Izumi S, Findley TW, Ikai T, Andrews J, Daum M, Chino N (1995) Facilitatory effect of thinking about movement on motor-evoked potentials to transcranial magnetic stimulation of the brain. Am J Phys Med Rehabil:6336–6353.

Jacob SN, Nieder A (2009) Notation-independent representation of fractions in the human parietal cortex. J Neurosci 29:4652–4657.

Johansen-Berg H, Christensen V, Woolrich M, Matthews PM (2000) Attention to touch modulates activity in both primary and secondary somatosensory areas.

Johnson J a, Zatorre RJ (2005) Attention to simultaneous unrelated auditory and visual events: behavioral and neural correlates. Cereb Cortex 15:1609–1620.

Kanwisher N (2010) Functional specificity in the human brain: a window into the functional architecture of the mind. Proc Natl Acad Sci U S A 107:11163–11170.

Kanwisher N, McDermott J, Chun MM (1997) The fusiform face area: a module in human extrastriate cortex specialized for face perception. J Neurosci 17:4302–4311.

Kastner S, Pinsk MA, Weerd P De, Desimone R, Ungerleider LG (1999) Increased Activity in Human Visual Cortex during Directed Attention in the Absence of Visual Stimulation. 22:751–761.

Kawashima R, O'Sullivan BT, Roland PE (1995) Positron-emission tomography studies of cross-modality inhibition in selective attentional tasks: closing the "mind's eye". Proc Natl Acad Sci U S A 92:5969–5972.

Kayser AS, Buchsbaum BR, Erickson DT, Esposito MD (2010) The Functional Anatomy of a Perceptual Decision in the Human Brain. :1179–1194.

Kayser C, Logothetis NK (2007) Do early sensory cortices integrate cross-modal information? Brain Struct Funct 212:121–132.

Kayser C, Petkov CI, Augath M, Logothetis NK (2005) Integration of touch and sound in auditory cortex. Neuron 48:373–384.

Kayser C, Petkov CI, Augath M, Logothetis NK (2007) Functional imaging reveals visual modulation of specific fields in auditory cortex. J Neurosci 27:1824–1835.

Kiani R, Shadlen MN (2009) Representation of confidence associated with a decision by neurons in the parietal cortex. Science 324:759–764.

Kim JN, Shadlen MN (1999) Neural correlates of a decision in the dorsolateral prefrontal cortex of the macaque. Nat Neurosci 2:176–185.

Kincade JM, Abrams R a, Astafiev S V, Shulman GL, Corbetta M (2005) An event-related functional magnetic resonance imaging study of voluntary and stimulus-driven orienting of attention. J Neurosci 25:4593–4604.

Konen CS, Mruczek REB, Montoya JL, Kastner S (2013) Functional organization of human posterior parietal cortex: grasping- and reaching-related activations relative to topographically organized cortex. J Neurophysiol 109:2897–2908.

Lamme V a, Roelfsema PR (2000) The distinct modes of vision offered by feedforward and recurrent processing. Trends Neurosci 23:571–579.

Laurienti PJ (2014) Neural murmurations: Comment on “Understanding brain networks and brain organization” by Luiz Pessoa. Phys Life Rev 11:452–454.

Laurienti PJ, Burdette JH, Wallace MT, Yen Y-F, Field AS, Stein BE (2002) Deactivation of sensory-specific cortex by cross-modal stimuli. J Cogn Neurosci 14:420–429.

Leon-Sarmiento FE, Bara-Jimenez W, Wassermann EM (2005) Visual deprivation effects on human motor cortex excitability. Neurosci Lett 389:17–20.

Lewis JW, Van Essen DC (2000) Corticocortical connections of visual, sensorimotor, and multimodal processing areas in the parietal lobe of the macaque monkey. J Comp Neurol 428:112–137.

Logothetis NK, Augath M, Murayama Y, Rauch A, Sultan F, Goense J, Oeltermann A, Merkle H (2010) The effects of electrical microstimulation on cortical signal propagation. Nat Neurosci 13:1283–1291.

Luck SJ, Chelazzi L, Hillyard SA, Desimone R (1997) Neural mechanisms of spatial selective attention in areas V1, V2, and V4 of macaque visual cortex. J Neurophysiol 77:24–42.

Macaluso E (2000) Modulation of Human Visual Cortex by Crossmodal Spatial Attention. Science (80-) 289:1206–1208.

Macaluso E, Driver J (2005) Multisensory spatial interactions: a window onto functional integration in the human brain. Trends Neurosci 28:264–271.

Macaluso E, Eimer M, Frith CD, Driver J (2003) Preparatory states in crossmodal spatial attention: spatial specificity and possible control mechanisms. Exp Brain Res 149:62–74.

Mangun GR, Buonocore MH, Girelli M, Jha AP (1998) ERP and fMRI measures of visual spatial selective attention. In: Human Brain Mapping, pp 383–389.

Maniscalco B, Lau H (2012) A signal detection theoretic approach for estimating metacognitive sensitivity from confidence ratings. Conscious Cogn 21:422–430.

Maunsell JH, van Essen DC (1983) The connections of the middle temporal visual area (MT) and their relationship to a cortical hierarchy in the macaque monkey. J Neurosci 3:2563–2586.

McAdams CJ, Maunsell JHR (1999) Effects of Attention on the Reliability of Individual Neurons in Monkey Visual Cortex. Neuron 23:765–773.

McDonald JJ, Teder-Sälejärvi WA, Di Russo F, Hillyard SA (2003) Neural substrates of perceptual enhancement by cross-modal spatial attention. J Cogn Neurosci 15:10–19.

McIntosh a. R (2000) Towards a network theory of cognition. Neural Networks 13:861–870.

McMains SA, Fehd HM, Emmanouil T-A, Kastner S (2007) Mechanisms of feature- and space-based attention: response modulation and baseline increases. J Neurophysiol 98:2110–2121.

Meehan TP, Bressler SL (2012) Neurocognitive networks: findings, models, and theory. Neurosci Biobehav Rev 36:2232–2247.

Mesulam MM (1990) Large-scale neurocognitive networks and distributed processing for attention, language, and memory. Ann Neurol 28:597–613.

Miller LM, D’Esposito M (2005) Perceptual fusion and stimulus coincidence in the cross-modal integration of speech. J Neurosci 25:5884–5893.

Moisa M, Pohmann R, Ewald L, Thielscher A (2009) New coil positioning method for interleaved transcranial magnetic stimulation (TMS)/functional MRI (fMRI) and its validation in a motor cortex study. J Magn Reson Imaging 29:189–197.

Moisa M, Pohmann R, Uludağ K, Thielscher A (2010) Interleaved TMS/CASL: Comparison of different rTMS protocols. Neuroimage 49:612–620.

Molholm S, Ritter W, Murray MM, Javitt DC, Schroeder CE, Foxe JJ (2002) Multisensory auditory–visual interactions during early sensory processing in humans: a high-density electrical mapping study. Cogn Brain Res 14:115–128.

Moliadze V, Giannikopoulos D, Eysel UT, Funke K (2005) Paired-pulse transcranial magnetic stimulation protocol applied to visual cortex of anaesthetized cat: effects on visually evoked single-unit activity. J Physiol 566:955–965.

Moliadze V, Zhao Y, Eysel U, Funke K (2003) Effect of transcranial magnetic stimulation on single-unit activity in the cat primary visual cortex. J Physiol 553:665–679.

Moran J, Desimone R (1985) Selective attention gates visual processing in the extrastriate cortex. Science 229:782–784.

Motter BC (1993) Focal attention produces spatially selective processing in visual cortical areas V1, V2, and V4 in the presence of competing stimuli. J Neurophysiol 70:909–919.

Mumford D (1992) On the computational architecture of the neocortex - II The role of cortico-cortical loops. Biol Cybern 66:241–251.

Munneke J, Heslenfeld DJ, Usrey WM, Theeuwes J, Mangun GR (2011) Preparatory effects of distractor suppression: Evidence from visual cortex. PLoS One 6.

Murray MM, Molholm S, Michel CM, Heslenfeld DJ, Ritter W, Javitt DC, Schroeder CE, Foxe JJ (2005) Grabbing your ear: Rapid auditory-somatosensory multisensory interactions in low-level sensory cortices are not constrained by stimulus alignment. Cereb Cortex 15:963–974.

Nahas Z, Lomarev M, Roberts DR, Shastri A, Lorberbaum JP, Teneback C, McConnell K, Vincent DJ, Li X, George MS, Bohning DE (2001) Unilateral left prefrontal transcranial magnetic stimulation (TMS) produces intensity-dependent bilateral effects as measured by interleaved BOLD fMRI. Biol Psychiatry 50:712–720.

Noppeney U, Ostwald D, Werner S (2010) Perceptual decisions formed by accumulation of audiovisual evidence in prefrontal cortex. J Neurosci 30:7434–7446.

O'Craven KM, Rosen BR, Kwong KK, Treisman A, Savoy RL (1997) Voluntary attention modulates fMRI activity in human MT-MST. Neuron 18:591–598.

O'Shea J, Taylor PCJ, Rushworth MFS (2008) Imaging causal interactions during sensorimotor processing. Cortex 44:598–608.

Oliver R, Bjoertomt O, Driver J, Greenwood R, Rothwell J (2009) Novel "hunting" method using transcranial magnetic stimulation over parietal cortex disrupts visuospatial sensitivity in relation to motor thresholds. Neuropsychologia 47:3152–3161.

Pasalar S, Ro T, Beauchamp MS (2010) TMS of posterior parietal cortex disrupts visual tactile multisensory integration. Eur J Neurosci 31:1783–1790.

Pessoa L (2014) Brain networks: Moving beyond graphs: Reply to comments on "Understanding brain networks and brain organization". Phys Life Rev 11:462–466.

Pinsk M a, Doniger GM, Kastner S (2004) Push-pull mechanism of selective attention in human extrastriate cortex. J Neurophysiol 92:622–629.

Pleger B, Ruff CC, Blankenburg F, Bestmann S, Wiech K, Stephan KE, Capilla A, Friston KJ, Dolan RJ (2006) Neural coding of tactile decisions in the human prefrontal cortex. J Neurosci 26:12596–12601.

Ploran EJ, Tremel JJ, Nelson SM, Wheeler ME (2011) High quality but limited quantity perceptual evidence produces neural accumulation in frontal and parietal cortex. Cereb Cortex 21:2650–2662.

Posner MI (1980) Orienting of attention. Q J Exp Psychol 32:3–25.

Price CJ (2010) The anatomy of language: A review of 100 fMRI studies published in 2009. Ann N Y Acad Sci 1191:62–88.

Price CJ, Friston KJ (2002) Degeneracy and cognitive anatomy. Trends Cogn Sci 6:416–421.

Ptak R (2012) The Frontoparietal Attention Network of the Human Brain: Action, Saliency, and a Priority Map of the Environment. Neurosci 18:502–515.

Ratcliff R, Smith PL (2004) A comparison of sequential sampling models for two-choice reaction time. Psychol Rev 111:333–367.

Rauss K, Pourtois G (2013) What is Bottom-Up and What is Top-Down in Predictive Coding? Front Psychol 4:276.

Reichenbach A, Bresciani JP, Peer A, Bülthoff HH, Thielscher A (2011) Contributions of the PPC to online control of visually guided reaching movements assessed with fMRI-Guided TMS. Cereb Cortex 21:1602–1612.

Rockland KS, Ojima H (2003) Multisensory convergence in calcarine visual areas in macaque monkey. In: International Journal of Psychophysiology, pp 19–26.

Roitman JD, Shadlen MN (2002) Response of neurons in the lateral intraparietal area during a combined visual discrimination reaction time task. J Neurosci 22:9475–9489.

Romei V, Murray MM, Merabet LB, Thut G (2007) Occipital transcranial magnetic stimulation has opposing effects on visual and auditory stimulus detection: implications for multisensory interactions. J Neurosci 27:11465–11472.

Rorie AE, Gao J, McClelland JL, Newsome WT (2010) Integration of sensory and reward information during perceptual decision-making in lateral intraparietal cortex (LIP) of the macaque monkey. PLoS One 5:e9308.

Rubinov M, Sporns O (2010) Complex network measures of brain connectivity: uses and interpretations. Neuroimage 52:1059–1069.

Ruff CC, Bestmann S, Blankenburg F, Bjoertomt O, Josephs O, Weiskopf N, Deichmann R, Driver J (2008) Distinct causal influences of parietal versus frontal areas on human visual cortex: evidence from concurrent TMS-fMRI. Cereb Cortex 18:817–827.

Ruff CC, Blankenburg F, Bjoertomt O, Bestmann S, Freeman E, Haynes J-D, Rees G, Josephs O, Deichmann R, Driver J (2006) Concurrent TMS-fMRI and psychophysics reveal frontal influences on human retinotopic visual cortex. Curr Biol 16:1479–1488.

Ruff CC, Blankenburg F, Bjoertomt O, Bestmann S, Weiskopf N, Driver J (2009) Hemispheric differences in frontal and parietal influences on human occipital cortex: direct confirmation with concurrent TMS-fMRI. J Cogn Neurosci 21:1146–1161.

Russ BE, Kim AM, Abrahamsen KL, Kiringoda R, Cohen YE (2006) Responses of neurons in the lateral intraparietal area to central visual cues. Exp Brain Res 174:712–727.

Sack AT, Kohler A, Bestmann S, Linden DEJ, Dechent P, Goebel R, Baudewig J (2007) Imaging the brain activity changes underlying impaired visuospatial judgments: simultaneous FMRI, TMS, and behavioral studies. Cereb Cortex 17:2841–2852.

Sadaghiani S, Maier JX, Noppeney U (2009) Natural, metaphoric, and linguistic auditory direction signals have distinct influences on visual motion processing. J Neurosci 29:6490–6499.

Santangelo V, Olivetti Belardinelli M, Spence C, Macaluso E (2009) Interactions between voluntary and stimulus-driven spatial attention mechanisms across sensory modalities. J Cogn Neurosci 21:2384–2397.

Saygin AP, Sereno MI (2008) Retinotopy and attention in human occipital, temporal, parietal, and frontal cortex. Cereb Cortex 18:2158–2168.

Schlack A, Sterbing-D'Angelo SJ, Hartung K, Hoffmann K-P, Bremmer F (2005) Multisensory space representations in the macaque ventral intraparietal area. J Neurosci 25:4616–4625.

Schönfeldt-Lecuona C, Thielscher A, Freudenmann RW, Kron M, Spitzer M, Herwig U (2005) Accuracy of stereotaxic positioning of transcranial magnetic stimulation. Brain Topogr 17:253–259.

Schridde U, Khubchandani M, Motelow JE, Sanganahalli BG, Hyder F, Blumenfeld H (2008) Negative BOLD with large increases in neuronal activity. Cereb Cortex 18:1814–1827.

Schroeder CE, Foxe J (2005) Multisensory contributions to low-level, "unisensory" processing. Curr Opin Neurobiol 15:454–458.

Seidl KN, Peelen M V., Kastner S (2012) Neural Evidence for Distracter Suppression during Visual Search in Real-World Scenes. J Neurosci 32:11812–11819.

Senkowski D, Molholm S, Gomez-Ramirez M, Foxe JJ (2006) Oscillatory beta activity predicts response speed during a multisensory audiovisual reaction time task: A high-density electrical mapping study. Cereb Cortex 16:1556–1565.

Serences JT, Kastner S (2014) A Multi-level Account of Selective Attention. In: The Oxford Handbook of attention, pp Chapter 4.

Serences JT, Yantis S (2007) Spatially selective representations of voluntary and stimulus-driven attentional priority in human occipital, parietal, and frontal cortex. Cereb Cortex 17:284–293.

Serences JT, Yantis S, Culberson A, Awh E (2004) Preparatory activity in visual cortex indexes distractor suppression during covert spatial orienting. J Neurophysiol 92:3538–3545.

Seyal M, Ro T, Rafal R (1995) Increased sensitivity to ipsilateral cutaneous stimuli following transcranial magnetic stimulation of the parietal lobe. Ann Neurol 38:264–267.

Shadlen MN, Newsome WT (2001) Neural basis of a perceptual decision in the parietal cortex (area LIP) of the rhesus monkey. J Neurophysiol 86:1916–1936.

Shams L, Kamitani Y, Shimojo S (2002) Visual illusion induced by sound. In: Cognitive Brain Research, pp 147–152.

Shams L, Kim R (2010) Crossmodal influences on visual perception. Phys Life Rev 7:269–284.

Shmuel A, Augath M, Oeltermann A, Logothetis NK (2006) Negative functional MRI response correlates with decreases in neuronal activity in monkey visual area V1. Nat Neurosci 9:569–577.

Shomstein S, Yantis S (2004) Control of attention shifts between vision and audition in human cortex. J Neurosci 24:10702–10706.

Silvanto J, Lavie N, Walsh V (2005) Double dissociation of V1 and V5/MT activity in visual awareness. Cereb Cortex 15:1736–1741.

Silver MA, Ress D, Heeger DJ (2005) Topographic maps of visual spatial attention in human parietal cortex. J Neurophysiol 94:1358–1371.

Smith D V, Davis B, Niu K, Healy EW, Bonilha L, Fridriksson J, Morgan PS, Rorden C (2010) Spatial attention evokes similar activation patterns for visual and auditory stimuli. J Cogn Neurosci 22:347–361.

Stewart LM, Walsh V, Rothwell JC (2001) Motor and phosphene thresholds: A transcranial magnetic stimulation correlation study. Neuropsychologia 39:415–419.

Sultan F, Augath M, Logothetis N (2007) BOLD sensitivity to cortical activation induced by microstimulation: comparison to visual stimulation. Magn Reson Imaging 25:754–759.

Talsma D, Senkowski D, Soto-Faraco S, Woldorff MG (2010) The multifaceted interplay between attention and multisensory integration. Trends Cogn Sci 14:400–410.

Taubert M, Dafotakis M, Sparing R, Eickhoff S, Leuchte S, Fink GR, Nowak DA (2010) Inhibition of the anterior intraparietal area and the dorsal premotor cortex interfere with arbitrary visuo-motor mapping. Clin Neurophysiol 121:408–413.

Thielscher A, Pessoa L (2007) Neural correlates of perceptual choice and decision making during fear-disgust discrimination. J Neurosci 27:2908–2917.

Thurlow WR, Jack CE (1973) Certain determinants of the "ventriloquism effect". Percept Mot Skills 36:1171–1184.

Thut G, Nietzel A, Brandt S a, Pascual-Leone A (2006) Alpha-band electroencephalographic activity over occipital cortex indexes visuospatial attention bias and predicts visual target detection. J Neurosci 26:9494–9502.

Tolias AS, Sultan F, Augath M, Oeltermann A, Tehovnik EJ, Schiller PH, Logothetis NK (2005) Mapping cortical activity elicited with electrical microstimulation using FMRI in the macaque. Neuron 48:901–911.

Tootell RB, Hadjikhani N, Hall EK, Marrett S, Vanduffel W, Vaughan JT, Dale a M (1998) The retinotopy of visual spatial attention. Neuron 21:1409–1422.

Tosoni A, Galati G, Romani GL, Corbetta M (2008) Sensory-motor mechanisms in human parietal cortex underlie arbitrary visual decisions. Nat Neurosci 11:1446–1453.

Treue S, Martínez Trujillo JC (1999) Feature-based attention influences motion processing gain in macaque visual cortex. Nature 399:575–579.

Tyll S, Budinger E, Noesselt T (2011) Thalamic influences on multisensory integration. Commun Integr Biol 4:378–381.

Weiskopf N, Josephs O, Ruff CC, Blankenburg F, Featherstone E, Thomas A, Bestmann S, Driver J, Deichmann R (2009) Image artifacts in concurrent transcranial magnetic stimulation (TMS) and fMRI caused by leakage currents: modeling and compensation. J Magn Reson Imaging 29:1211–1217.

Werner S, Noppeney U (2010) Distinct functional contributions of primary sensory and association areas to audiovisual integration in object categorization. J Neurosci 30:2662–2675.

Werner S, Noppeney U (2011) The contributions of transient and sustained response codes to audiovisual integration. Cereb Cortex 21:920–931.

White CN, Mumford J a, Poldrack R a (2012) Perceptual criteria in the human brain. J Neurosci 32:16716–16724.

Worden MS, Foxe JJ, Wang N, Simpson G V (2000) Anticipatory biasing of visuospatial attention indexed by retinotopically specific alpha-band electroencephalography increases over occipital cortex. J Neurosci 20:RC63.

Yantis S, Schwarzbach J, Serences JT, Carlson RL, Steinmetz M a, Pekar JJ, Courtney SM (2002) Transient neural activity in human parietal cortex during spatial attention shifts. Nat Neurosci 5:995–1002.

Yau JM, Hua J, Liao D a, Desmond JE (2013) Efficient and robust identification of cortical targets in concurrent TMS-fMRI experiments. Neuroimage 76:134–144.

Yau JM, Jalinous R, Cantarero GL, Desmond JE (2014) Static Field Influences on Transcranial Magnetic Stimulation: Considerations for TMS in the Scanner Environment. Brain Stimul:1–6.

Yeung N, Summerfield C (2012) Metacognition in human decision-making: confidence and error monitoring. Philos Trans R Soc Lond B Biol Sci 367:1310–1321.

Ziemann U (2004) TMS and drugs. Clin Neurophysiol 115:1717–1729.